MURINE CENP-F REGULATES MICROTUBULE NETWORK FUNCTION AND IS ESSENTIAL IN HEART DEVELOPMENT

By

Katherine Lynn Moynihan

Dissertation

Submitted to the Faculty of the

Graduate School of Vanderbilt University

in partial fulfillment of the requirements

for the degree of

DOCTOR OF PHILOSOPHY

In

Cell and Developmental Biology

December, 2009

Nashville, Tennessee

Approved:

Professor Vivien Casagrande, Chair

Professor David Bader

Associate Professor Patricia Labosky

Associate Professor Maureen Gannon

Assistant Professor Irina Kaverina

ACKNOWLEDGEMENTS

In my first year here at Vanderbilt, I would see senior graduate students and could never imagine myself in their shoes, at the finish line. And yet, here I am, primarily due to those who guided and supported me along the way. First, I would like to thank my mentor, David Bader, for making graduate school both remarkably fun and educational. I learned and laughed so much in your lab, thoroughly enjoyed Glamorous Kt/Frog outings, and, despite our blustering, truly appreciate our friendship. I would also like to thank my incredibly helpful committee members for their suggestions and encouragement: Vivien Casagrande, Trish Labosky, Irina Kaverina, and Maureen Gannon. Overall, the Department of Cell and Developmental Biology and Program in Developmental Biology have been invaluable in supporting me as a graduate student and fostering the spirit of scientific community. Additionally, the work presented here was produced with the help of funding from the Vascular Biology Training Grant (T32 HL07751) and American Heart Association Predoctoral Fellowship (09PRE2170006).

Critical to the success of this project, as well as the addition of joy and friendship to the workday, was the entirety of the Bader laboratory: Hillary Hager Carter, Emily Cross, Pierre Hunt, Ryan Pooley, Samyukta Reddy, Ryan Roberts, Alexis Schaible, Cheryl Seneff, Elaine Shelton, Travis Smith, Becca Thomason, and Niki Winters. Pierre and Alexis deserve special mention for their patient and

infinite work with mouse models, sectioning, and genotyping. I would also like to thank several colleagues offering reagents and expertise: Ellen Dees, Paul Miller, Scott Baldwin, John Lowe, Helmut Kramer, Joe Roland with the Imaging Resources of the Epithelial Biology Center, and Jeff Rottman with the Mouse Metabolic Phenotyping Center.

Graduate school has passed with its own set of trials and triumphs. To the Bader Babes, we have banded together as friends far beyond the lab and I owe you my sanity. I will always treasure the memories of those trips to South Dakota and California, the many happy hours, birthday cupcakes, as well as various unmentionable quotes! To my family, thank you for your belief in me from the beginning – I have always wanted to make you proud and I dedicate this document to you. To Dad, for always recognizing how right we both are and to Mom, for our morning phone calls and therapy sessions. To Meghan and David, you mean the world to me and I value the strength of our friendships even as we are spread all across the country. Finally, to Brian, thank you for your strength, encouragement, and love throughout this journey. Your patience and understanding are exceptional and despite the 500 miles that have separated us, you have always been there for me.

TABLE OF CONTENTS

Page

ACKNOWLEDGEMENTS ii

LIST OF FIGURES vii

Chapter

I. INTRODUCTION 1
- CENP-F Family 1
- Microtubule Network 6
- CENP-F and the MT Network 11
- Summary of this Thesis 12

II. MURINE CENP-F INTERACTS WITH SYNTAXIN 4 IN THE REGULATION OF VESICULAR TRANSPORT 14

- Abstract 14
- Introduction 15
- Materials and Methods 19
  - Yeast two-hybrid screen (Y2H) 19
  - Cell culture, transfection and constructs 20
  - Immunostaining and microscopy 20
  - Co-immunoprecipitation using transient transfections 21
  - Co-immunoprecipitation of endogenous protein complexes containing murine CENP-F 22
  - MO antisense oligomer treatment 22
  - 2-Deoxy-D-glucose transport assay 22
  - Cell coupling 23
  - Antibodies 24
- Results 24
  - Identification of syntaxin 4 as a murine CENP-F binding partner 24
  - Transiently expressed N-terminal murine CENP-F and syntaxin 4 colocalize in cells 27
  - Endogenous CENP-F and syntaxin 4 associate in mammalian cells 29
  - Transient expression of NT-CENP-F redistributes endogenous SNAP-25 and syntaxin 4 32
  - Disruption of CENP-F function interferes with cell coupling 37
  - Inhibition of CENP-F function inhibits glucose transport 39
- Discussion 40
  - The CENP-F family regulates diverse cellular processes 40
  - Interaction with syntaxin 4 reveals a potentially broad role for murine CENP-F in vesicular transport 43

Murine CENP-F is critical in regulation of vesicular transport 44
References 45

III. MURINE CENP-F REGULATES CENTROSOMAL MICROTUBULE NUCLEATION AND INTERACTS WITH HOOK2 AT THE CENTROSOME 51

Abstract 51
Introduction 52
Materials and Methods 55
Yeast two-hybrid screen 55
Antibodies 56
Cell culture, transfection and DNA constructs 56
Immunostaining, microtubule assays, and microscopy 57
Co-immunoprecipitation using transient transfections and endogenous proteins 59
Isolation of mouse embryonic fibroblasts (MEFs) 60
Results 61
Identification of a novel interaction between murine CENP-F and Hook2 61
Transiently expressed Hook2 and NT-CENP-F interact and co-localize at the centrosome in mammalian cells 64
Endogenous Hook2 and CENP-F interact and co-localize at the centrosome 67
Ablated and disrupted CENP-F expression attenuates MT repolymerization after nocodazole challenge 69
CENP-F regulation of MT repolymerization is centrosome specific 74
CENP-F regulates MT nucleation 78
CENP-F regulates nucleation and anchoring of MT polymerization from the centrosome 79
Disruption of CENP-F function redistributes centrosomal proteins 83
Discussion 88
CENP-F displays a novel endogenous localization, binding partner, and function at the centrosome 89
CENP-F regulates MT nucleation and anchoring at the centrosome with other centrosomal proteins 91
CENP-F is a possible master regulator of MT network processes with cellular organelles 94
Acknowledgements 95
References 95

IV. AN OVERVIEW OF AVIAN HEART STRUCTURE AND DEVELOPMENT 100

Overview 100

Anatomy of the chicken heart 101
Circulation, chambers, and valves 102
Coronary circulation and conduction 104
Histology 106
Development: an overview 107
Determination and earliest development 108
Cardiogenic determination 116
Inducers of cardiomyogenic determination 118
In vitro analysis of cardiogenic mesoderm 119
Early morphogenetic changes in the forming heart tube 120
Diversification of myogenic cell lineages 123
Trabeculation and cardiac myocytes 129
Summary 135
References 135

V. MURINE CENP-F IS ESSENTIAL TO PROPER HEART DEVELOPMENT AND FUNCTION 142

Introduction 142
Materials and Methods 145
Developing the CENP-F$^{-/-}$ mouse 145
Genotyping 145
Organ and tissue preparation for histochemical analysis 146
Echocardiography 147
Electrocardiography (ECG) 148
Results 148
CENP-F is successfully excised by cTNT-Cre to generate a heart-specific knockout model 148
CENP-F$^{-/-}$ hearts display morphological differences in size and chamber wall thickness 153
CENP-F$^{-/-}$ hearts show impaired function 156
Discussion and Future Directions 161

VI. CONCLUSIONS AND FUTURE DIRECTIONS 169

Conclusions 169
Future Directions 175
Determine mechanism underlying the heart-specific CENP-F$^{-/-}$ phenotype 175
Characterize potential mitotic and migration phenotypes of CENP-F$^{-/-}$ MEFs 177
Develop and characterize global CENP-F$^{-/-}$ murine model 181

REFERENCES 184

LIST OF FIGURES

Figure Page

2.1. Identification of syntaxin 4 as an mCENP-F interacting protein 26

2.2. Transfected NTmCENP-F redistributes in COS-7 cells expressing GFP-syntaxin 4 28

2.3. Endogenous mCENP-F and syntaxin 4 co-localize in murine cells 30

2.4. N-terminal mCENP-F expression localizes to foci containing both TGN and recycling endosome markers 33

2.5. Transiently expressed NTmCENP-F and syntaxin 4 co-localize at the TGN in COS-7 cells 35

2.6. NTmCENP-F expression interferes with cell coupling 38

2.7. Depletion of mCENP-F alters GLUT4 trafficking 41

3.1. Identification of CENP-F/Hook2 interaction and characterization of binding domains 62

3.2. Transiently expressed CENP-F and Hook2 proteins interact at the centrosome 65

3.3. Endogenous CENP-F and Hook2 proteins interact and co-localize at the centrosome 68

3.4. Disrupting the CENP-F/Hook2 interaction interferes with MT repolymerization after nocodazole challenge 70

3.5. Inhibited MT nucleation is not a permanent condition, but significant 75

3.6. CENP-F disruption of MT repolymerization is centrosome specific and inhibits MT aster nucleation 76

3.7. CENP-F functions in MTOC nucleation and anchoring 81

3.8. Centrosomal proteins are redistributed by CENP-F disruption and deletion 84

3.9. Some centrosomal proteins are not redistributed by expression of NT-CENP-F 87

4.1. Anterior view of adult chicken heart 103

4.2. Fate maps of cardiogenic progenitors and myocytes in the early avian embryo 110

4.3. Position of cardiogenic cells at stage 6 in the developing chicken embryo 115

4.4. Closure of the bilateral wings of the cardiogenic crescent and formation of a heart tube 122

4.5. Position of ventricular and atrial MHC-expressing cells at stage 10 125

4.6. Diagram of the morphogenetic events regulating trabeculation and compaction 130

4.7. Prominence of the atrioventricular canal in the early chicken heart 133

4.8. Early morphogenetic moments of the heart tube 134

5.1. Deletion of the CENP-F gene with Cre-lox technology 150

5.2. CENP-F$^{-/-}$ hearts display morphological differences in size and chamber wall thickness 154

5.3. CENP-F$^{-/-}$ mice show enlarged ventricles and impaired function 158

6.1. CENP-F disruption induces spindle pole fragmentation but does not affect dynein localization to KTs 179

6.2. CENP-F$^{-/-}$ MEFs display aberrant lamellipodia 182

CHAPTER I

INTRODUCTION

CENP-F Family

CENP-F (mitosin) was independently discovered as a human, cell cycle-dependent, kinetochore (KT) associated protein and as a binding partner of the Retinoblastoma (Rb) tumor suppressor protein (Rattner et al., 1993; Zhu et al., 1995b). Since those initial discoveries, CENP-F has been shown to be well conserved; homologous proteins have been described in other vertebrates, invertebrates, and prokaryotes (Moore et al., 1999; Ortiz et al., 1999). Avian and rodent orthologs are single gene family members that share multiple conserved regions of interest and function (Goodwin et al., 1999; Litvin et al., 1993; Redkar et al., 2002). Murine, avian, and primate family members are large proteins and have a predicted coiled-coil structure with multiple intervening protein/protein binding domains (Goodwin et al., 1999; Zhou et al., 2005; Zhu et al., 1995a). Each homolog has been investigated fairly independently, leading to characterization of many functions of this large protein without a unifying theme.

The chronological nature of these investigations shows the hazy history concerning the analysis of CENP-F function. As stated above, the human homolog was the first family member discovered; in the context of cell cycle progression with KT localization, it was called CENP-F (Rattner et al., 1993), and

as an Rb-binding protein, named mitosin (Zhu et al., 1995b). Following these reports, Wei, et al. discovered the avian homolog CMF1 in myogenic populations of the chicken heart (Wei et al., 1996). Additionally, other family members were identified in *S. cerevisiae* and *C. elegans* that also showed KT localization (Moore et al., 1999; Ortiz et al., 1999). These discoveries of protein function and localization were treated very separately until Goodwin, et al. outlined a familial link via homology comparisons in the context of discovery of the murine family member (then LEK1, now murine CENP-F) (Goodwin et al., 1999). Throughout functional investigation of all emerging family members, CENP-F appeared as a cancer marker in many different tissues (de la Guardia et al., 2001; Dees et al., 2005; Erlanson et al., 1999; Esguerra et al., 2004; O'Brien et al., 2007; Rattner et al., 1997; Shigeishi et al., 2005; Ueda et al., 2008). However, beyond this link to cancer, most familial orthologs have been pursued separately without reference to species variation and without consideration to overarching concepts in gene and protein function.

As these protein family members have been explored further, fundamental divergence in temporal and spatial patterns of the gene expression has become apparent. Both murine and avian homologs are developmentally regulated, reaching peak expression throughout the embryo and then down-regulated in the adult (Dees et al., 2000; Goodwin et al., 1999). Cell lines and neoplastic tissue have been used to characterize human CENP-F, hence endogenous expression patterns are as yet unknown. However, intracellularly, the protein has primarily

been detected in the nucleus leading up to mitosis (Ashar et al., 2000; Holt et al., 2005; Hussein and Taylor, 2002; Liao et al., 1995; Rattner et al., 1993; Yang et al., 2005; Yang et al., 2003; Zhou et al., 2005; Zhu et al., 1995a; Zhu et al., 1995b). The cell cycle regulatory properties of human CENP-F have been probed extensively via RNAi, yet inconsistencies prevent consensus on the role of CENP-F in mitosis (Holt et al., 2005; Laoukili et al., 2005; Toralova et al., 2009; Yang et al., 2005). This is reviewed by Varis, et al. extensively and I will not go through it here (Varis et al., 2006). In the chicken, CMF1 localizes to the nucleus in culture myoblasts, and then becomes cytoplasmic as the myoblasts differentiate (Dees et al., 2000). Interestingly, in the mouse, both cytoplasmic and nuclear localization of CENP-F has been described (Ashe et al., 2004; Evans et al., 2007; Pooley et al., 2008b; Pooley et al., 2006; Soukoulis et al., 2005).

Despite the various localizations seen in the analysis of CENP-F across species, many well-conserved domains have been shown to function and/or bind similar partners in more than one family member. As stated above, the discovery of human CENP-F was initially a result of a Retinoblastoma protein-binding screen (Zhu et al., 1995b), and its orthologs share the E2F1-like domain in the C-terminus of the protein (Goodwin et al., 1999; Pabón-Peña et al., 2000). This domain binds other pocket proteins such as p107 and p130 (Ashe et al., 2004) and plays a significant role in cell cycle regulation and myogenic differentiation. This family of pocket proteins also functions in regulation of the G1/S checkpoint via suppression of cell cycle regulatory gene transcription (Classon et al., 2000).

CENP-F has another transcriptional target in ATF-4; Zhou, et al. has shown that two domains within the C-terminus CENP-F negatively regulate this transcription factor (Zhou et al., 2005). The bipartite nuclear localization signal adjacent to these regulatory domains is necessary for nuclear localization and, presumably, the activity with these nuclear proteins (Dees et al., 2006; Zhu et al., 1995a). Furthermore, there exists a farnesylation domain in the carboxyl-terminus that is necessary for CENP-F association with microtubules (MTs), CENP-F degradation, and G2/M progression in general (Ashar et al., 2000; Hussein and Taylor, 2002). Other computer-modeled structures within the carboxyl region of the protein predict interaction with transcriptional and structural regulators of cell division and differentiation (Wei et al., 1996; Zhu et al., 1995a). CENP-F has been widely described as a KT-associated protein, and the conserved region responsible for this localization is again found in the C-terminus (Zhu et al., 1995a). Though the exact function of CENP-F at this mitotic structure is still not completely clear, CENP-F does accumulate at the outer KT plate in early mitosis and remains there throughout M phase (Liao et al., 1995). Studies of the assembly of KT proteins place CENP-F within this interdependent accumulation pathway of various KT and spindle checkpoint proteins; CENP-F is necessary for CENP-E, BubR1, and Mad1 recruitment (Jablonski et al., 1998; Johnson et al., 2004), yet is dependent on Bub1 (Taylor et al., 1998; Taylor et al., 2001), Zwint-1 (Wang et al., 2004), CENP-I (Liu et al., 2003), Sgt1 (Steensgaard et al., 2004), and Shugoshin (Salic et al., 2004) for KT localization. The KT is an important scaffold of the G2/M cell cycle checkpoint and CENP-F C-terminal

overexpression studies have revealed a role of this domain in mitotic progression (Evans et al., 2007; Hussein and Taylor, 2002; Zhu et al., 1995a). Clearly, the variable domains within CENP-F contribute to the various processes in which this protein functions and further integration of those functions will make significant contributions in advancing the understanding of CENP-F.

More recently, analyses of CENP-F function have moved beyond the carboxyl terminus into the central and N-terminal regions of the proteins. Again, there are predicted and characterized domains within this family throughout the entire CENP-F protein in the various vertebrate species analyzed to this point (Feng et al., 2006; Pooley et al., 2008a; Pooley et al., 2006; Soukoulis et al., 2005). A spectrin repeat region is positioned central to the C-terminus, which is a potential domain for cytoskeletal and signal transduction docking (Djinovic-Carugo et al., 2002), and several leucine zippers, candidates for protein-protein interaction (O'Shea et al., 1989), are distributed throughout N-terminal sequences. Soukoulis, et al. demonstrated a novel binding domain within murine CENP-F adjacent to the spectrin repeat region that binds Nde1/Nudel and regulates MT network organization via association with the LIS1 pathway (Soukoulis et al., 2005). Nde1/Nudel and the LIS1 pathway are important in neuronal migration, as well as microtubule network regulation (Liu et al., 2000). Binding partner Nde1/Nudel was also confirmed with the human CENP-F homolog (Vergnolle and Taylor, 2007). Additionally, both the N and C-termini of CENP-F were recently established as MT-binding domains, with polymerization

mediated with the C-terminal domain *in vitro* (Feng et al., 2006). Finally, the N-terminus of CENP-F also binds soluble N-ethylmaleimide-sensitive factor attachment protein receptor (SNARE) proteins SNAP25 and syntaxin 4, proteins involved in vesicular transport along the MT network and its tracks (Pooley et al., 2008a; Pooley et al., 2006). Thus, it is clear that CENP-F as a whole has varied nuclear and cytoplasmic functions in mitotic and interphase cells, but these activities have yet to be integrated into an overall pattern of cellular, developmental, and/or organ function.

The overall CENP-F family functional theme has become more evident given our recent data demonstrating the novel localization and role of CENP-F at the centrosome (Moynihan et al., 2009a). These new findings highlight the importance of the less characterized N-terminus in MT nucleation. This important additional link between CENP-F and the MT network illuminates a MT theme throughout the CENP-F literature. Here, I discuss the roles of CENP-F in the context of MT network function – a new way to conceptualize seemingly disparate functions of CENP-F family members that do indeed fit together.

Microtubule Network

The MT network is a fundamental platform of major cellular processes. Microtubules of the cytoskeleton carry responsibilities in both cycling and quiescent cells; MTs form the mitotic spindle and attach to KTs as well as guide cell polarity and trafficking of proteins and organelles. The MT network as a

whole is regulated by the centrosome. The centrosome has multiple roles: nucleating and anchoring microtubules as well as duplicating during the cell cycle to form the poles of the mitotic spindle (Urbani and Stearns, 1999). MT nucleation occurs at the centrosome with the assistance of the γ-tubulin ring complex as a scaffold, and then, the minus-ends of the MTs are capped and anchored by other centrosomal proteins. In the cell cycle, the interphase radial array of MTs transforms into a bipolar spindle as the newly duplicated centrosomes move to opposite sides of the cell at the G2/M stage. Kinesins, generally plus-end directed MT motors, facilitate spindle formation at this stage (Allan and Schroer, 1999). During mitosis, as the nuclear envelope breaks down, the chromosomes are available to bind the probing spindle MTs at the KT attachment points (Hill, 1985; Holy and Leibler, 1994; Kirschner and Mitchison, 1986). The KT is a specialized structure on the centromere of chromosomes necessary for effective alignment and segregation of the DNA during mitosis. There is strong evidence of conservation across species in this three-layered structure that harbors motor proteins such as cytoplasmic dynein and other protein complexes governing MT attachment and the spindle checkpoint (Santaguida and Musacchio, 2009). The MTs penetrate only the outer layer of the KT, the accepted location of CENP-F, and these MT attachments allow for the alignment of the chromosomes along the metaphase plate and ultimate separation toward opposite poles (Biggins and Walczak, 2003; Maiato et al., 2004). Thus, although the precise role of CENP-F in this process has yet to be determined, the localization of CENP-F to the MT attachment point indicates a general function in this MT endpoint function. The

additional spindle checkpoint role of CENP-F discussed above fits with this localization, as the checkpoint proteins are also associated with the KT. Historically, studies of the role of MTs and the spindle checkpoint have found it difficult to tease apart the contributions of each (Maiato et al., 2004).

The cytoskeleton also regulates transport of proteins and organelles along MT tracks. The MT network plays an important role in positioning of organelles throughout the cell, including mitochondria, Golgi, and even the nucleus via centrosomal linkage (Bornens, 2008; Frederick and Shaw, 2007; Walenta et al., 2001). In fact, the recently identified CENP-F binding partner Hook2 has homologs implicated in the MT-facilitated positioning of two of these examples: the nucleus-centrosome attachment by *zyg-12* in *C. elegans* and the MT-regulated Golgi localization by eukaryotic Hook3 (Malone et al., 2003; Walenta et al., 2001). In *D. melanogaster*, multivesicular endosomes are regulated by the Hook ortholog in trafficking of both transmembrane and soluble ligands from multivesicular bodies to late endosomes and lysosomes (Krämer and Phistry, 1996; Krämer and Phistry, 1999; Sunio et al., 1999). In eukaryotes, the hook family of proteins has an N-terminal conserved MT-binding domain, and they function as linker proteins with divergent C-termini. Hook1 regulates linkage between the MT manchette and flagellum of spermatozoa, and Hook2 functions at the centrosome in regulating the radial array of MTs (Mendoza-Lujambio et al., 2002; Szebenyi et al., 2007). As mentioned before, Hook3 binds Golgi membranes and has been implicated in regulating class A scavenger receptor

function (Sano et al., 2007; Walenta et al., 2001). Thus, the hook family is an integral part of organelle positioning in coordination with the MT network as a whole.

Additionally, MTs serve as tracks along which cargo is transported by different motor proteins throughout the cell. Due to the intrinsic polarity of the MT monomer and the uniform arrangement of α– and β–monomer subunits within the protofilaments, the entire MT is polar. This polarity is characterized as a plus-end, generally the site of dynamic instability, and a minus-end, commonly the site of anchoring the MT (Rodionov et al., 1999). This inherent polarity of the MT is recognized by motor proteins and allows for differential targeting of specific cargos to distinct areas of the cell (Allan and Schroer, 1999; Rodriguez-Boulan et al., 2005; Rogers and Gelfand, 2000). The kinesin family of motor proteins predominantly travels toward the plus-end of the MT – typically at the cell periphery, KT, or basolateral surface of an epithelial cell. This type of directional trafficking is termed anterograde transport. Retrograde transport, conversely, is mediated by cytoplasmic dynein and is directed toward the minus-end of the MT. The minus-end is commonly anchored at the centrosome, basal body, or apical surface of an epithelial cell. Cytoplasmic dynein plays an essential role in protein and membrane trafficking amid the Golgi, lysosomes, and late and recycling endosomes (Höök and Vallee, 2006), and this mode of transport is thought to be additionally regulated by the dynactin complex in cargo selection and motor activation (Kamal and Goldstein, 2000). Protein and membrane trafficking along

MTs is an essential component of cell homeostasis and requires a diverse set of associated proteins to assist in its regulation.

One such set of trafficking-associated proteins is the SNARE family; these proteins are commonly regarded as specificity regulators and membrane fusion facilitators in vesicular transport between membranes (Bock et al., 2001). The family members are widely varied in structure but share a conserved helical motif, which is thought to be the primary participant in binding other SNARE helices and thus, targeting vesicles to specific destinations. The binding affinity of these SNARE helices and the influence of calcium allows membrane fusion between the vesicle and target membranes, and therefore, cargo delivery (Jena, 2009). SNARE proteins are divided into three classes: syntaxins and VAMPs, both having C-terminal transmembrane domains, and SNAPs, which are post-translationally modified to allow membrane attachment (Bock et al., 2001). The N-terminus of CENP-F binds both SNAP25 and syntaxin 4 and affects vesicular transport regulated by each of these SNARE proteins (Pooley et al., 2008a; Pooley et al., 2006). Together, linker proteins such as the hook family, motor proteins such as dynein, and SNARE proteins such as SNAP25 and syntaxin 4 all regulate transport of organelles and proteins throughout the cell using the MT network as a base. The potential regulative role of CENP-F throughout these processes is the focus of this work.

CENP-F and the MT Network

While the roles of the MT network described above run along the same vein as many of the characterized functions of CENP-F, a conceptual framework linking CENP-F to the broader functions of the MT network have not been put forward. Given all of the functions throughout the CENP-F family, there is a definite pattern of CENP-F acting along or at the ends of MTs. In simply looking at the different subcellular localizations of CENP-F and MTs, they overlap at the KT and centrosome, and with vesicular trafficking and dynein/Nde1 in varied cellular activities and times. Additionally, CENP-F itself can bind and promote polymerization of tubulin (Feng et al., 2006). Our recent demonstration of CENP-F disruption inhibiting centrosomal nucleation is a direct example of this relationship at the MT end within the MT organizing center (MTOC) (Moynihan et al., 2009a). Moreover, links to the MT network have appeared again and again with different CENP-F orthologs, even from the onset of research investigating this protein family. The outer plate of the KT, as discussed, is the site of MT attachment and CENP-F has been established as an early KT protein residing in this vicinity (Rattner et al., 1993; Santaguida and Musacchio, 2009). Though it is difficult to distinguish the exact mechanism of MT/KT attachment from the mechanism of spindle checkpoint activation, it is clear from studies on human CENP-F that CENP-F interference can affect both (Biggins and Walczak, 2003; Bomont et al., 2005; Feng et al., 2006; Holt et al., 2005; Vergnolle and Taylor, 2007; Yang et al., 2005). Additionally, the interaction of N-terminal CENP-F with SNARE proteins SNAP25 and syntaxin 4 indicates a role in trafficking, which

occurs along MT tracks (Pooley et al., 2008b; Pooley et al., 2006). Another CENP-F domain more centrally located interacts with Nde1 and is involved with the dynein/LIS1 pathway, also present along MTs (Soukoulis et al., 2005). And most recently, we found that CENP-F binds Hook2 and regulates MT nucleation at the centrosome (Moynihan et al., 2009a). Taken together, these data all suggest a global role for CENP-F in coordination with the activities of the MT network.

Summary of this Thesis

Given the framework of previously depicted CENP-F function described above, the work presented here grew out of a general multi-faceted approach in systematically deconstructing protein function: identifying binding partners and examining effects of CENP-F deletion and truncation expression. Specifically, I concentrated on the N-terminus of CENP-F, as that area of the protein was the least well-characterized. The first binding partner established in these studies was syntaxin 4, a SNARE protein that regulates vesicular docking and fusion. The binding of CENP-F to syntaxin 4 regulates vesicular trafficking, as evidenced by impaired GLUT4 trafficking when CENP-F is depleted (Chapter II). Furthermore, CENP-F also binds Hook2, a centrosomal MT linker protein. This interaction opened a new avenue of investigation of CENP-F function at the centrosome, resulting in data demonstrating the role of CENP-F in centrosomal MT nucleation (Chapter III). Additionally, I have examined CENP-F function in the context of organogenesis, specifically the heart, which is the first organ to

develop and function in the embryo. To this point, I leave the introduction of heart development to Chapter IV and the initial section of Chapter V. Chapter IV specifically details the development of the avian heart, whereas Chapter V presents our studies of murine CENP-F heart-specific deletion. CENP-F is highly expressed in the murine heart, and this expression peaks during the period of extensive remodeling. Cardiomyocyte-specific CENP-$F^{-/-}$ animals clearly display a smaller heart phenotype, which then develops into dilated cardiomyopathy. As a whole, this thesis examines the roles of CENP-F in trafficking and MT nucleation at the cellular level and the effect of CENP-F deletion in heart development to illuminate the larger role this protein plays in organogenesis.

CHAPTER II

MURINE CENP-F INTERACTS WITH SYNTAXIN 4 IN THE REGULATION OF VESICULAR TRANSPORT

This chapter is published under the same title in *Journal of Cell Science*, October, 2008 (Pooley and Moynihan, et al., 2008). This publication was a joint effort; Ryan Pooley and myself were co-first authors.

Abstract

Syntaxin 4 is a component of the SNARE complex that regulates membrane docking and fusion. Using a yeast-two hybrid screen, we identify a novel interaction between syntaxin 4 and cytoplasmic murine CENP-F (CENP-F), a protein previously demonstrated to associate with the microtubule network and SNAP-25. The binding domain for syntaxin 4 in CENP-F was defined by yeast two-hybrid and co-immunoprecipitation. Confocal analyses in cell culture reveal a high degree of co-localization between endogenously expressed proteins in interphase cells. Additionally, the endogenous SNARE proteins can be isolated as a complex with CENP-F in immunoprecipitation experiments. Further analyses demonstrate that CENP-F and syntaxin 4 co-localize with components of plasma membrane recycling: SNAP-25 and VAMP2. Depletion of endogenous CENP-F disrupts GLUT4 trafficking while expression of a dominant-negative form of CENP-F inhibits cell coupling. Taken together, these studies demonstrate that CENP-F provides a direct link between proteins of the SNARE system and the

microtubule network and indicate a diverse role for CENP-F in vesicular transport.

Introduction

Movement of membrane bound vesicles to and from the cell membrane is dependent on the cytoskeleton. Along with the actin network, microtubules serve as tracks for the efficient and directed movement of organelles and vesicles (Caviston and Holzbaur, 2006; Hehnly and Stamnes, 2007; Ishiki and Klip, 2005; Soldati and Schliwa, 2006; Vedrenne and Hauri, 2006). A wide range of studies report the importance of the microtubule network in the transport of specific cargos in polarized and non-polarized cells. For example, microtubule-based transport and dynein activity are essential for TrkA signaling to Rap1 and MAPK1/2 as inhibition of dynein activity results in altered vesicular trafficking (Miyamoto et al., 2006; Wu et al., 2007). Similarly, kinesin motors regulate vesicular cargo along microtubules (Schnapp, 2003). Furthermore, a PKA- and calcium-dependent pathway controls non-polarized macrophage secretion of apoE along the microtubule network (Kockx et al., 2007). Additionally, treatment with agents that disrupt microtubule function such as nocodozale and rotenone inhibit movement of proteins from the Golgi to the cell surface (Feng, 2006; Zheng et al., 2007). However, identification and characterization of proteins directly linking membrane bound vesicles to the microtubule network remain elusive.

Human CENP-F (also called mitosin) was independently identified by the Yen and Lee groups utilizing auto-immune antibodies and Rb-binding properties (Rattner et al., 1993; Zhu et al., 1995b). Our group discovered the murine homolog and, though previous publications have used the term LEK1 (Ashe et al., 2004; Goodwin et al., 1999; Pooley et al., 2006; Soukoulis et al., 2005), we now refer to this protein as murine CENP-F to more accurately describe the gene product. Murine CENP-F, like other family members, is a large protein (2998 aa) and shares significant sequence and domain homology with related proteins in both humans and avians (Ashe et al., 2004; Dees et al., 2000; Goodwin et al., 1999; Liao et al., 1995; Pabon-Pena et al., 2000; Zhu et al., 1995a; Zhu et al., 1995b). The human homolog binds the kinetochore and is an important regulator of mitosis and cell division (Feng et al., 2006; Liang et al., 2004; Liao et al., 1995; Rattner et al., 1993; Yang et al., 2005; Zhu et al., 1995a; Zhu et al., 1997; Zhu et al., 1995b). In addition, both human and murine CENP-F bind proteins associated with the microtubule network, including tubulin (Feng et al., 2006) and Nde1 (Soukoulis et al., 2005). The binding of CENP-F to Nde1 is of particular interest as Nde1 interacts with Lis1 and dynein to modulate the microtubule network in regulation of cell shape and movement (Faulkner et al., 2000; Gibbons, 1996; Rattner et al., 1993; Smith et al., 2000; Zhu et al., 1997). Relevant to the current study, the Lis1 pathway functions with the Golgi network and in membrane trafficking (Kondratova et al., 2005; Liang et al., 2004). Utilizing dominant-negative protein expression and induced suppression of CENP-F expression, we demonstrate that interference with CENP-F function severely

alters the microtubule network (Soukoulis et al., 2005). In addition, several studies show that membrane trafficking and positioning of organelles are dependent on interaction of the microtubule network with Nde1 and Lis1 (Banks and Heald, 2001; Faulkner et al., 2000; Gibbons, 1996; Smith et al., 2000; Terada et al., 1996; Xiang et al., 1999).

Budding and fusion events between donor and acceptor membranes are essential for vesicular transport. The SNARE (soluble N-ethylmaleimide-sensitive fusion protein attachment protein receptors) family of proteins is responsible, at least in part, for regulation of such fusion events (Chen and Scheller, 2001; Ishiki and Klip, 2005). Apposing SNARE proteins, which consist of vesicle-associated membrane proteins (VAMPs), plasma membrane-associated syntaxins, and cytoplasmic synaptosomal-associated proteins (SNAPs), form coiled-coil aggregates that are important in regulating membrane fusion events (Aikawa et al., 2006; Chen and Scheller, 2001; Ishiki et al., 2005; Martin et al., 1998; McMahon et al., 1993; Rowe et al., 1999). Plasma membrane trafficking of proteins between subcellular domains and translocation to the cell surface is mediated, in part, by SNARE proteins (Chen and Scheller, 2001; Jahn and Sudhof, 1999; Mallard et al., 2002; Sollner et al., 1993; Wilcke et al., 2000). The SNARE protein syntaxin 4 is an integral membrane protein that localizes to the plasma membrane and is essential in vesicular docking and fusion (Aikawa et al., 2006; Bajohrs et al., 2005; Band et al., 2002; Pooley et al., 2006). Specifically, syntaxins are critical in vesicular transport of GLUT4-containing vesicles in

skeletal muscle, cardiomyocytes, and adipose tissue after insulin stimulation (Bryant et al., 2002; Cain et al., 1992; Martin et al., 1996; Pessin et al., 1999). Determining the physical linkage of SNAREs to the microtubule network is essential for understanding the role of this cytoskeletal component in the myriad of trafficking events.

In a recent study, we reported that CENP-F physically associates with SNAP-25, and together these proteins form a complex with Rab11a, myosinVb, and VAMP2 in the recycling endosome pathway (Pooley et al., 2006). Furthermore, disruption of endogenous CENP-F function by dominant-negative protein expression or protein knock-down severely retarded the recycling endosome network and transferrin trafficking (Chen and Scheller, 2001). While this is the only report of CENP-F regulating vesicular transport, the family has been shown to function with the cytokeleton (Goodwin et al., 1999; Feng et al., 2006), and from this, we postulate that CENP-F may have a extensive role in controlling SNARE-mediated vesicular transport by the microtubule network. Further data is critical to establish the roles for CENP-F in the diverse processes of vesicular transport.

In the current study using yeast two hybrid (Y2H) and biochemical analyses, we demonstrate that syntaxin 4 and CENP-F physically interact. These data are consistent with the hypothesis that CENP-F is a critical component in the dynamic regulation of plasma membrane trafficking with the microtubule

network through its interaction with SNARE proteins and Nde1 (Soukoulis et al., 2005). Using genetic, immunolocalization, and immunoprecipitation studies, we demonstrate that both transiently expressed and endogenous cytoplasmic CENP-F directly associate with syntaxin 4 at the Golgi and this complex also contains VAMP2 and SNAP-25. Additionally, disruption of CENP-F interferes with cell coupling in 3T3 fibroblasts, demonstrating inhibition of gap junction function at the cell membrane (Francis and Lo, 2006) and indicating the essential role of CENP-F in membrane trafficking. Finally, we show that disruption of CENP-F function inhibits GLUT4 trafficking, a system used to model syntaxin 4 function in membrane trafficking in 3T3 adipocytes. Thus, the present study establishes a physical link between CENP-F and the SNARE complex and suggests a role for CENP-F in the regulation for vesicular transport by the microtubule network.

Materials and Methods

Yeast two-hybrid screen

This screen was previously described by Pooley et al. (2006). Briefly, a large N-terminal region of cytoplasmic CENP-F (amino acids 1-689, termed "LCR") was utilized in the Matchmaker Y2H System 3 (BD Biosciences Clontech). Library plasmids were isolated from yeast colonies that survived on Quadruple Dropout Medium (QDO; SD/-Ade/-His/-Leu/-Trp/X-a-Gal) and exhibited *lacZ* expression. The inserts were then sequenced by the Vanderbilt Sequencing Core Facility and identified using NCBI Blast (Altschul et al., 1990).

For each identified protein product, false positive tests with empty vector and random protein matings were conducted to eliminate spurious interactions according to manufacturer's recommendations.

Cell culture, transfection, and constructs

COS-7, 3T3-L1, and C2C12 cells (ATCC) were maintained in Dulbecco's modified Eagle's medium supplemented with 10, 10, and 20% FBS respectively, 100 μg/mL penicillin/streptomycin, and L- glutamine, in a 5% CO_2 atmosphere at 37^{o}C. 3T3-L1 pre-adipocytes were differentiated by treatment with insulin, dexamethasone, and isobutylmethlxanthine as previously described (Frost and Lane, 1985), and cells were used for experimentation 9-12 days after initiation of differentiation. For transfection, cells were grown to 50-75% confluency and transfected with DNA using FuGENE 6 (Roche) according to manufacturer's recommendations. N-terminal CENP-F (NT-CENP-F) was constructed by placing the N-terminal 474 amino acids of CENP-F into pCMV-myc vector and full length syntaxin 4 was placed into the EGFP-C3 vector (BD Biosciences Clontech).

Immunostaining and microscopy

For transient and endogenous studies, cells were gently washed with 1X PBS and fixed with either 4% paraformaldehyde to visualize endogenous proteins or with methanol to visualize transient protein for 20 minutes. Subsequently, cells were washed with 1X PBS, permeabilized with 0.25% Triton X-100 in 1X PBS for 10 minutes, and blocked for at least 1 hour in 2% BSA in 1X

PBS at room temperature. Primary antibodies were incubated overnight at 4^{o}C. Cells were then washed 3 times in 1X PBS and secondary antibodies were added for 1 hour at room temperature. Cells were again washed 3 times with 1X PBS and coverslips mounted with AquaPoly/Mount (PolySciences). Cells were visualized by fluorescence microscopy with an AX70 (Olympus), or for confocal analysis, with a LSM510 (Ziess) microscope. Images were captured using Magnafire (Olympus). All images of control and experimental cells were processed identically.

Co-immunoprecipitation using transient transfections

COS-7 cells were grown on 10 cm plates; lysates were harvested 48 hours post transfection. The ProFound Mammalian c-Myc Tag Co-IP Kit (Pierce) was utilized according to manufacturer's protocol. Briefly, cells were washed once with ice-cold TBS, incubated with M-Per Extraction Reagent (Pierce) containing protease inhibitor (Sigma), and centrifuged at 16,000 X g for 20 minutes at 4^{o}C. Lysate protein concentration of the supernatant was determined using a bicinchoninic acid solution assay (Pierce). For 2 hours, 100 µg total lysate was incubated with gentle shaking at 4^{o}C with 10 µL anti-c-myc agarose slurry. Columns were washed 3 times with 1X TBS-Tween. Protein was eluted with 2X non-reducing sample buffer (Pierce) at 95^{o}C for 5 minutes. To reduce proteins for SDS-PAGE analysis and western blot analysis, 2 µL 2-mercaptoethanol was added. Ten µL of total lysate supernatant was used to

confirm protein expression. Blots were developed using NBT-BCIP (Roche) and scanned into digital images (Hewlett-Packard).

Co-immunoprecipitation of endogenous protein complexes containing CENP-F

C2C12 cells were lysed with Nonidet P-40 buffer with gentle sonication. Whole cell lysates were recovered and samples containing 2-3 mg total protein were precleared with GammaBind Plus Sepharose (Amersham Biosciences) for 20 minutes with gentle rotation at 4^{o}C. Cell lysates were collected and incubated overnight with 3 µg polyclonal syntaxin 4 antibody (Sigma). GammaBind Plus Sepharose was added to bind the antibody-protein complex. Beads were washed 3 times with cold 1X PBS and proteins were eluted with Laemmli sample buffer at a boiling temperature for 5 minutes. Proteins were resolved on a 6% SDS-PAGE gel and analyzed by western blot analysis. Twenty µg of protein lysate was loaded to visualize CENP-F in whole cell lysate.

MO antisense oligomer treatment

Production of and methods utilizing MO to specifically knock down endogenous CENP-F have been previously reported (Ashe et al., 2004; Pooley et al., 2006; Soukoulis et al., 2005).

2-Deoxy-D-Glucose transport assay

Forty-eight hours after MO addition, 3T3-L1 adipocytes were serum-starved for 1 hour. The cells were then incubated with 100 nM insulin in KRH

buffer for 20 minutes. Glucose transport was initiated by addition of 0.5 mM 2-deoxy-D-[1,2-^{3}H] glucose (0.25 µCi). After 10 minutes, transport was terminated by washing the cells 3X with cold KRH buffer. Cells were then solubilized with 0.5% SDS, and the incorporated radioactivity was measured by liquid scintillation counting. All quantitative data are representative of three separate experiments conducted over three days, each with n=6-8. As a control to demonstrate the insulin-dependent nature of glucose transport with morpholino inhibition, standard control and CENP-F MO-treated cultures were assayed for glucose uptake with and without insulin stimulation. A one sample Student's t-test was used after normalization to standard control (SC) cell populations.

Cell coupling

Cultured 3T3 fibroblasts were transfected with GFP alone as a control, both NT-CENP-F and GFP-SNAP-25, or both NT-CENP-F and GFP-syntaxin 4. Living transfected cells were identified and to quantitatively assess dye coupling, intracellular impalement was carried out with microelectrode filled with sulforhodamine101. The fluorescent dye was injected into the impaled cells iontophoretically using a current pulse of 1-3 nA of 0.5 second duration once per second for a total duration of 2 minutes. After an additional 3 minutes, the total extent of dye spread was recorded as the number of surrounding cells containing the injected dye. Transfer of dye was quantified and outlined according to published methods in 1st and 2nd tier cells (Francis and Lo, 2006).

Antibodies

Rab11a (a gift from Dr. James Goldenring, Vanderbilt University) and CENP-F antibodies were previously described (Pooley et al., 2006; Soukoulis et al., 2005). SNAP-25, syntaxin 4, and β-tubulin antibodies were obtained from Sigma. Golgin-97 was obtained from Molecular Probes, while VAMP2 and VAMP3 antibodies were purchased from StressGen. Syntaxin 4, EEA1, α-myc and α-GFP, antibodies were obtained from BD Bioscience. Alexa Fluor 488- and 568- conjugated secondary antibodies were also utilized (Molecular Probes). For triple labeled immunofluorescence studies, polyclonal anti-myc (Novus) was directly labeled with the Zenon Alexa-647 labeling kit (Molecular Probes). Alkaline phosphatase-conjugated secondary antibodies for western blot were also purchased from Sigma.

Results

Identification of syntaxin 4 as a CENP-F binding partner

Despite the significant literature characterizing CENP-F family members, most work has focused on the C terminus of the protein (Clark et al., 1997; Feng et al., 2006; Konstantinidou et al., 2003; Liao et al., 1995; Zhou et al., 2005; Zhu et al., 1995a; Zhu et al., 1997; Zhu et al., 1995b). Relatively little else was known concerning potential molecular interactions and functions in the major N-terminal regions of the molecule until recently. Feng et al. have identified a microtubule binding domain in the initial 385 amino acids of human CENP-F (Feng et al.,

2006), and our group demonstrated the interaction of CENP-F with Nde1 and SNAP-25 (Pooley et al., 2006; Soukoulis et al., 2005). To identify binding partners in this domain, and thus, ascribe molecular function, we conducted an extensive Y2H screen using the N-terminal coiled-coil domain (amino acids 1-689; coding sequences for exons 1-6) of CENP-F as bait. From this screen, we identified specific proteins known to regulate organelle positioning and membrane trafficking, one of which was the cytoplasmic SNARE protein SNAP-25 (Pooley et al., 2006). The screen yielded CENP-F interaction with a second SNARE protein: syntaxin 4, the binding partner of SNAP proteins which helps mediate vesicular docking and fusion. Y2H analysis was used to further define binding domains within these proteins. From this assay, the first 474 amino acids of CENP-F (NT-CENP-F) were determined to be required for syntaxin 4 interaction (Figure 2.1), while further reduction of this sequence eliminated syntaxin 4 binding altogether. Interestingly, our group identified this region of CENP-F for its interaction with SNAP-25, while Feng et al. recognized the same area for the interaction of the human homolog with tubulin (Feng et al., 2006; Pooley et al., 2006). Y2H analysis determined that the C-terminal 144 amino acids of syntaxin 4 were indispensable for CENP-F binding (Figure 2.1).

Transient protein expression within mammalian cells further confirmed the interaction of CENP-F and syntaxin 4. The minimal syntaxin 4 binding domain of CENP-F (myc-tagged N-terminal 474 amino acids of CENP-F, termed NT-CENP-F), and GFP-tagged syntaxin 4 were expressed in COS-7 cells. Lysates were

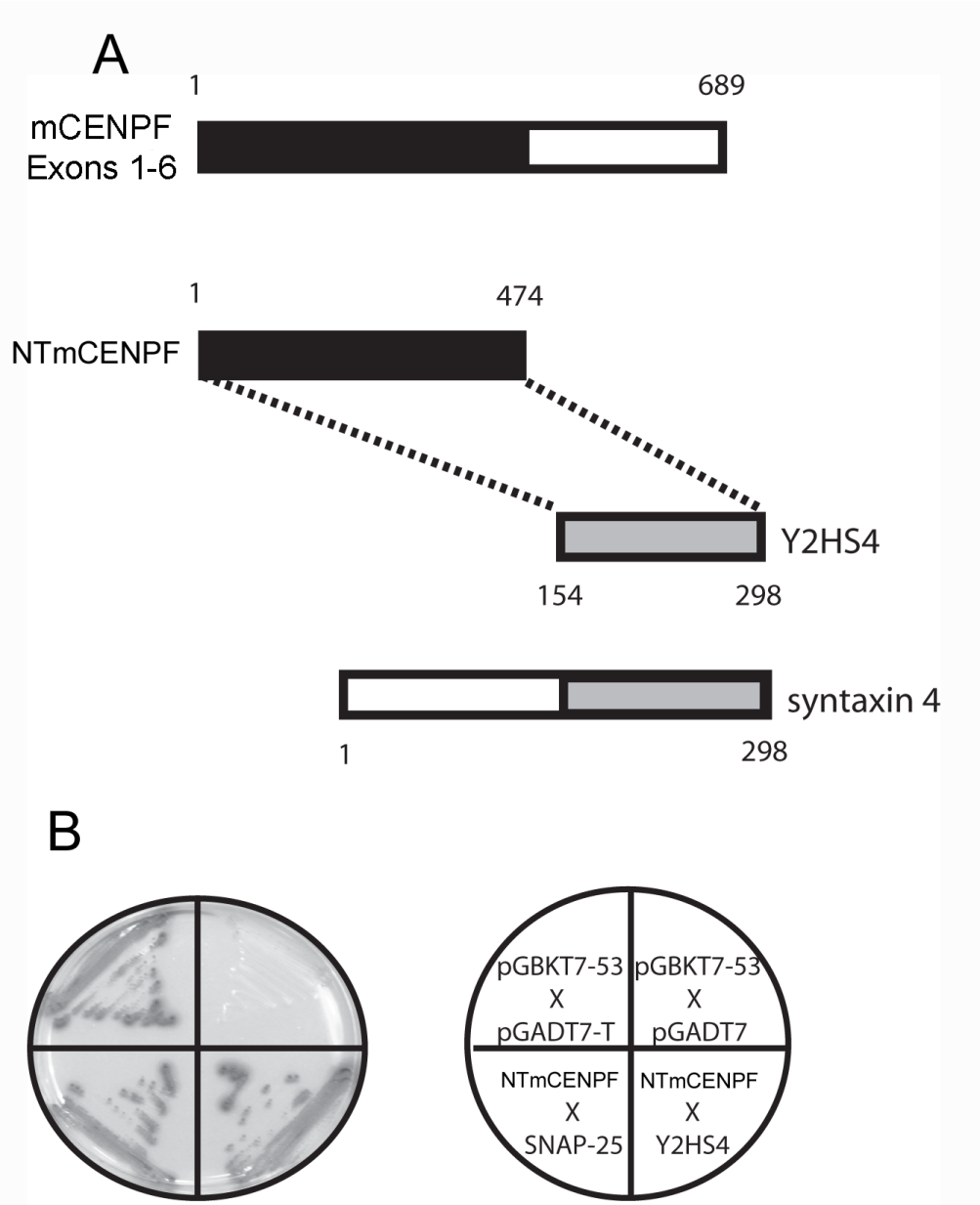

Figure 2.1. Identification of syntaxin 4 as an mCENP-F interacting protein. A) A Y2H screen was conducted and described previously (Pooley et al., 2006). One of the interacting proteins with mCENP-F was identified as syntaxin 4. The plasmid was isolated from a colony that survived on QDO media and subsequently sequenced. The resulting sequence was identified as the C-terminal 144 aa of syntaxin 4, labeled Y2HS4. The N-terminal 474 aa region of mCENP-F, NTmCENP-F, was further characterized as being the region of mCENP-F sufficient for syntaxin 4 interaction by Y2H. B) Positive associations grew on QDO media and exhibited blue color upon β-Gal testing. As a positive control, growth was indicated by yeast transformed with pGBKT7-53 and pGADT7-T. The previously described interaction of NTmCENP-F with SNAP-25 was also used as a positive control (Pooley et al., 2006). The negative control with yeast co-expressing pGBTK-53 and the empty vector pGADT7 demonstrated no growth on the media. The test interaction clearly demonstrates that NTmCENP-F does associate with the Y2HS4 portion of syntaxin 4 in yeast.

prepared and co-immunoprecipitations (co-IP) were conducted with the appropriate antibodies. As seen in Figure 2.2F, we were able to co-precipitate GFP-syntaxin 4 utilizing NT-CENP-F, while all control experiments demonstrated no spurious GFP-syntaxin 4 association with CENP-F. Syntaxin 4 did not react with any other sequences in CENP-F except NT-CENP-F (unpublished data). Taken together, these results demonstrate that the N-terminal 474 amino acids of CENP-F are necessary and sufficient for syntaxin 4 association.

Transiently expressed N-terminal CENP-F and syntaxin 4 co-localize in cells

Knowing that these proteins interacted in Y2H and co-IP analyses, we investigated the subcellular localization of these proteins. Transient expression of NT-CENP-F in COS-7 cells results in strong protein localization to the perinuclear region of cells and more diffusely to the cell periphery (Figure 2.2A). As previously reported for syntaxins in COS cells (Banfield et al., 1994; Quinones et al., 1999), transient expression of GFP-syntaxin 4 leads to protein localization in multiple foci located throughout the cell (Figure 2.2B). This punctuate perinuclear distribution is very similar to previous reports of exogenously-expressed syntaxin in COS cells (Bandfield et al, 1994; Quinones et al, 1999). However, in cells co-expressing both proteins, NT-CENP-F redistributed to GFP-syntaxin 4-positive foci with a high degree of co-localization (Figure 2.2C-E). Taken together, these data support our Y2H and co-IP data and demonstrate an interaction between CENP-F and syntaxin 4.

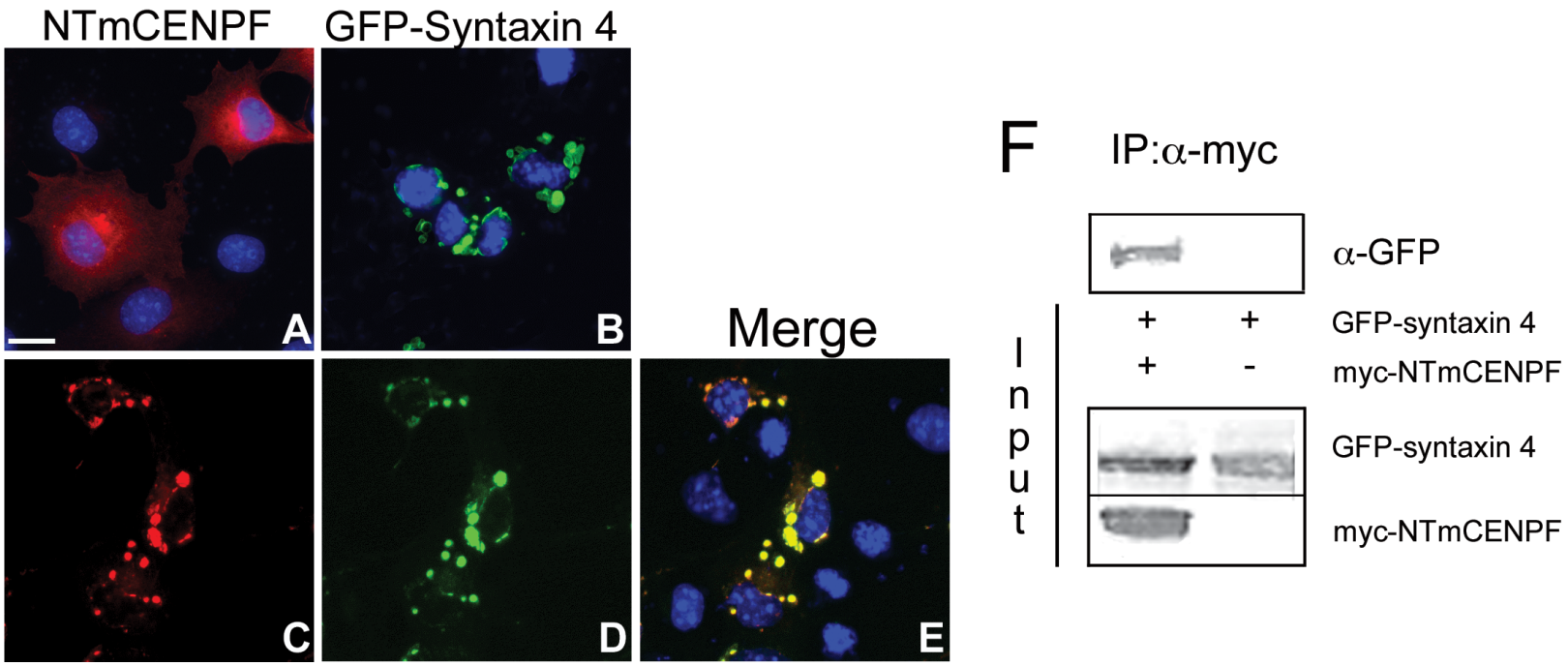

Figure 2.2. Transfected NTmCENP-F redistributes in COS-7 cells expressing GFP-syntaxin 4. A) COS-7 cells singly transfected with NTmCENP-F show a cytoplasmic distribution of the protein with a high perinuclear distribution. B) Cells singly transfected with GFP-syntaxin 4 show a significantly different distribution at defined foci throughout the cell. C-E) When cells are co-transfected with syntaxin 4 and NTmCENP-F, syntaxin 4 remained at the multiple intracellular foci, and NTmCENP-F demonstrated a significant redistribution to the same foci occupied by GFP-syntaxin 4 as seen in the merged image (E). NTmCENP-F is indicated in red, while GFP-syntaxin 4 is shown in green. DAPI (blue) is used to visualize the nucleus. F) COS-7 cells were transfected with NTmCENP-F-myc and GFP-syntaxin or with GFP-syntaxin 4 alone for a negative control. An immunoprecipitation was conducted with α-myc antibody, and blots were probed with α-GFP antibody. Input lanes show transfected protein expression in the lysate. GFP-syntaxin 4 was precipitated in the presence of NTmCENP-F-myc. The singly transfected control shows there was no spurious binding of GFP-syntaxin 4 to the beads.

Endogenous CENP-F and syntaxin 4 associate in mammalian cells

We next examined the endogenous localization of CENP-F and syntaxin 4 in murine cell lines. Two cell lines previously shown to express endogenous CENP-F and syntaxin 4 were used: C2C12 myoblasts and 3T3 L1 adipocytes (Pooley et al., 2006; Soukoulis et al., 2005; Tortorella and Pilch, 2002). As seen in the myoblast line in Figure 2.3A, confocal analysis demonstrated significant co-localization in the perinuclear region of the cell extending into the cell periphery. Band et al (2002) have previously observed this perinuclear to peripheral distribution of endogenous syntaxin 4 in cultured NRK cells. In the present study, overlap was not absolute, as the staining pattern of CENP-F extended further in the cell periphery than that of syntaxin 4. This is to be expected given that both proteins have been shown to bind other proteins and function in multiple pathways.

Analysis of syntaxin 4 function has been studied extensively in 3T3-L1 adipocytes (Cain et al., 1992; Pessin et al., 1999; Volchuk et al., 1996). Therefore, in prelude to our functional studies of this novel interaction, we examined the subcellular distribution of CENP-F and syntaxin 4 in this cell line (Figure 2.3C). The intense perinuclear staining of both CENP-F and syntaxin 4 mirrored the cytoplasmic expression observed in C2C12 cells, but both proteins demonstrated more significant staining at the cell periphery as compared to the myoblast cell line (Figure 2.3B). This pattern of syntaxin 4 localization reflects results previously reported for this cell type (Band et al., 2002). Furthermore,

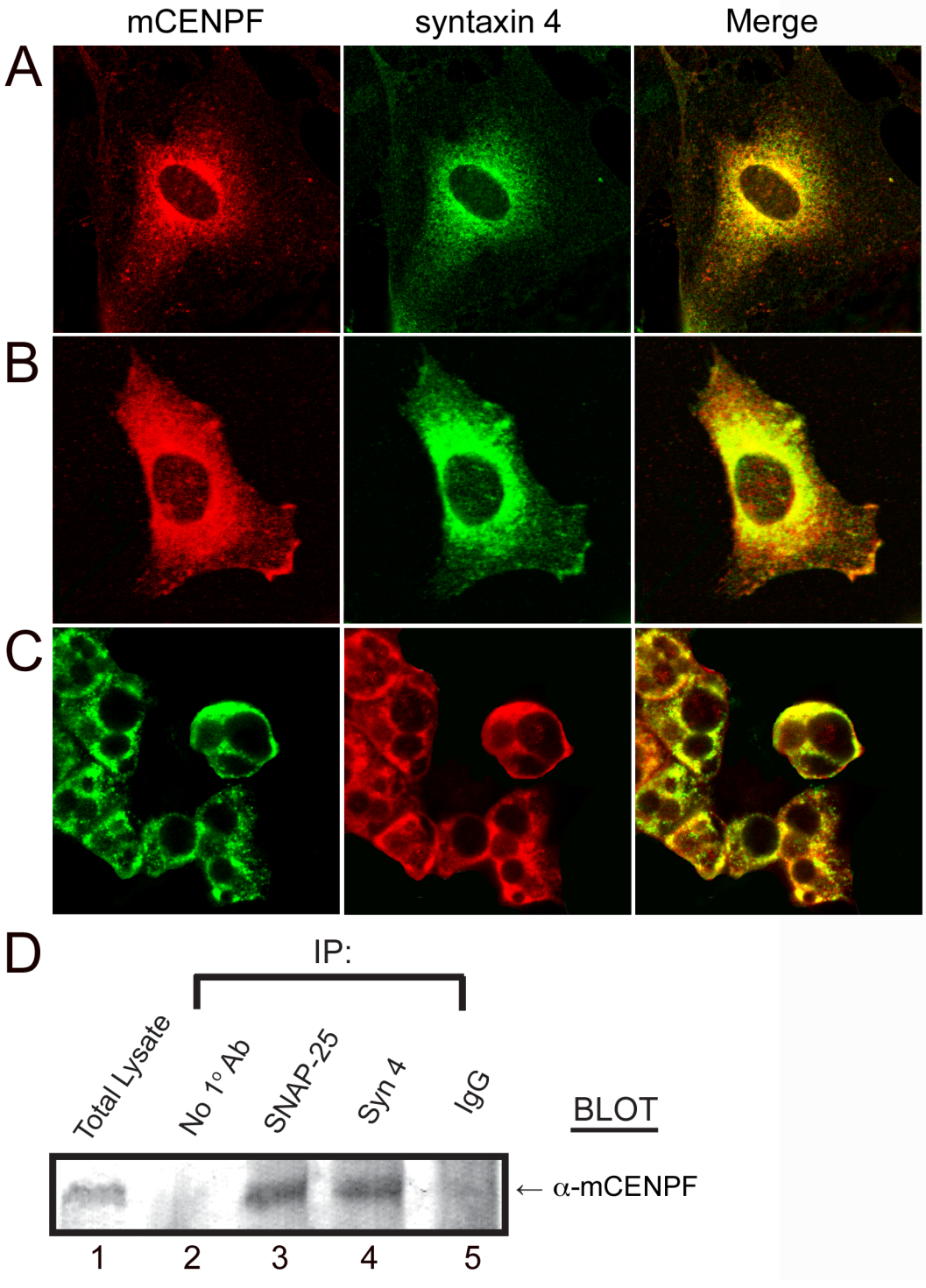
mCENPF
syntaxin 4
Merge
A
B
C
D
IP:
Total Lysate
No 1° Ab
SNAP-25
Syn 4
IgG
BLOT
← α-mCENPF
1
2
3
4
5

Figure 2.3. Endogenous mCENP-F and syntaxin 4 co-localize in murine cells. A) Endogenous mCENP-F and syntaxin 4 demonstrated significant overlap in expression throughout the cytoplasm in C2C12 myoblasts (merge). They share a high degree of co-localization in the perinuclear region, but mCENP-F has a broader distribution extending further into the cell periphery. **B)** 3T3-L1 pre-adipocytes also demonstrate similar expression patterns of mCENP-F and syntaxin 4 to that seen in C2C12 cells. However, both endogenous proteins demonstrate higher expression at the cell periphery than that seen in C2C12 myoblasts. **C)** 3T3-L1 cells were differentiated as described in methods. Both endogenous mCENP-F and syntaxin 4 appear to have a high expression distribution throughout the cells. All images are from confocal microscopy. (Bar, 10 μm) **D)** Murine CENP-F forms an endogenous complex with syntaxin 4. Endogenous protein complexes were analyzed using C2C12 cell lysates for co-immunoprecipitation analysis with Sepharose beads alone, α-SNAP-25 antibody, syntaxin 4 antiserum, or IgG antibody alone. After precipitation, elution, and Western blotting, the blot was probed with α-mCENP-F antibody. **Lane 1** demonstrates the presence of mCENP-F in the lysate. **Lane 2** demonstrates the absence of precipitation with beads alone. **Lane 3** is a positive control that demonstrates mCENP-F precipitation with SNAP-25. **Lane 4** shows that mCENP-F precipitates with syntaxin 4. **Lane 5** demonstrates the lack of precipitation with non-immune IgG.

differentiated 3T3-L1 adipocytes demonstrated a high degree of endogenous CENP-F and syntaxin 4 co-localization (Figure 2.3C). Protein localization is broader in the differentiated cells and extends to the cell periphery.

To corroborate these results, we probed for the presence of endogenous complexes containing both CENP-F and syntaxin 4 using immunoprecipitation of C2C12 lysates. As seen in Figure 2.3D, CENP-F was readily co-precipitated with syntaxin 4 (Lane 4). In contrast, precipitations with beads alone (Lane 2) and non-immune IgG (Lane 5) were negative. As a positive control, we co-precipitated CENP-F from the same lysate with an antiserum against the CENP-F binding partner SNAP-25 (Figure 2.3D, lane 3). Taken together, these data identifying endogenous colocalization and biochemical interaction through antibody coimmunoprecipitation support the hypothesis that CENP-F associates with the endogenous SNARE complex within eukaryotic cells.

Transient expression of NT-CENP-F redistributes endogenous SNAP-25 and syntaxin 4

In an effort to define the role of CENP-F in the regulation of vesicular function, we examined whether expression of its syntaxin 4-binding domain might influence subcellular localization of the trafficking apparatus in C2C12 cells. As seen in Figure 2.4, forced expression of NT-CENP-F resulted in the concentration of syntaxin 4 in perinuclear foci (compare Figure 2.3 with Figure 2.4A). SNAP-25, a known binding partner of both syntaxin 4 and CENP-F also accumulated in this position but not completely as other regions of the cytoplasm

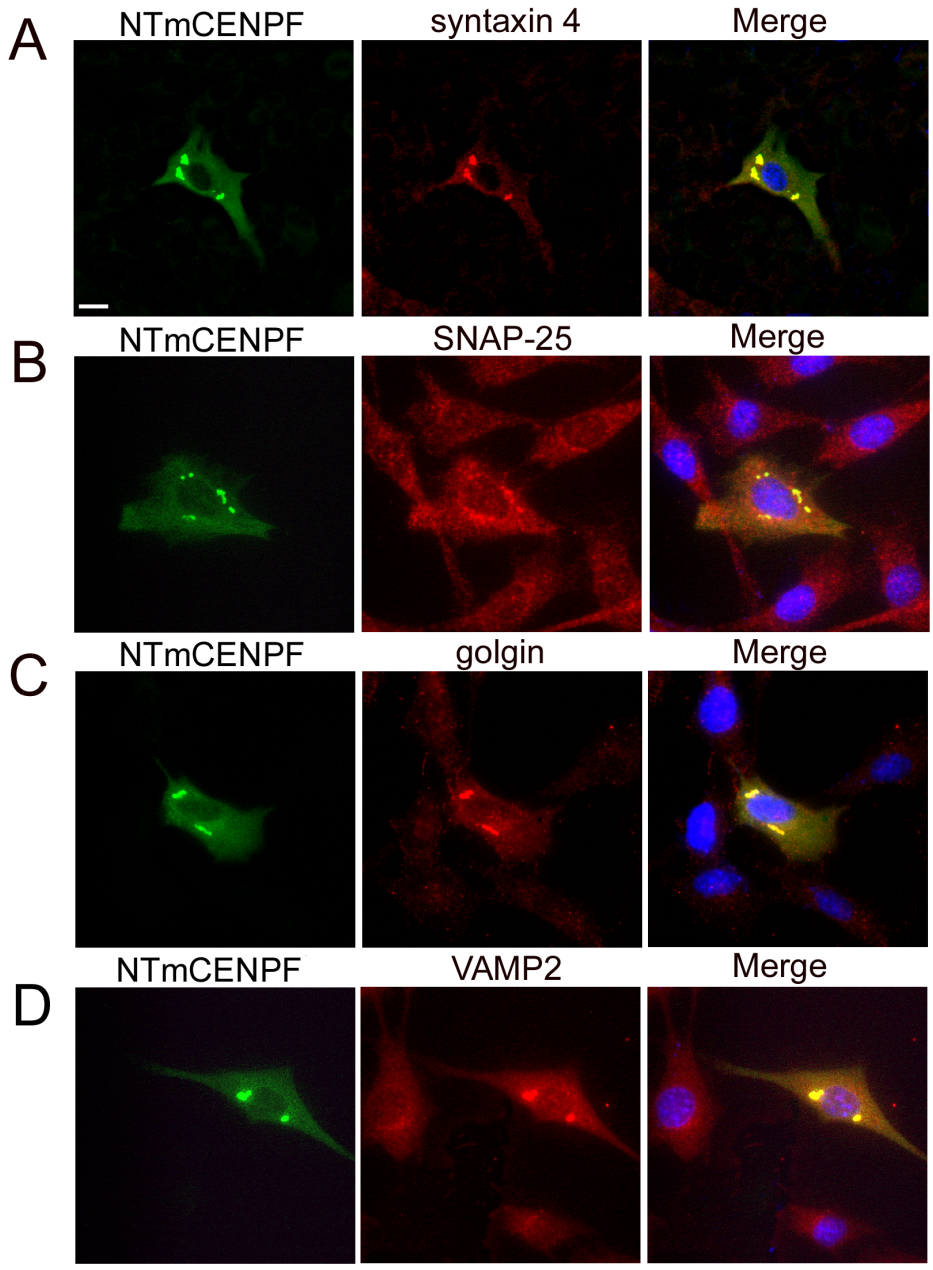

Figure 2.4. N-terminal mCENP-F expression localizes to foci containing both TGN and recycling endosome markers. NTmCENP-F was transfected into C2C12 cells and markers for SNAREs, TGN, and recycling endosomes were immunolabelled. A) Syntaxin 4 did not co-localize with NTmCENP-F-myc, but there was a redistribution of the protein in cells that were transfected. B-D) SNAP-25, golgin, and VAMP2 did co-localize with NTmCENP-F. NTmCENP-F immunofluorescence is shown in green, while endogenous markers are in red. DAPI was used to visualize the nuclei (blue) (Bar, 10 μm).

remained weakly positive for the anti-SNAP-25 antibody (Figure 2.4B). Utilizing the trans-Golgi network (TGN) marker golgin-97, we determined that these NT-CENP-F/syntaxin 4/SNAP-25 foci co-localized within TGN (Figure 2.4C) and not with markers of the early or recycling endosome (data not shown). VAMP2, but not VAMP3, also accumulated in the TGN of cells expressing NT-CENP-F (Figure 2.4D). We would also note that expression of GFP-syntaxin 4 alone also results in accumulation of endogenous CENP-F in the TGN in C2C12 cells (Data not shown).

Co-transfection was used to determine whether redistribution of components was a consistent feature of transient expression of NT-CENP-F and syntaxin 4. As seen in Figure 2.5A, expression of exogenous proteins resulted in the same accumulation of product in the Golgi/TGN. It should be noted that previous studies have reported that exogenously expressed syntaxin accumulates in the Golgi (Rowe et al., 1999; Salaun et al., 2004; Takuma et al., 2002; Washbourne et al. 2001). Consistent with expression of NT-CENP-F alone, VAMP2 (Figure 2.5B) and SNAP-25 (data not shown) were readily seen in this compartment, while VAMP3, Rab11a, and EEA1 were excluded from the TGN. The dramatic redistribution of syntaxin 4, VAMP2 and SNAP-25 to the TGN after expression of NT-CENP suggests a role for this protein in vesicular transport.

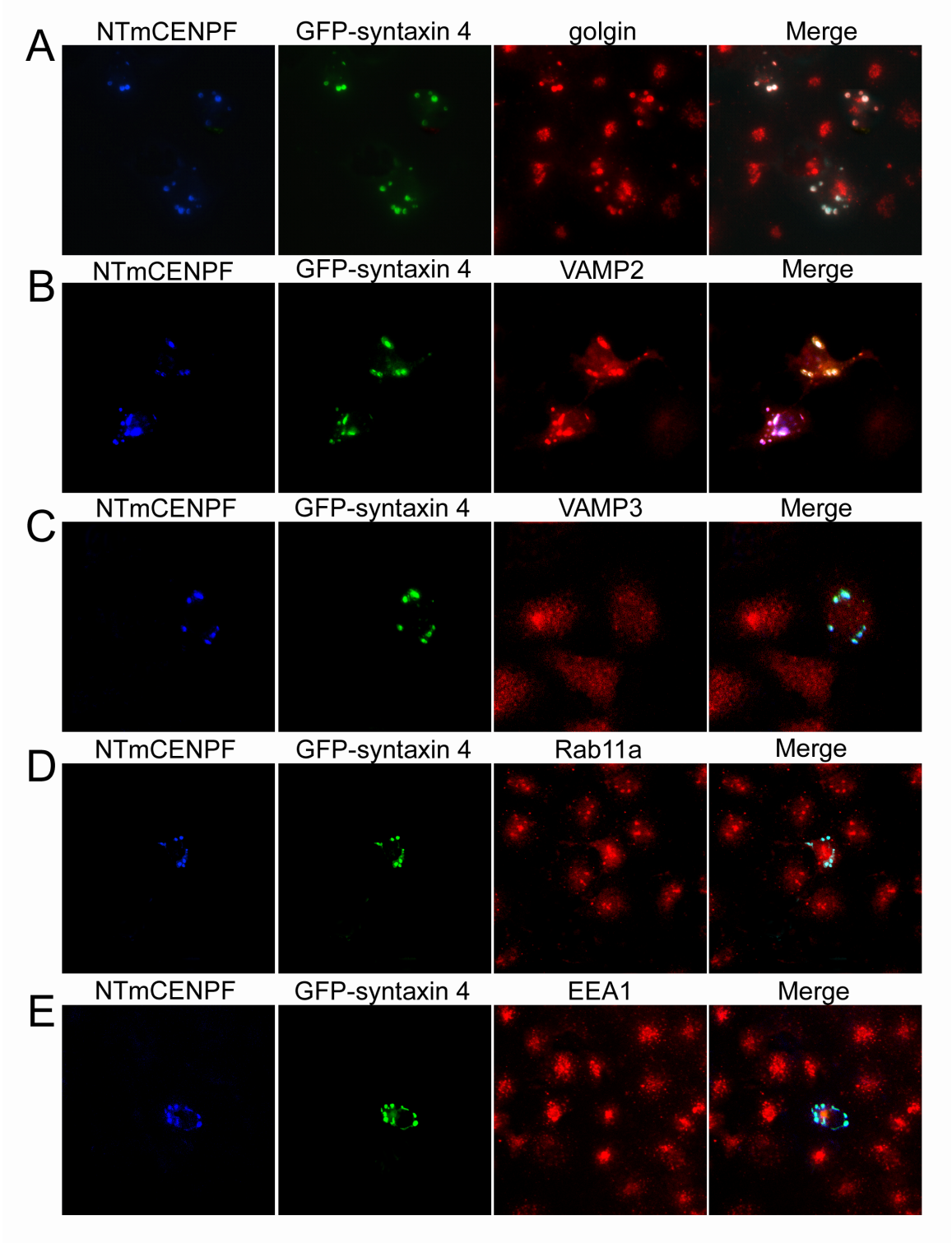
A
NTmCENPF
GFP-syntaxin 4
golgin
Merge
B
NTmCENPF
GFP-syntaxin 4
VAMP2
Merge
C
NTmCENPF
GFP-syntaxin 4
VAMP3
Merge
D
NTmCENPF
GFP-syntaxin 4
Rab11a
Merge
E
NTmCENPF
GFP-syntaxin 4
EEA1
Merge

Figure 2.5. Transiently expressed NTmCENP-F and syntaxin 4 co-localize at the TGN in COS-7 cells. COS-7 cells were co-transfected with NTmCENP-F and GFP-syntaxin 4, and only those cells expressing both transient proteins were analyzed. **A)** NTmCENP-F and GFP-syntaxin 4 co-localize with the TGN marker golgin-97. **B)** VAMP2 also demonstrates a high degree of co-localization with NTmCENP-F and GFP-syntaxin 4. **C)** VAMP3 does not demonstrate any significant redistribution to NTmCENP-F/GFP-syntaxin 4 foci. **D)** Rab11a, a marker of recycling endosomes, does not demonstrate noticeable co-localization. **E)** Early endosomes, stained by EEA1, also show no significant redistribution to NTmCENP-F/GFP-syntaxin 4 foci. Therefore, the NTmCENP-F/GFP-syntaxin 4 complex is specific for localization at the TGN. NTmCENP-F staining is indicated in blue, GFP-syntaxin 4 in green, and the third marker, as indicated, is in red (Bar, 10 μm).

Disruption of CENP-F function interferes with cell coupling

Coupling of cells is dependent, in part, on the efficient trafficking of connexin molecules to and from the cell membrane (Wei et al., 2004). Transfer of molecular dyes in cultured cells is an efficient and sensitive measure of connexin-based cell coupling (Francis et al., 2006). Dye coupling has the advantage of allowing the direct visualization of gap junction communication and function in a community of cells. For our purposes, 3T3 fibroblasts were transfected with GFP vector, GFP-syntaxin and NT-CENP-F or GFP-SNAP-25 and NT-CENP-F. Living transfected cells were identified by GFP expression and loaded with sulforhodamine101 dye (dark red cell with yellow spot, Figure 2.6A). Dye transfer from injected cell to first tier cells (those in direct contact with the injected cell) and second tier cells (those in contact with first tier cells) were quantified using established methods (Francis et al., 2006). As seen in Figure 2.6, dye is efficiently transferred to first and second tier cells after injection into control GFP transfected cells. In addition, the results in this figure demonstrate that control transfection of cells in the first and second tier cells adjacent to the injected cells have no apparent affect on cell coupling. In contrast, expression of NT-CENP-F with either GFP-labeled SNAP-25 or syntaxin 4 in the injected cell alone significantly inhibits the transfer of dye to neighboring cells, especially second tier cells (Figure 2.6A and B). Inhibition of coupling is observed with co-expression of NT-CENP-F with either syntaxin 4 or SNAP-25 even though NT-CENP-F/syntaxin 4 complexes accumulate in the TGN (Figure 2.5A) while SNAP-25/NT-CENP-F concentrates in the recycling endosome (Pooley et al.,

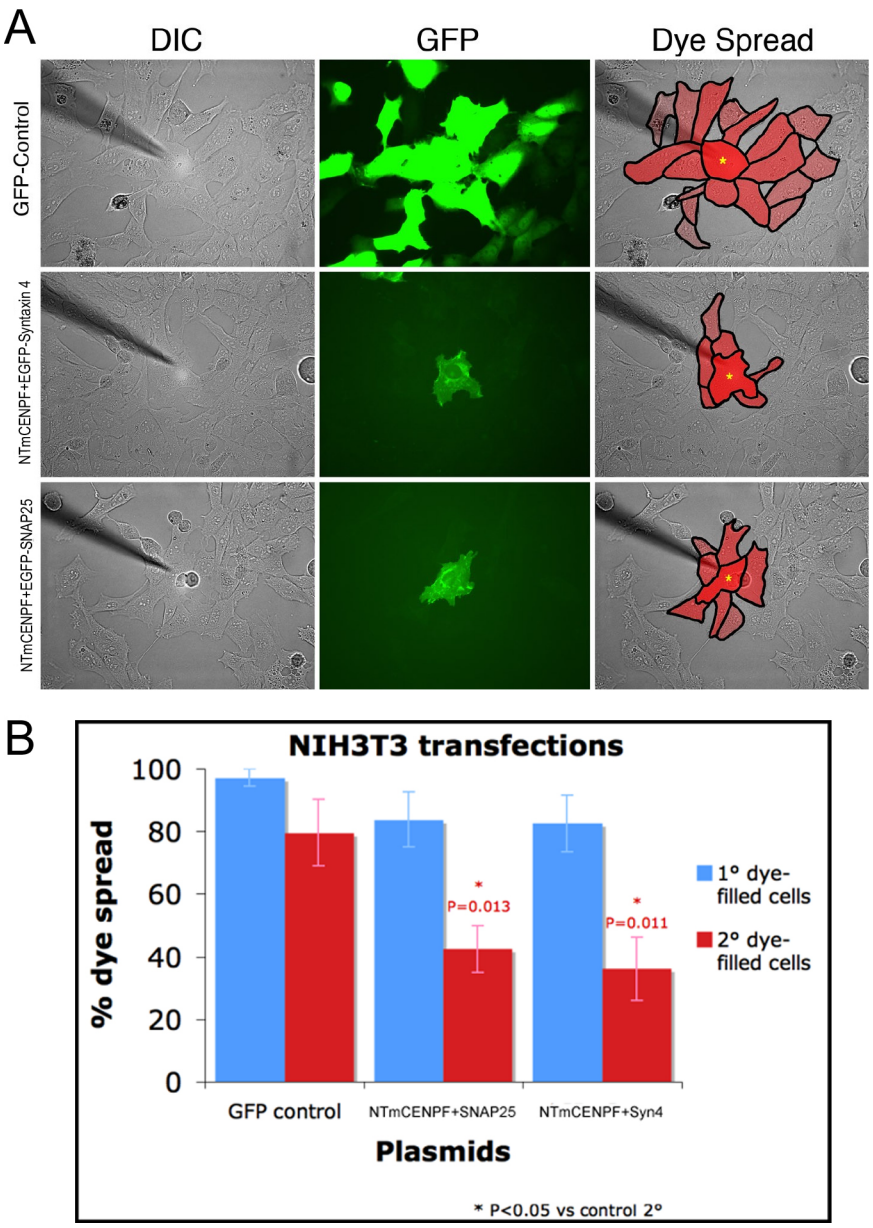

Figure 2.6. NTmCENP-F expression interferes with cell coupling. A) Cultured 3T3 fibroblasts were transfected with control GFP or NTmCENP-F and GFP-SNAP-25 or NTmCENP-F and GFP-Syntaxin 4 and living, transfected cells were loaded with sulforhodamine101 dye (dark red cell with yellow spot). The first and second tier cells were outlined to quantify transfer; first tier cells touch the injected cell while second tier cells are those dye-transferred cells not touching the injected cell. B) Percentage of dye spread was quantified according to methods described and the cells expressing NTmCENP-F showed significantly less coupling at the second tier level.

2006). Expression of NT-CENP-F alone results in the same disruption of dye transfer (data not shown). These data provide direct evidence that CENP-F function is important for proper cell coupling.

Inhibition of CENP-F function inhibits glucose transport

Syntaxin 4 has a critical role in GLUT4 trafficking in insulin-responsive tissues (Martin et al., 1998; Cain et al., 1992; Pessin et al., 1999; Volchuk et al., 1996). Insulin stimulates the translocation of intracellular GLUT4 vesicle pools to the plasma membrane in target tissues, which include cardiac myocytes, skeletal muscle, and adipose tissue. Activation of insulin receptors triggers a large increase of GLUT4 vesicle trafficking and exocytosis as compared to basal conditions. Additionally, while studies have concentrated on the function of SNAP-23 in GLUT4 trafficking, SNAP-25 has been isolated from GLUT4 positive cells (Jagadish et al, 1996). Thus, confident that this model could directly measure CENP-F function in vesicular transport, we analyzed whether inhibition of CENP-F function would inhibit GLUT4 trafficking. Briefly, 3T3-L1 cells were differentiated and CENP-F function was inhibited using MO knockdown, a method previously described by our group (Ashe et al., 2004; Soukoulis et al., 2005; Pooley et al., 2006) in conjunction with the 2-Deoxy-D-Glucose transport assay (Kawanishi et al., 2000). The level of GLUT 4 trafficking was compared between differentiated 3T3-L1 adipocyte cultures treated with control (SC) or those treated with CENP-F MO. To determine whether CENP-F MO treatment was specific for CENP-F depletion, replicate SC control and experimental MO-

treated cultures were processed for western blot analysis. Figure 2.7A demonstrates that CENP-F protein levels drop significantly with experimental but not control MO application. In contrast, levels of tubulin, syntaxin 4, GLUT4, and β-actin remain unchanged. As seen in Figure 2.7B, depletion of CENP-F resulted in a 53% reduction of 2-deoxy-D- [1,2-3H] glucose binding at the cell surface over that of control MO cultures ($p<0.01$). These results prove functional evidence that depletion of CENP-F has a direct effect on GLUT4 trafficking. As a control, SC and CENP-F MO-treated cultures were assayed for glucose uptake with and without insulin stimulation. As seen in Figure 2.7C, strong induction of glucose uptake was observed with insulin treatment in SC MO-treated cultures and this response was statistically significant in comparison to no insulin treatment ($p < 0.01$). In contrast, glucose uptake was not observed in CENP-F MO-treated cultures with or without insulin treatment. These data indicate that MO treatment alone is neither stimulatory nor inhibitory to glucose uptake.

Discussion

The CENP-F family regulates diverse cellular processes

The CENP-F family has diverse roles in cell cycle, division, and differentiation. While sequences in the C-terminus have even been shown to regulate gene expression (Ma et al., 2006; Zhou et al., 2005), many important functions associated with CENP-F are thought to be mediated through the microtubule network (Ashe et al., 2004; Dees et al., 2000; Pooley et al., 2006; Rattner et al., 1993; Soukoulis et al., 2005; Zhu et al., 1995b). For example,

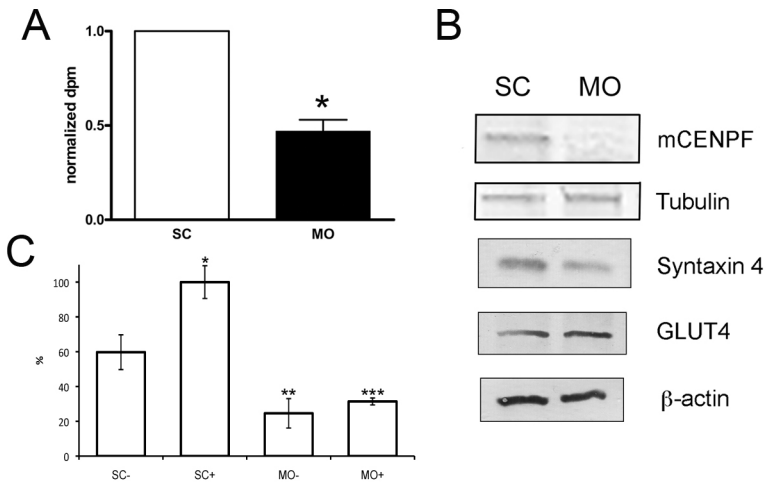

Figure 2.7. Depletion of mCENP-F alters GLUT4 trafficking. A) After 48 hours post-MO treatment, cells were processed according to described methods. Normalized to SC cell populations, cells with MO addition had a two-fold decrease in radio-labeled glucose trafficking to the plasma membrane as counted by disintegration per minute (dpm). Data are normalized against the SC counts and are shown as means + SE from three independent experiments. (*) one sample Student's t-test, $p<0.01$ vs. SC control. B) 3T3-L1 adipocytes were differentiated and depleted of mCENP-F by addition of MO. As shown previously (Ashe et al., 2004; Pooley et al., 2006; Soukoulis et al., 2005), MO addition is specific to mCENP-F depletion as demonstrated by Western blot. MO treatment also demonstrated no effect on tubulin, syntaxin 4, GLUT4, or β-actin levels. C) 3T3-L1 adipocytes were differentiated, treated with either standard control or mCENP-F MO, and assayed for glucose uptake as noted in the text. Control (SC) and experimental (MO) treatment were conducted in the presence (+) and absence (-) of insulin. Glucose uptake values were normalized to SC+ and shown as percentages of that result. There is a statistically significant difference between SC- and SC+ populations ($p < 0.01$; indicated by *), SC- and MO- populations ($p < 0.001$; indicated by **), and SC+ and MO+ populations ($p = 0.0001$; indicated by ***). There was not a statistically significant difference between the MO- and MO+ populations.

human CENP-F binds the kinetochore and is highly expressed at the G_1/S boundary (Zhu et al., 1997; Zhu et al., 1995b). The kinetochore is located at the centromere of the chromosome and serves as the site for microtubule spindle attachment during mitosis (Cleveland et al., 2003; Rieder and Salmon, 1998). Silencing of CENP-F results in misalignment of chromosomes during mitosis and premature cell death (Yang et al., 2005), demonstrating a central role for this protein in microtubule regulation of mitosis and cell division. CENP-F is also critical in the modulation of cell shape and motility. This protein directly interacts with Nde1, a regulator of dynein and microtubules (Soukoulis et al., 2005; Vergnolle and Taylor, 2007). Dynein, a microtubule-based motor, is also important for chromosome positioning and segregation through this interaction (Cleveland et al., 2003; Heald and Walczak, 1999; Sharp et al., 2000). In turn, Nde1 interacts with Lis1 in organelle positioning and movement, especially relating to developing neurons in the CNS (Feng et al., 2000; Feng and Walsh, 2004). Taken together, CENP-F family proteins demonstrate diverse roles in organelle dynamics associated with microtubule-based processes. While it is clear from this current study and previously reported data that CENP-F family proteins are involved in organelle positioning, to date, the interacting proteins and regulators of such functions are largely unknown. Through a series of experiments to identify interacting proteins, we have now determined that CENP-F provides a link between the MT network and vesicular transport.

Interaction with syntaxin 4 reveals a potentially broad role for CENP-F in vesicular transport

Using genetic, biochemical, and immunochemical analyses, we demonstrate that CENP-F has a direct interaction with syntaxin 4. This interaction is mediated through sequences in the N-terminal portion of CENP-F that are highly conserved in various vertebrate genomes (NCBI search) and predicted to form the same tertiary coiled coil structure. The highly conserved nature of these sequences, their broad distribution in vertebrate genomes, the ubiquitous nature of CENP-F expression in developing organisms, and the diversity of putative cellular function suggests a general role for this protein in cell function.

Both transiently expressed NT-CENP-F and endogenous CENP-F associate with syntaxin 4 in co-IP analyses. Furthermore, NT-CENP-F and syntaxin 4 co-localize specifically to the TGN. Expression of the truncated form of NT-CENP-F results in accumulation of this protein and syntaxin 4 in the TGN. As seen in previous studies (Rowe et al., 1999; Salaun et al., 2004; Takuma et al., 2002; Washbourne et al., 2001), exogenous expression of syntaxin 4 leads to its accumulation in the TGN (Figure 2.5). Our data demonstrate that NT-CENP-F also localizes to the TGN with the SNARE proteins SNAP-25 and VAMP2, both of which are associated with vesicular movement to and from the cell membrane. This is expected as both SNAP-25 and VAMP2 interact with syntaxin 4 (Pevsner et al., 1994). This result suggests a function for CENP-F in vesicular transport and provides a method to analyze its potential role in this basic cell activity.

Murine CENP-F is critical in regulation of vesicular transport

Previous studies on CENP-F have demonstrated its roles in mitosis and cell division (Feng et al., 2006; Hussein and Taylor, 2002; Konstantinidou et al., 2003; Liao et al., 1995; Zhou et al., 2005; Zhu et al., 1995a; Zhu et al., 1997; Zhu et al., 1995b) and even gene transcription (Ma et al., 2006; Zhou et al., 2005). Still, further in vivo and in vitro analyses of CENP-F and its binding partners suggest additional roles in cell movement and organelle positioning and translocation (Sasaki et al., 2000; Soukoulis et al., 2005; Vergnolle and Taylor, 2007). Identification of CENP-F interaction with syntaxin 4 and the dramatic redistribution of these proteins with exogenous expression of these binding partners strongly suggests a potential role in regulation of vesicular transport. To test the significance of CENP-F-syntaxin 4 interaction, we employed two different experimental interventions. First, GLUT4 assay was used as a model of plasma membrane trafficking, as syntaxin 4 is critical in GLUT4 vesicle trafficking (Foster and Klip, 2000; Thurmond et al., 1998; Watson and Pessin, 2001). In depleting cells of CENP-F, there was a significant decrease in the amount of labeled glucose recovered from 3T3-L1 adipocyte plasma membranes as compared to control groups. This is completely consistent with its role in movement of receptors to the cell surface by vesicular transport (Foster and Klip, 2000; Thurmond et al., 1998; Watson and Pessin, 2001). In addition, the inhibition of dye transfer between cells is a model to test the integrity of cell coupling after disruption of CENP-F function by directly assaying for gap junction function at the

cell surface (Francis and Lo, 2006; Lauf et al., 2002; Moskalewski et al., 1994). Our analyses show that disruption of CENP-F function significantly diminished dye transfer between treated cells and clearly demonstrates inhibition of gap junction activity at the cell surface, resulting from mis-regulated protein trafficking to the cell membrane. Taken together with our previous work, the current data predict a broad role for CENP-F in vesicular transport.

References

Aikawa, Y., Xia, X. and Martin, T. F. (2006). SNAP25, but not syntaxin 1A, recycles via an ARF6-regulated pathway in neuroendocrine cells. *Mol Biol Cell* **17**, 711-22.

Altschul, S. F., Gish, W., Miller, W., Myers, E. W. and Lipman, D. J. (1990). Basic local alignment search tool. *J Mol Biol* **215**, 403-10.

Ashe, M., Pabon-Pena, L., Dees, E., Price, K. L. and Bader, D. (2004). LEK1 is a potential inhibitor of pocket protein-mediated cellular processes. *J Biol Chem* **279**, 664-76.

Bajohrs, M., Darios, F., Peak-Chew, S. Y. and Davletov, B. (2005). Promiscuous interaction of SNAP-25 with all plasma membrane syntaxins in a neuroendocrine cell. *Biochem J* **392**, 283-9.

Band, A. M., Ali, H., Vartiainen, M. K., Welti, S., Lappalainen, P., Olkkonen, V. M. and Kuismanen, E. (2002). Endogenous plasma membrane t-SNARE syntaxin 4 is present in rab11 positive endosomal membranes and associates with cortical actin cytoskeleton. *FEBS Lett* **531**, 513-9.

Banfield, D. K., Lewis, M. J., Rabouille, C., Warren, G. and Pelham, H. R. (1994). Localization of Sed5, a putative vesicle targeting molecule, to the cis-Golgi network involves both its transmembrane and cytoplasmic domains. *Journal of Cell Biology* **127**, 357-71.

Banks, J. D. and Heald, R. (2001). Chromosome movement: dynein-out at the kinetochore. *Curr Biol* **11**, R128-31.

Bryant, N. J., Govers, R. and James, D. E. (2002). Regulated transport of the glucose transporter GLUT4. *Nat Rev Mol Cell Biol* **3**, 267-77.

Cain, C. C., Trimble, W. S. and Lienhard, G. E. (1992). Members of the VAMP family of synaptic vesicle proteins are components of glucose transporter-containing vesicles from rat adipocytes. *J Biol Chem* **267**, 11681-4.

Caviston, J. P. and Holzbaur, E. L. (2006). Microtubule motors at the intersection of trafficking and transport. *Trends Cell Biol* **16**, 530-7.

Chen, Y. A. and Scheller, R. H. (2001). SNARE-mediated membrane fusion. *Nat Rev Mol Cell Biol* **2**, 98-106.

Clark, G. M., Allred, D. C., Hilsenbeck, S. G., Chamness, G. C., Osborne, C. K., Jones, D. and Lee, W. H. (1997). Mitosin (a new proliferation marker) correlates with clinical outcome in node-negative breast cancer. *Cancer Res* **57**, 5505-8.
Cleveland, D. W., Mao, Y. and Sullivan, K. F. (2003). Centromeres and kinetochores: from epigenetics to mitotic checkpoint signaling. *Cell* **112**, 407-21.
Dees, E., Pabon-Pena, L. M., Goodwin, R. L. and Bader, D. (2000). Characterization of CMF1 in avian skeletal muscle. *Dev Dyn* **219**, 169-81.
Faulkner, N. E., Dujardin, D. L., Tai, C. Y., Vaughan, K. T., O'Connell, C. B., Wang, Y. and Vallee, R. B. (2000). A role for the lissencephaly gene LIS1 in mitosis and cytoplasmic dynein function. *Nat Cell Biol* **2**, 784-91.
Feng, J. (2006). Microtubule: a common target for parkin and Parkinson's disease toxins. *Neuroscientist* **12**, 469-76.
Feng, J., Huang, H. and Yen, T. J. (2006). CENP-F is a novel microtubule-binding protein that is essential for kinetochore attachments and affects the duration of the mitotic checkpoint delay. *Chromosoma* **115**, 320-9.
Feng, Y., Olson, E. C., Stukenberg, P. T., Flanagan, L. A., Kirschner, M. W. and Walsh, C. A. (2000). LIS1 regulates CNS lamination by interacting with mNudE, a central component of the centrosome. *Neuron* **28**, 665-79.
Feng, Y. and Walsh, C. A. (2004). Mitotic spindle regulation by Nde1 controls cerebral cortical size. *Neuron* **44**, 279-93.
Foster, L. J. and Klip, A. (2000). Mechanism and regulation of GLUT-4 vesicle fusion in muscle and fat cells. *Am J Physiol Cell Physiol* **279**, C877-90.
Francis, R. J. and Lo, C. W. (2006). Primordial germ cell deficiency in the connexin 43 knockout mouse arises from apoptosis associated with abnormal p53 activation. *Development* **133**, 3451-60.
Frost, S. C. and Lane, M. D. (1985). Evidence for the involvement of vicinal sulfhydryl groups in insulin-activated hexose transport by 3T3-L1 adipocytes. *J Biol Chem* **260**, 2646-52.
Gibbons, I. R. (1996). The role of dynein in microtubule-based motility. *Cell Struct Funct* **21**, 331-42.
Goodwin, R. L., Pabon-Pena, L. M., Foster, G. C. and Bader, D. (1999). The cloning and analysis of LEK1 identifies variations in the LEK/centromere protein F/mitosin gene family. *J Biol Chem* **274**, 18597-604.
Heald, R. and Walczak, C. E. (1999). Microtubule-based motor function in mitosis. *Curr Opin Struct Biol* **9**, 268-74.
Hehnly, H. and Stamnes, M. (2007). Regulating cytoskeleton-based vesicle motility. *FEBS Lett* **581**, 2112-8.
Hussein, D. and Taylor, S. S. (2002). Farnesylation of Cenp-F is required for G2/M progression and degradation after mitosis. *J Cell Sci* **115**, 3403-14.
Ishiki, M. and Klip, A. (2005). Minireview: recent developments in the regulation of glucose transporter-4 traffic: new signals, locations, and partners. *Endocrinology* **146**, 5071-8.
Ishiki, M., Randhawa, V. K., Poon, V., Jebailey, L. and Klip, A. (2005). Insulin regulates the membrane arrival, fusion, and C-terminal unmasking of glucose

transporter-4 via distinct phosphoinositides. *Journal of Biological Chemistry* **280**, 28792-802.
Jagadish, M.N., et al., Insulin-responsive tissues contain the core complex protein SNAP-25 (synaptosomal-associated protein 25) A and B isoforms in addition to syntaxin 4 and synaptobrevins 1 and 2. Biochem J, 1996. **317 (Pt 3)**: p. 945-54
Jahn, R. and Sudhof, T. C. (1999). Membrane fusion and exocytosis. *Annu Rev Biochem* **68**, 863-911.
Kawanishi, M., et al., Role of SNAP23 in insulin-induced translocation of GLUT4 in 3T3-L1 adipocytes. Mediation of complex formation between syntaxin4 and VAMP2. J Biol Chem, 2000. **275**(11): p. 8240-7.
Kockx, M., Guo, D. L., Huby, T., Lesnik, P., Kay, J., Sabaretnam, T., Jary, E., Hill, M., Gaus, K., Chapman, J. et al. (2007). Secretion of apolipoprotein E from macrophages occurs via a protein kinase A and calcium-dependent pathway along the microtubule network. *Circulation Research* **101**, 607-16.
Kondratova, A. A., Neznanov, N., Kondratov, R. V. and Gudkov, A. V. (2005). Poliovirus protein 3A binds and inactivates LIS1, causing block of membrane protein trafficking and deregulation of cell division. *Cell Cycle* **4**, 1403-10.
Konstantinidou, A. E., Korkolopoulou, P., Kavantzas, N., Mahera, H., Thymara, I., Kotsiakis, X., Perdiki, M., Patsouris, E. and Davaris, P. (2003). Mitosin, a novel marker of cell proliferation and early recurrence in intracranial meningiomas. *Histol Histopathol* **18**, 67-74.
Lauf, U., Giepmans, B. N., Lopez, P., Braconnot, S., Chen, S. C. and Falk, M. M. (2002). Dynamic trafficking and delivery of connexons to the plasma membrane and accretion to gap junctions in living cells. *Proc Natl Acad Sci U S A* **99**, 10446-51.
Liang, Y., Yu, W., Li, Y., Yang, Z., Yan, X., Huang, Q. and Zhu, X. (2004). Nudel functions in membrane traffic mainly through association with Lis1 and cytoplasmic dynein. *J Cell Biol* **164**, 557-66.
Liao, H., Winkfein, R. J., Mack, G., Rattner, J. B. and Yen, T. J. (1995). CENP-F is a protein of the nuclear matrix that assembles onto kinetochores at late G2 and is rapidly degraded after mitosis. *J Cell Biol* **130**, 507-18.
Ma, L., Zhao, X. and Zhu, X. (2006). Mitosin/CENP-F in mitosis, transcriptional control, and differentiation. *J Biomed Sci* **13**, 205-13.
Mallard, F., Tang, B. L., Galli, T., Tenza, D., Saint-Pol, A., Yue, X., Antony, C., Hong, W., Goud, B. and Johannes, L. (2002). Early/recycling endosomes-to-TGN transport involves two SNARE complexes and a Rab6 isoform. *J Cell Biol* **156**, 653-64.
Martin, L. B., Shewan, A., Millar, C. A., Gould, G. W. and James, D. E. (1998). Vesicle-associated membrane protein 2 plays a specific role in the insulin-dependent trafficking of the facilitative glucose transporter GLUT4 in 3T3-L1 adipocytes. *J Biol Chem* **273**, 1444-52.
Martin, S., Tellam, J., Livingstone, C., Slot, J. W., Gould, G. W. and James, D. E. (1996). The glucose transporter (GLUT-4) and vesicle-associated membrane protein-2 (VAMP-2) are segregated from recycling endosomes in insulin-sensitive cells. *J Cell Biol* **134**, 625-35.

McMahon, H. T., Ushkaryov, Y. A., Edelmann, L., Link, E., Binz, T., Niemann, H., Jahn, R. and Sudhof, T. C. (1993). Cellubrevin is a ubiquitous tetanus-toxin substrate homologous to a putative synaptic vesicle fusion protein. *Nature* **364**, 346-9.
Miyamoto, Y., Yamauchi, J., Tanoue, A., Wu, C. and Mobley, W. C. (2006). TrkB binds and tyrosine-phosphorylates Tiam1, leading to activation of Rac1 and induction of changes in cellular morphology. *Proc Natl Acad Sci U S A* **103**, 10444-9.
Moskalewski, S., Popowicz, P. and Thyberg, J. (1994). Functions of the Golgi complex in cell division: formation of cell-matrix contacts and cell-cell communication channels in the terminal phase of cytokinesis. *J Submicrosc Cytol Pathol* **26**, 9-20.
Pabon-Pena, L. M., Goodwin, R. L., Cise, L. J. and Bader, D. (2000). Analysis of CMF1 reveals a bone morphogenetic protein-independent component of the cardiomyogenic pathway. *J Biol Chem* **275**, 21453-9.
Pessin, J. E., Thurmond, D. C., Elmendorf, J. S., Coker, K. J. and Okada, S. (1999). Molecular basis of insulin-stimulated GLUT4 vesicle trafficking. Location! Location! Location! *J Biol Chem* **274**, 2593-6.
Pevsner, J., Hsu, S. C., Braun, J. E., Calakos, N., Ting, A. E., Bennett, M. K. and Scheller, R. H. (1994). Specificity and regulation of a synaptic vesicle docking complex. *Neuron* **13**, 353-61.
Pooley, R. D., Reddy, S., Soukoulis, V., Roland, J. T., Goldenring, J. R. and Bader, D. M. (2006). CytLEK1 is a regulator of plasma membrane recycling through its interaction with SNAP-25. *Mol Biol Cell* **17**, 3176-86.
Quinones, B., Riento, K., Olkkonen, V. M., Hardy, S. and Bennett, M. K. (1999). Syntaxin 2 splice variants exhibit differential expression patterns, biochemical properties and subcellular localizations. *J Cell Sci* **112**, 4291-304.
Rattner, J. B., Rao, A., Fritzler, M. J., Valencia, D. W. and Yen, T. J. (1993). CENP-F is a .ca 400 kDa kinetochore protein that exhibits a cell-cycle dependent localization. *Cell Motil Cytoskeleton* **26**, 214-26.
Rieder, C. L. and Salmon, E. D. (1998). The vertebrate cell kinetochore and its roles during mitosis. *Trends Cell Biol* **8**, 310-8.
Rowe, J., Corradi, N., Malosio, M. L., Taverna, E., Halban, P., Meldolesi, J. and Rosa, P. (1999). Blockade of membrane transport and disassembly of the Golgi complex by expression of syntaxin 1A in neurosecretion-incompetent cells: prevention by rbSEC1. *J Cell Sci* **112 (Pt 12)**, 1865-77.
Salaun, C., James, D. J., Greaves, J. and Chamberlain, L. H. (2004). Plasma membrane targeting of exocytic SNARE proteins. *Biochim Biophys Acta* **1693**, 81-9.
Sasaki, S., Shionoya, A., Ishida, M., Gambello, M. J., Yingling, J., Wynshaw-Boris, A. and Hirotsune, S. (2000). A LIS1/NUDEL/cytoplasmic dynein heavy chain complex in the developing and adult nervous system. *Neuron* **28**, 681-96.
Schnapp, B. J. (2003). Trafficking of signaling modules by kinesin motors. *J Cell Sci* **116**, 2125-35.
Sharp, D. J., Rogers, G. C. and Scholey, J. M. (2000). Microtubule motors in mitosis. *Nature* **407**, 41-7.

Smith, D. S., Niethammer, M., Ayala, R., Zhou, Y., Gambello, M. J., Wynshaw-Boris, A. and Tsai, L. H. (2000). Regulation of cytoplasmic dynein behaviour and microtubule organization by mammalian Lis1. *Nat Cell Biol* **2**, 767-75.
Soldati, T. and Schliwa, M. (2006). Powering membrane traffic in endocytosis and recycling. *Nature Reviews Molecular Cell Biology* **7**, 897-908.
Sollner, T., Whiteheart, S. W., Brunner, M., Erdjument-Bromage, H., Geromanos, S., Tempst, P. and Rothman, J. E. (1993). SNAP receptors implicated in vesicle targeting and fusion. *Nature* **362**, 318-24.
Soukoulis, V., Reddy, S., Pooley, R. D., Feng, Y., Walsh, C. A. and Bader, D. M. (2005). Cytoplasmic LEK1 is a regulator of microtubule function through its interaction with the LIS1 pathway. *Proc Natl Acad Sci U S A* **102**, 8549-54.
Takuma, T., Arakawa, T., Okayama, M., Mizoguchi, I., Tanimura, A. and Tajima, Y. (2002). Trafficking of green fluorescent protein-tagged SNARE proteins in HSY cells. *J Biochem* **132**, 729-35.
Terada, S., Nakata, T., Peterson, A. C. and Hirokawa, N. (1996). Visualization of slow axonal transport in vivo. *Science* **273**, 784-8.
Thurmond, D. C., Ceresa, B. P., Okada, S., Elmendorf, J. S., Coker, K. and Pessin, J. E. (1998). Regulation of insulin-stimulated GLUT4 translocation by Munc18c in 3T3L1 adipocytes. *J Biol Chem* **273**, 33876-83.
Tortorella, L. L. and Pilch, P. F. (2002). C2C12 myocytes lack an insulin-responsive vesicular compartment despite dexamethasone-induced GLUT4 expression. *Am J Physiol Endocrinol Metab* **283**, E514-24.
Vedrenne, C. and Hauri, H. P. (2006). Morphogenesis of the endoplasmic reticulum: beyond active membrane expansion. *Traffic* **7**, 639-46.
Vergnolle, M. A. and Taylor, S. S. (2007). Cenp-F links kinetochores to Ndel1/Nde1/Lis1/dynein microtubule motor complexes. *Curr Biol* **17**, 1173-9.
Volchuk, A., Wang, Q., Ewart, H. S., Liu, Z., He, L., Bennett, M. K. and Klip, A. (1996). Syntaxin 4 in 3T3-L1 adipocytes: regulation by insulin and participation in insulin-dependent glucose transport. *Mol Biol Cell* **7**, 1075-82.
Washbourne, P., Cansino, V., Mathews, J. R., Graham, M., Burgoyne, R. D. and Wilson, M. C. (2001). Cysteine residues of SNAP-25 are required for SNARE disassembly and exocytosis, but not for membrane targeting. *Biochem J* **357**, 625-34.
Watson, R. T. and Pessin, J. E. (2001). Transmembrane domain length determines intracellular membrane compartment localization of syntaxins 3, 4, and 5. *Am J Physiol Cell Physiol* **281**, C215-23.
Wei, C. J., Xu, X. and Lo, C. W. (2004). Connexins and cell signaling in development and disease. *Annu Rev Cell Dev Biol* **20**, 811-38.
Wilcke, M., Johannes, L., Galli, T., Mayau, V., Goud, B. and Salamero, J. (2000). Rab11 regulates the compartmentalization of early endosomes required for efficient transport from early endosomes to the trans-golgi network. *J Cell Biol* **151**, 1207-20.
Wu, C., Ramirez, A., Cui, B., Ding, J., Delcroix, J. D., Valletta, J. S., Liu, J. J., Yang, Y., Chu, S. and Mobley, W. C. (2007). A functional dynein-microtubule

network is required for NGF signaling through the Rap1/MAPK pathway. *Traffic* **8**, 1503-20.
Xiang, X., Zuo, W., Efimov, V. P. and Morris, N. R. (1999). Isolation of a new set of Aspergillus nidulans mutants defective in nuclear migration. *Curr Genet* **35**, 626-30.
Yang, Z., Guo, J., Chen, Q., Ding, C., Du, J. and Zhu, X. (2005). Silencing mitosin induces misaligned chromosomes, premature chromosome decondensation before anaphase onset, and mitotic cell death. *Mol Cell Biol* **25**, 4062-74.
Zheng, H., McKay, J. and Buss, J. E. (2007). H-Ras does not need COP I- or COP II-dependent vesicular transport to reach the plasma membrane. *Journal of Biological Chemistry* **282**, 25760-8.
Zhou, X., Wang, R., Fan, L., Li, Y., Ma, L., Yang, Z., Yu, W., Jing, N. and Zhu, X. (2005). Mitosin/CENP-F as a negative regulator of activating transcription factor-4. *J Biol Chem* **280**, 13973-7.
Zhu, X., Chang, K. H., He, D., Mancini, M. A., Brinkley, W. R. and Lee, W. H. (1995a). The C terminus of mitosin is essential for its nuclear localization, centromere/kinetochore targeting, and dimerization. *J Biol Chem* **270**, 19545-50.
Zhu, X., Ding, L. and Pei, G. (1997). Carboxyl terminus of mitosin is sufficient to confer spindle pole localization. *J Cell Biochem* **66**, 441-9.
Zhu, X., Mancini, M. A., Chang, K. H., Liu, C. Y., Chen, C. F., Shan, B., Jones, D., Yang-Feng, T. L. and Lee, W. H. (1995b). Characterization of a novel 350-kilodalton nuclear phosphoprotein that is specifically involved in mitotic-phase progression. *Mol Cell Biol* **15**, 5017-29.

CHAPTER III

MURINE CENP-F REGULATES CENTROSOMAL MICROTUBULE NUCLEATION AND INTERACTS WITH HOOK2 AT THE CENTROSOME

This chapter is published under the same title in *Molecular Biology of the Cell*, November, 2009 (Moynihan et al., 2009).

Abstract

The microtubule network (MT) is essential in a broad spectrum of cellular functions. Many studies have linked CENP-F to MT-based activities as disruption of this protein leads to major changes in MT structure and function. Still the basis of CENP-F regulation of the MT network remains elusive. Here, our studies reveal a completely novel and critical localization and role for CENP-F at the centrosome, the major MT organizing center (MTOC) of the cell. Using a yeast two-hybrid screen, we identify Hook2, a linker protein that is essential for regulation of the MT network at the centrosome, as a binding partner of CENP-F. With recently developed immunochemical reagents, we confirm this interaction and reveal the novel localization of CENP-F at the centrosome. Importantly, in this first report of CENP-F$^{-/-}$ cells, we demonstrate that ablation of CENP-F protein function eliminates MT repolymerization after standard nocodazole treatment. This inhibition of MT regrowth is centrosome-specific as MT repolymerization is readily observed from the Golgi in CENP-F$^{-/-}$ cells. The centrosome-specific function of CENP-F in the regulation of MT growth is

confirmed by expression of truncated CENP-F containing only the Hook2-binding domain. Further, analysis of partially reconstituted MTOC asters in cells that escape complete repolymerization block, we show that disruption of CENP-F function impacts MT nucleation and anchoring rather than promoting catastrophe. Our studies reveal a major new localization and function of CENP-F at the centrosome that is likely to impact a broad array of MT-based actions in the cell.

Introduction

Characterization of CENP-F has revealed many different domains, binding partners, and functions. The large size of this protein lends itself to a multifaceted role within the cell and the orthologs studied in different species show significant variation in overall function and localization. Initially, CENP-F was visualized at the kinetochore (KT), the attachment point for MT at the centromere (Rattner *et al.*, 1993). KT function of CENP-F has not yet been completely elucidated, but knockdown of CENP-F leads to mitotic delay, decreased KT tension, and MT instability (Bomont et al., 2005; Feng et al., 2006; Holt et al., 2005; Laoukili et al., 2005; Yang et al., 2005). Furthermore, the farnesylation site located at the extreme carboxyl terminus is necessary for KT targeting of CENP-F (Ashar *et al.*, 2000; Hussein and Taylor, 2002) and KT localization of CENP-F is also vital to normal KT recruitment of CENP-E and $p150^{glued}$(Yang *et al.*, 2005). The diversity of function within the C terminus of CENP-F is further illustrated by the recent characterization of its binding partner nucleoporin protein Nup133, an integral

component of the nuclear pore complex (Zuccolo *et al.*, 2007). Moreover, within the carboxyl terminus resides an E2F1-like Rb-binding domain that interacts with not only Rb, but also other pocket proteins p107 and p130 (Ashe *et al.*, 2004). Recently, analysis of the avian ortholog demonstrated that interaction with Rb is important for myogenic differentiation (Robertson *et al.*, 2008). CENP-F was initially identified as an Rb-binding protein (Zhu *et al.*, 1995b) and mutation of this site results in impaired differentiation of myotubes and reduced contractile protein expression (Robertson *et al.*, 2008). Finally, the C-terminus of CENP-F, the focus of the majority of studies on this protein, has also been established as a negative regulator of the transcription factor ATF-4 (Zhou *et al.*, 2005). All of these functions are nuclear and are attributed to domains of CENP-F adjacent to the C-terminal NLS characterized by Zhu, et al. (Zhu *et al.*, 1995a). However, given the substantial size of CENP-F and other predicted structural and interactive domains throughout the molecule, this nuclear region governs only a subset of functions of this protein.

Previous studies have also characterized cytoplasmic localization and function of CENP-F (Pooley et al., 2008; Pooley et al., 2006; Soukoulis et al., 2005; Vergnolle and Taylor, 2007). CENP-F contains a spectrin repeat region central to the C-terminus and adjacent to these repeats is the Nde1/Ndel1 binding domain originally identified by Soukoulis, et al. (Soukoulis *et al.*, 2005) and confirmed by Vergnolle and Taylor (Vergnolle and Taylor, 2007). This interaction domain regulates MT network organization through Nde1/Ndel1

interaction with the LIS1 pathway. Additionally, both termini of CENP-F have tubulin binding capabilities and the C terminus domain is capable of tubulin polymerization *in vitro* (Feng *et al.*, 2006). Moreover, the N-terminus of CENP-F has been shown to bind SNARE proteins SNAP25 and syntaxin 4, linking MTs to vesicles in the regulation of protein trafficking (Pooley et al., 2008; Pooley et al., 2006). These interactions with tubulin and the MT network further support additional functions of CENP-F in the cytoplasm.

Many studies have linked CENP-F to MT-based activities as disruption of this protein leads to major changes in MT structure and function. Still, the basis of CENP-F regulation of the MT network remains elusive. Here, our studies reveal a novel role for CENP-F at the centrosome, the major MT organizing center (MTOC) of the cell. We demonstrate that Hook2, a newly identified centrosomal protein that is essential for centrosomal regulation of the MT network, as a binding partner of CENP-F. Using novel immunochemical reagents, we confirm this interaction and establish the localization of CENP-F at the centrosome. Importantly, we demonstrate that ablation of CENP-F in newly developed CENP-F$^{-/-}$ cells dramatically attenuates MT repolymerization after standard nocodazole treatment. Further, this effect is centrosome-specific as MT repolymerization is readily observed from the Golgi in CENP-F$^{-/-}$ cells. This centrosome-specific function of CENP-F is confirmed by expression of the Hook2-binding domain in CENP-F (NT-CENP-F). From analysis of NT-CENP-F-expressing cells where partially reconstituted MTOC asters are observed, we

show that disruption of CENP-F function impacts MT nucleation and anchoring rather than promoting catastrophe. Thus, our studies reveal a major new function of CENP-F at the centrosome that is likely to impact a broad array of MT-based actions in the cell.

Materials and Methods

Yeast two-hybrid (Y2H) screen

The large N-terminal region of cytoplasmic murine CENP-F (amino acids 1-689, termed "LCR"), was used as bait in a Y2H screen performed using our published methods with the Matchmaker Y2H System 3 (BD Biosciences Clontech, San Jose, CA) (Pooley *et al.*, 2008). The bait was mated with a yeast strain pretransformed with a whole mouse embryonic day 17.5 cDNA library. Library plasmids were isolated from yeast colonies that survived on Quadruple Dropout Medium (QDO; SD/-Ade/-His/-Leu/-Trp/X-a-Gal) and exhibited *lacZ* expression. The inserts were then sequenced by the Vanderbilt Sequencing Core Facility and identified using NCBI Blast (Altschul and Lipman, 1990). A series of truncations of each of protein were constructed by PCR and transformed into appropriate yeast strains. Yeast were grown and plated on QDO medium; positive associations grew and exhibited blue color upon Gal testing. Positive control growth was indicated by yeast transformed with pGBKT7–53 and pGADT7-T and the negative control utilized yeast expressing pGBTK-53 and the empty vector pGADT7. False positive tests with empty vector and random protein

matings were conducted to eliminate spurious interactions according to manufacturer's recommendations.

Antibodies

A novel polyclonal murine CENPF antibody was generated in rabbits from the peptide NTNKHSMSATD (aa1122-1132; Biosynthesis). Antisera were affinity purified using the injected peptide and a SulfoLink kit (Pierce). The polyclonal Hook2 antibody (epitope aa 427-719) was a generous gift from Dr. Helmut Kramer, UT Southwestern. Gamma and β-tubulin antibodies were obtained from Sigma, myc and GFP antibodies were obtained from BD Biosciences. The ninein, pericentrin, centrin1, and MT network marker YL1/2 antibodies were purchased from Abcam. The PCM-1 antibody was from Novus Biological. Alexa Fluor 488- and 568-conjugated secondary antibodies were also utilized (Molecular Probes). For primary-antibody direct labeling immunofluorescence studies, polyclonal anti-CENP-F was directly labeled with the Zenon Alexa-488 labeling kit (Molecular Probes). Alkaline phosphatase-conjugated secondary antibodies for western blot were also purchased from Sigma.

Cell culture, transfection, and DNA constructs

COS-7 (ATCC), 3T3 (ATCC), mouse embryonic fibroblasts (MEFs), RPE (Clontech), and C2C12 cells (ATCC) were maintained in Dulbecco's Modified Eagle's Medium (Hyclone) supplemented with 10, 10, 10, and 20% FBS respectively, 100 ug/mL penicillin/streptomycin, and L- glutamine, in a 5% CO_2

atmosphere at 37°C. For transfection, cells were grown to 50-75% confluency and transfected with DNA using FuGENE 6 according to manufacturer's recommendations (Roche). Full length Hook2 cDNA (Invitrogen) was cloned into the pEGFP-C3 vector. This construct was then used as the PCR template for the truncation constructs, which were cloned into the manufactured yeast vector for Y2H analysis. NT-CENP-F was constructed by cloning the N-terminal 474 amino acids of CENP-F in frame into the pCMV-myc, pCerulean, and the pEGFP-C1 vectors (BD Biosciences, Clontech). The 3GFP-EMTB construct was a kind gift of Dr. J.C. Bulinski (Columbia University, New York).

Immunostaining, microtubule assays, and microscopy

For studies of transiently transfected protein expression and analysis of endogenous protein localization, cells were gently washed with 1X PBS and fixed for 20 minutes at room temperature with either 4% paraformaldehyde to visualize directly labeled antibodies or with 70% methanol at room temperature to visualize all other proteins. Cells used for γ-tubulin labeling were fixed at -20°C. Subsequently, cells were washed with 1X PBS, permeabilized with 0.25% Triton X-100 in 1X PBS for 10 minutes, and blocked for 1 hour in 2% BSA in 1X PBS at room temperature. Primary antibodies were incubated overnight at 4°C. Cells were then washed 3 times in 1X PBS and incubated with secondary antibodies for 1 hour at room temperature. Cells were again washed 3 times with 1X PBS and coverslips mounted with Poly AquaMount (PolySciences).

For MT repolymerization assays, cells were incubated with nocodazole (Sigma) for 2 hours (2.5ug/mL in culture medium). Cells were then washed 3 times with fresh culture medium and held in fresh medium at 37 degrees to allow repolymerization for a specific time period, dependent on the experiment. Cells were then washed once with PHEM buffer (60 mM PIPES, 25 mM HEPES, 10 mM EGTA, 3 mM MgCl2 pH 6.8) and treated for 1 min with 0.5% Triton-X in PHEM buffer before fixations, as described above.

Cells were visualized by fluorescence microscopy with an AX70 (Olympus) or a LSM510 (Zeiss) microscope for confocal analysis. Widefield images were captured using Nikon Elements Basic Science software and confocal images with Laser Scanning Microscope ZEN LE (Zeiss). Additional widefield images were captured with an Olympus IX71 inverted microscope and a CoolSNAP-HQ2 CCD camera (Photometrics), in a temperature and CO2-controlled WeatherStation (Precision Control) as part of the DeltaVision platform (Applied Precision) and deconvolved with the SoftWorx software included in the DeltaVision core. Image processing with performed with Photoshop, contrasting with histrogram stretching and using gamma correction in MT images to ensure visualization of all MTs. All images of control and experimental cells were processed identically. Statistical analysis of MTOC reformation in COS-7 cells was done with the Student's T-test and the incomplete MT repolymerization statistical analysis was performed with the G test.

In live imaging studies of MT regrowth, cells were initially positioned and recorded in nocodazole medium before they were washed with new culture medium on the microscope stage for repolymerization. Live imaging experiments used cells plated on MatTek glass bottom dishes. A heated stage (Warner Instruments) maintained cultures at 37°C. IPLab software (Scanalytics) was used to capture images on a Nikon TE2000E inverted microscope (CFI PLAN APO VC 100× oil lens, NA 1.4, with or without 1.5× intermediate magnification) with an automated focusing device (PerfectFocus), Yokogawa QLC-100/CSU-10 spinning disk head (Visitec assembled by Vashaw), and a back-illuminated EM-CCD camera Cascade 512B (Photometrics). A krypton-argon laser (75 mW 488/568; Melles Griot) with AOTF was used for two-color excitation. Custom double dichroic mirror and filters (Chroma) in a filter wheel (Ludl) were used in the emission light path (Efimov *et al.*, 2007).

Co-immunoprecipitation using transient transfections and endogenous proteins

Transfected COS-7 cells were grown on 10 cm plates; lysates were harvested 48 hours post transfection. The ProFound Mammalian c-Myc Tag Co-IP Kit (Pierce) was utilized according to previous methods established by our laboratory (Pooley et al., 2008). Briefly, cells were washed once with ice-cold TBS, incubated with M-Per Extraction Reagent (Pierce) containing protease inhibitor (11 697 498 001, Roche), and centrifuged at 16,000 X g for 20 minutes at 4°C. Protein lysate concentration of the supernatant was determined using a bicinchoninic acid solution assay (Pierce); 100 µg total lysate was incubated for

two hours with gentle shaking at 4°C with 10 µL anti-c-myc agarose slurry. Columns were washed 3 times with 1X TBS-Tween. Protein was eluted with 2X non-reducing sample buffer (Pierce) at 95°C for 5 minutes. To reduce proteins for SDS-PAGE analysis and western blot analysis, 2 µL 2-mercaptoethanol was added. Ten µL of total lysate supernatant was used to confirm protein expression. Blots were developed using NBT-BCIP (Roche) and scanned into digital images (Hewlett-Packard).

For analysis of endogenous protein-protein interaction, Dynabeads Protein G (Invitrogen) were washed 3x with citrate phosphate buffer, incubated with CENPF antibody for 1 hour at RT, and washed again. C2C12 cells were lysed with NP-40 buffer with gentle sonication. Whole cell lysates were recovered and incubated with antibody-Dynabead complexes for 1 hour at 4°C. The Dynabead magnet apparatus was used to wash with cold 1X PBS 3x and proteins were eluted with Laemmli sample buffer at a boiling temperature for 5 minutes. Proteins were resolved on a 10% SDS-PAGE gel after addition of β-mercaptoethanol and analyzed by western blot analysis. Twenty µg of protein lysate was loaded to visualize Hook2 in whole cell lysate.

Isolation of mouse embryonic fibroblasts (MEFs)

Embryos from a CENP-F$^{-/WT}$ x CENP-F$^{-/WT}$ cross were isolated from the uteri of 13.5-day-pregnant females, washed with PBS, and the head and visceral organs were dissected out. The remainder of the embryos were washed with

PBS and finely minced before placement into individual tubes with fresh PBS. This mixture was well-triturated and plated into 10cm cell culture dishes with MEF medium (DMEM, 4.5g/mL glucose, 10% FBS, 2mM glutamine, and 1% pen/strep). These were maintained as described above and MEFs were used within 3 passages to avoid replicative senescence. Genotyping was done with two sets of primers. The first flank the 5 prime loxP site and the sequences are: 5': AATAATGAAGCTGACACCAAAAACT, 3': GAACCTACCGTCTGAGAACCACTG. The same 5' primer is used for the recombination test PCR, only with a 3' primer outside of the sixth exon: 3': GAGGAGCACAGGAGGGAAATG.

Results

Identification of a novel interaction between murine CENP-F and Hook2

Molecular analysis of CENP-F function has been confined predominantly to the C-terminal sequences of the protein. As the largely uncharacterized and extensive N-terminus has several predicted protein-protein binding motifs, we utilized a yeast two-hybrid (Y2H) approach to identify novel binding partners of CENP-F. The schematic in Figure 3.1A summarizes CENP-F domains previously studied as well as the N-terminal domains described here. The bait in this screen encompassed the first 689 amino acids of N-terminal CENP-F (bp 1-2067) and was screened against an embryonic whole mouse E17.5 cDNA library (Pooley et al., 2008). This screen identified specific proteins associated with the MT network

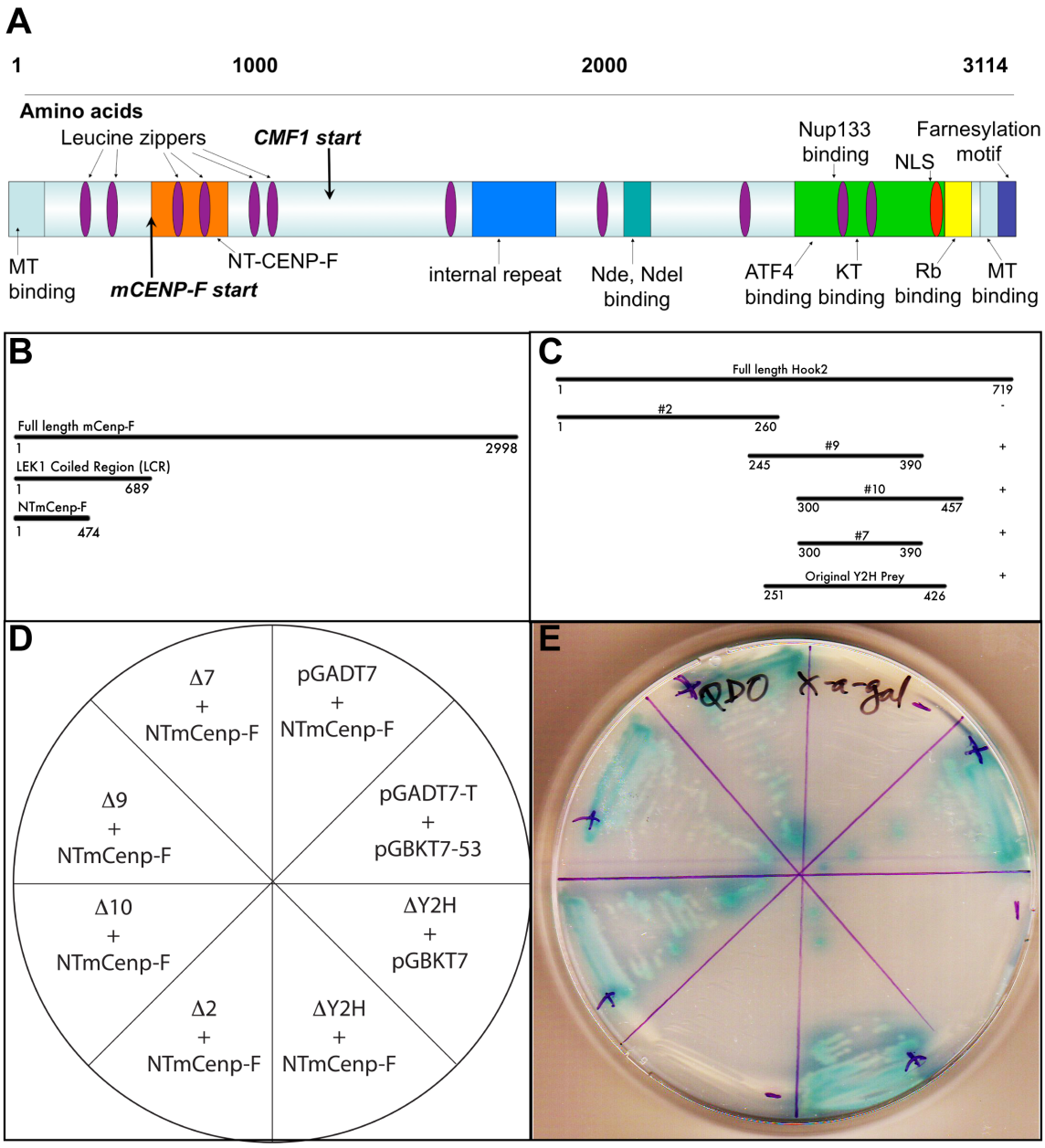

Figure 3.1. Identification of CENP-F/Hook2 interaction and characterization of binding domains. (A) Schematic of CENP-F protein domains. Our initial Y2H screen used the LEK Coiled Region (LCR) as bait and identified Hook2 directly interacting with CENP-F. (B) CENP-F truncation constructs. (C) Hook2 truncation constructs. In the column on the right, "+" indicates positive growth and "-" indicates no growth. Truncations were transformed into respective yeast strains to determine positive interactions. (D) Schematic of Hook2 truncation matings with NT-CENP-F and controls and plate of yeast growth. (E) Positive interactions grew and exhibited blue color upon Gal testing. Positive control growth was indicated by yeast transformed with pGBKT7–53 and pGADT7-T and our negative control utilized yeast expressing pGBTK-53 and the empty vector pGADT7.

and its various functions. Four independent hits matched the sequence of Hook homolog 2 (Hook2) and passed all false positive tests. Hook2 has been shown to regulate MT repolymerization at the centrosome and binds centrosomal protein CEP-110/centriolin (Szebenyi *et al.*, 2007). Our laboratory has shown that a central region of CENP-F distant from the N-terminus regulates the microtubule network via interaction with NudE (Soukoulis *et al.*, 2005) and given this potential connection, we examined the interaction of Hook2 and CENP-F in greater detail.

We again used a Y2H approach to define the smallest effective binding domain of each protein with a series of truncation constructs. We determined that the first 474 amino acids of CENP-F are necessary to retain Hook2 binding, and amino acids 300-390 of Hook2 must be present to bind CENP-F (Figure 3.1B-E). This N-terminal region of CENP-F contains a predicted leucine zipper, but no other predicted motifs. No other CENP-F sequences interact with Hook2 (Moynihan and Bader, unpublished data). The CENP-F-binding domain within Hook2 corresponds with a region between the microtubule-binding domain and organelle-binding domain previously identified by Szebenyi, et al. (2007). Thus, the interaction of these two proteins reveals a third protein binding region within Hook2. These data also support the use of these interaction domains as endogenous function inhibitors in future experiments.

Transiently expressed Hook2 and NT-CENP-F interact and co-localize at the centrosome in mammalian cells

Given these initial data demonstrating CENP-F binding with Hook2, we sought to confirm this interaction in mammalian cell lines. Full length Hook2 and NT-CENP-F were each tagged and expressed in COS-7 cells. As seen in Figure 3.2A, lysates from these cells were prepared, immunoprecipitated with an antibody to myc and blotted for GFP (Pooley et al., 2008). Effective immunoprecipitation of Hook2-GFP with NT-CENP-F-myc was readily observed, whereas no Hook2-GFP is pulled down in control lysates. This is consistent with the direct interaction found initially in yeast and led us to characterize the subcellular localization of these proteins. Again, the two tagged constructs were expressed in COS-7 cells and labeled with the respective antibodies to their epitope tags. NT-CENP-F was visualized at the centrosome by its co-localization with γ-tubulin (Figure 3.2B-D), indicating the sufficiency of this peptide region for centrosomal targeting. Other expressed CENP-F constructs lacking amino acids 1-474 do not target to the centrosome, suggesting, along with our biochemical data, that this sequence contains information necessary to direct CENP-F to this subcellular domain (Evans et al., 2007; Feng et al., 2006). Full length Hook2-GFP also localized to the centrosome when transfected in COS-7 cells (Figure 3.2E-G). This result was not surprising, given the previously described role of Hook2 in MT dynamics at the centrosome (Szebenyi *et al.*, 2007). As also demonstrated in Figure 3.2, transiently co-expressed NT-CENP-F-myc and Hook2-GFP co-localize at the centrosome, as identified by γ-tubulin (Figure 3.2H-K). Therefore, these data with transiently expressed constructs support a novel

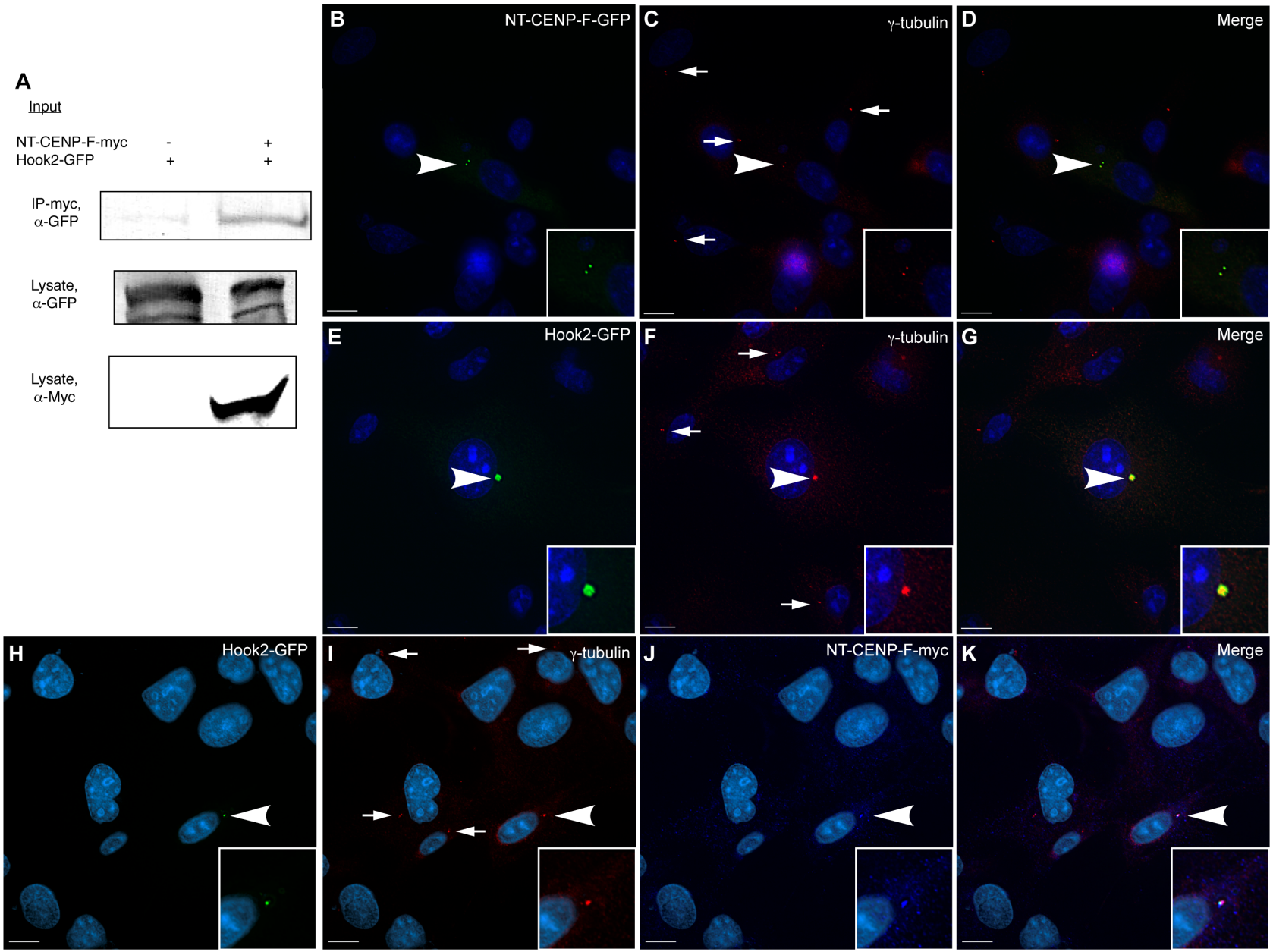
A
Input
NT-CENP-F-myc - +
Hook2-GFP + +
IP-myc, α-GFP
Lysate, α-GFP
Lysate, α-Myc
B NT-CENP-F-GFP
C γ-tubulin
D Merge
E Hook2-GFP
F γ-tubulin
G Merge
H Hook2-GFP
I γ-tubulin
J NT-CENP-F-myc
K Merge

Figure 3.2. Transiently expressed CENP-F and Hook2 proteins interact at the centrosome. COS-7 cells were co-transfected with NT-CENP-F-myc and Hook2-GFP. (A) Co-immunoprecipitation from transfected COS-7 cells. Lysate samples were pulled down with α-myc and blotted with α-GFP. (B-D) Singly transfected NT-CENP-F-GFP co-localizes with γ-tubulin centrosome marker (arrowhead). (E-G) Singly transfected Hook2-GFP co-localizes with γ-tubulin (arrowhead). (H-K) Co-expressed NT-CENP-F-myc and Hook2-GFP co-localized with γ-tubulin (arrowhead). Untransfected γ-tubulin at the centrosome marked with arrows. Scale bars 10 μm.

localization of CENP-F to the centrosome and we next examined endogenous localization and interaction.

Endogenous Hook2 and CENP-F interact and co-localize at the centrosome

The myoblast C2C12 cell line was used to co-immunoprecipitate CENP-F with binding partner Hook2 from murine cells. C2C12 cells were used in this experiment because the newly developed CENP-F antibody epitope is murine-specific and does not recognize primate cells and tissue tested thus far. As seen in Figure 3.3A, Hook2 is identified in the CENP-F immunoprecipitant with an antibody to Hook2 (a generous gift of Dr. H. Kramer, UT Southwestern), further confirming the interaction of these two proteins. While we do see an additional band in crude lysate, upon affinity purification with the CENP-F antibody, this non-specific band is lost in Western blots. C2C12 murine myoblasts were also used to characterize the endogenous localization of these proteins. Cells were labeled with γ-tubulin centrosome marker and either Hook2 or CENP-F. Figure 3.3B-G shows the co-localization of each binding partner to the centrosome, while Figure 3.3H-J demonstrates co-localization of CENP-F and Hook2, with direct-labeled CENP-F antibody and Hook2. It should be noted that the centrosome is not the only site for CENP-F or Hook2; these antibodies and previously reported antibodies show additional subcellular localizations (arrowheads, Figure 3.3). As CENP-F plays roles within the cell separate from the centrosome, this result was expected. Taken together, these data demonstrate a novel localization and binding partner at the centrosome for

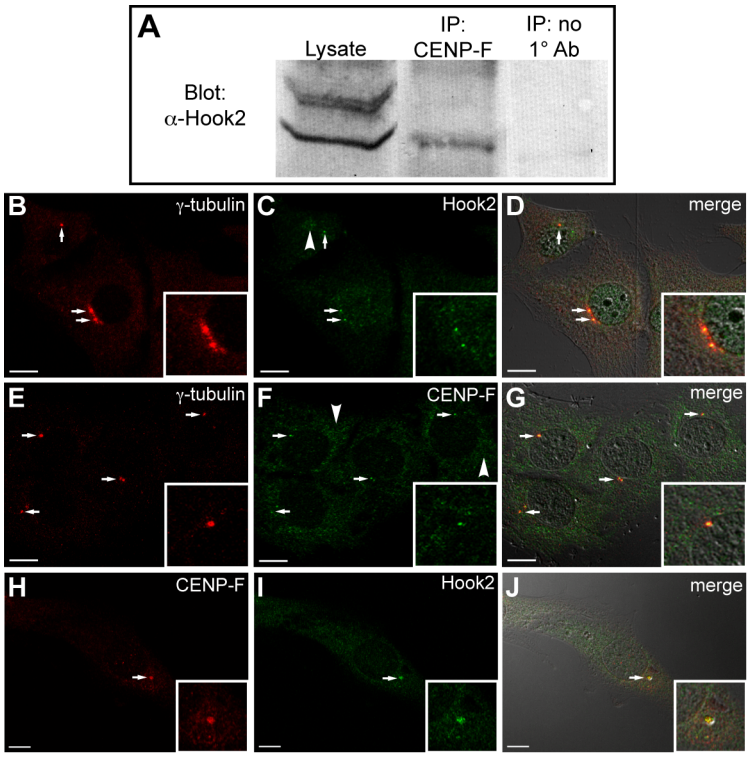

Figure 3.3. Endogenous CENP-F and Hook2 proteins interact and co-localize at the centrosome. (A) Endogenous co-immunoprecipitation with C2C12 cells. Lysate samples were pulled down with CENP-F antibody and blotted with Hook2 antibody. The third column shows no Hook2 pulled down when no CENP-F antibody was used in the pull-down. (B-J) Endogenous antibodies to CENP-F, Hook2, and γ-tubulin were used in C2C12 cells to show co-localization of all three proteins. (B) γ-tubulin centrosome marker (C) Hook2 (D) Merge with DIC (E) γ-tubulin (F) CENP-F (G) Merge (H) CENP-F (I) Hook2 (J) Merge with DIC. Arrows show co-localization and arrowheads show additional protein localizations. Scale bars 10 μm.

CENP-F and predict another regulative capacity of this protein in MT network function.

Ablated and disrupted CENP-F expression attenuates MT repolymerization after nocodazole challenge

CENP-F function has been probed in a variety of ways: RNAi, expression of truncation constructs, and morpholino knockdown (Feng et al., 2006; Holt et al., 2005; Pooley et al., 2008; Soukoulis et al., 2005). Here we present the first report using CENP-F$^{-/-}$ mouse embryonic fibroblasts as a model to examine CENP-F function. To that effect, we utilized a genetic mouse model developed in the laboratory, in which the first five exons of CENP-F, containing the Hook2 binding domain, were flanked with loxP sites (see Chapter V). This mouse line then crossed with the ubiquitously expressed CMV-Cre recombinase model (The Jackson Laboratory). Figure 3.4A demonstrates effective excision and recombination of genomic DNA by PCR and the data in Figure 3.4B confirms the loss of CENP-F mRNA in the floxed region by RT-PCR. A complete characterization of the phenotype of this animal model is underway (Moynihan et al, in preparation). Several preparations of mouse embryonic fibroblasts (MEFs) were isolated from E13.5 embryos and cultured for genotyping before experiments to analyze CENP-F function. Given the centrosomal localization of CENP-F described above and the role of the centrosome in MT initiation and organization, we utilized the WT and CENP-F$^{-/-}$ MEF populations in an assay of MT regulation: nocodazole washout and MT repolymerization.

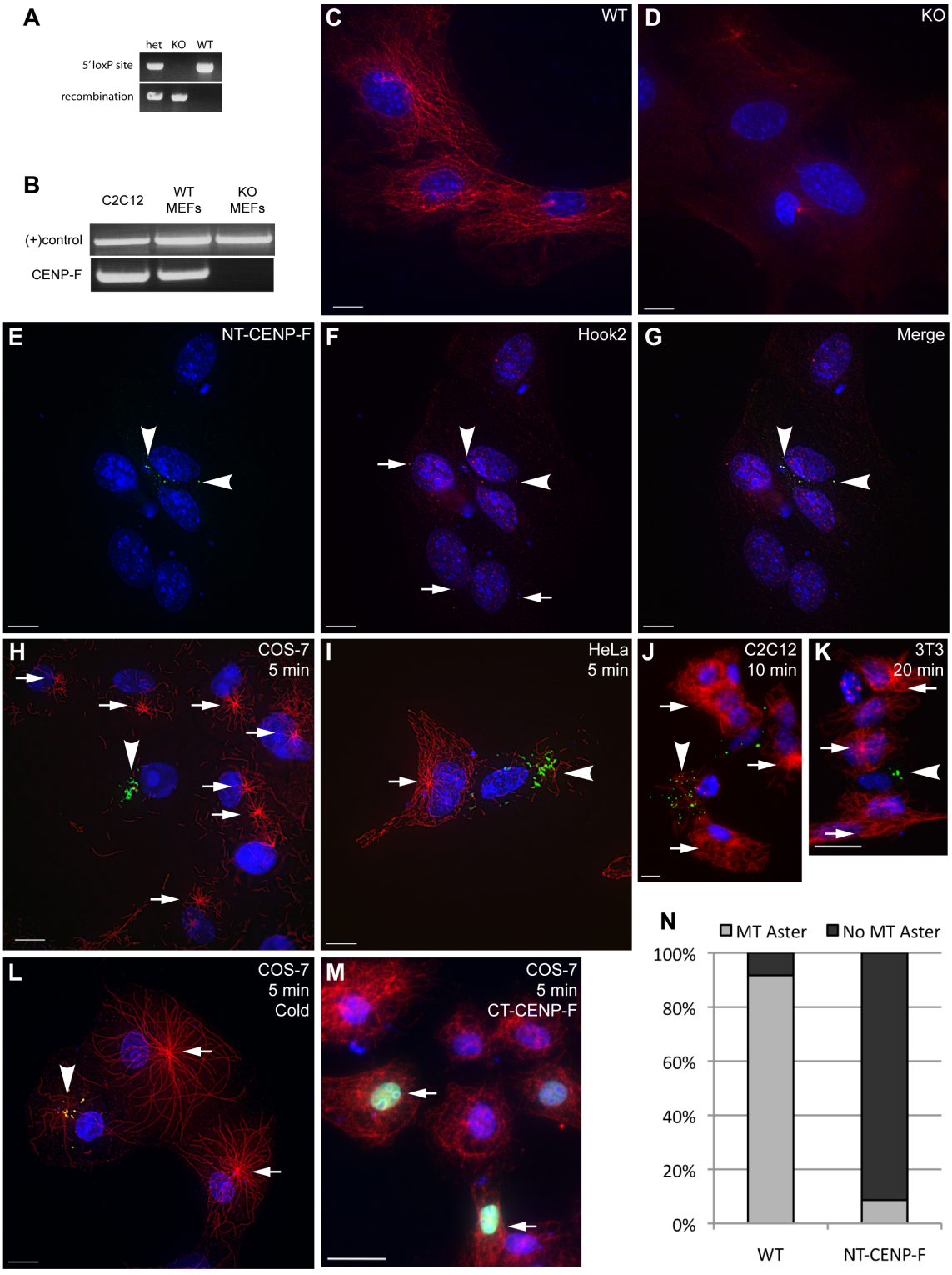
A
het KO WT
5' loxP site
recombination
B
C2C12
WT MEFs
KO MEFs
(+)control
CENP-F
C
WT
D
KO
E
NT-CENP-F
F
Hook2
G
Merge
H
COS-7
5 min
I
HeLa
5 min
J
C2C12
10 min
K
3T3
20 min
L
COS-7
5 min
Cold
M
COS-7
5 min
CT-CENP-F
N
MT Aster
No MT Aster
100%
80%
60%
40%
20%
0%
WT
NT-CENP-F

Figure 3.4. Disrupting the CENP-F/Hook2 interaction interferes with MT repolymerization after nocodazole challenge. (A) WT and CENP-F$^{-/-}$ MEFs were isolated and genotyped. The top bands use PCR primers flanking the 5' loxP site of the floxed CENP-F allele, determining floxed vs. WT. The bottom bands use PCR primers flanking the entire floxed sequence, thus allowing effective PCR only once the internal sequence has been excised, thus "recombination" has occurred. (B) RT-PCR confirmation of CENP-F$^{-/-}$ MEFs. NDRG4 primers and C2C12 lysate were used as positive controls. (C-D) WT and CENP-F$^{-/-}$ cells were treated with nocodazole, washed with fresh medium and fixed after 5 minutes. (C) WT MEFs display reconstituted MT networks whereas (D) CENP-F$^{-/-}$ MEFs show absence of MT repolymerization. MTs are labeled in red. (E-G) Expression of NT-CENP-F (green) displaces endogenous Hook2 (red) expression from centrosome (arrowheads). Arrows indicate typical Hook2 localization to centrosome in untransfected cells. (H-M) Four cell lines were transfected with NT-CENP-F-GFP, treated with nocodazole for 2 hours, washed with media, and allowed to recover. Transfected constructs are labeled green with an arrow, MTs are labeled red, and nuclei are labeled blue with DAPI. (H-L) Arrows indicate MTOC aster formation in untransfected cells, whereas arrowheads point to NT-CENP-F-expressing cells without MTOC asters. (H) COS-7 cells at 5 minutes post-washout (I) HeLa cells at 5 minutes (J) C2C12 cells at 10 minutes (K) 3T3 cells at 20 minutes. (L) Cold-treatment phenocopies nocodazole treatment in COS-7 cells (M) Negative control C-terminal CENP-F construct, arrow, does not have the same effect, showing the specificity of this phenotype. (N) Quantification of MTOC aster formation in COS-7 cells after 5 minutes. Gray indicates percentage of counted cells with a MTOC aster, while black represents the percentage with no MTOC aster. WT cells reconstitute MTOC asters in over 90% of cells, whereas NT-CENP-F-expressing cells repolymerize less than 10% MTOC asters. $p < 0.0001$. Scale bars 10 μm.

Both WT and CENP-F$^{-/-}$ MEFs were plated and incubated with nocodazole, thoroughly washed with fresh medium, and allowed to recover for 5 minutes before fixation and labeling. WT MEFs display fully reconstituted MT networks and a substantive MTOC aster within this time period (Figure 3.4C). In contrast, Figure 3.4D demonstrates the markedly absent MT aster repolymerization in CENP-F$^{-/-}$ MEFs even at 5 minutes post-washout. Some cytoplasmic MT repolymerization is seen in these null cells (see below, Figure 3.6B) but no clear MT aster forms. The lack of MT repolymerization from the centrosome in CENP-F$^{-/-}$ cells demonstrates a clear role for CENP-F in MTOC function. Specifically, these data signify a role for CENP-F in regulation of the MT network in correlation with MT repolymerization at the centrosome.

Given that CENP-F$^{-/-}$ cells do not effectively repolymerize MT asters and the knowledge that centrosomal binding partner Hook2 affects MT organization, we next examined the effect of expression of the Hook2-binding domain of CENP-F on MT aster formation. Figure 3.2 shows that NT-CENP-F, the domain of CENP-F that binds Hook2, localizes to the centrosome. With expression of NT-CENP-F, cell viability was not adversely affected over the period of analysis (3-4 days) and, in contrast to expression of the Nde-binding domain of CENP-F (Figure 3.1), the steady state MT network is not overtly altered. However, the expression of NT-CENP-F does redistribute the localization of binding partner Hook2 away from the centrosome after nocodazole treatment, indicating a dominant disruption of endogenous CENP-F function (Figure 3.4E-G,

arrowheads). Endogenous Hook2 localization in untransfected cells (indicated by arrows in Figure 3.4F) marks the centrosome. Therefore, the NT-CENP-F truncation is a useful tool to study the function of CENP-F/Hook2 interaction at the centrosome. Previous studies of Hook2 function utilized protein truncations to elucidate function in MT repolymerization (Szebenyi *et al.*, 2007) and we have used a similar strategy with NT-CENP-F as a analogous tool. To probe the effect of NT-CENP-F on MTOC function and further validate CENP-F$^{-/-}$ data, nocodazole treatment and washout with MT repolymerization analysis was employed. For nocodazole assays, COS-7 cells were used as standard single-MTOC aster cells (Clark and Meyer, 1999; Quintyne *et al.*, 1999). Nonetheless, in total, four different mammalian cell lines were transfected with the tagged NT-CENP-F construct for nocodazole challenge and MT repolymerization experiments. MT repolymerization after washout varies slightly by cell type but generally, MTs begin to repopulate the cell within 180 seconds (Efimov *et al.*, 2007). Similar to CENP-F-ablated MEFs, cells expressing NT-CENP-F exhibit a dramatic attenuation of MT repolymerization in COS-7 (Figure 3.4H), HeLa (Figure 3.4I), C2C12 (Figure 3.4J), and NIH-3T3 (Figure 3.4K) cell lines. Importantly, reduced MT repolymerization is not nocodazole specific, as depolymerization of MTs with cold treatment induces a similar phenotype in COS-7 cells (Figure 3.4L). Attenuation is specific to the expression of NT-CENP-F, as expression of C-terminal CENP-F does not result in any barrier to MT repolymerization (Figure 3.4M). Reformation of the MTOC aster was quantified in COS-7 cells and experimental cells showed fewer than 10% MTOC aster

reformation, whereas WT cells show over 90% MTOC aster reformation (Figure 3.4N, $p<0.0001$). The impaired MT repolymerization can persist for a remarkably lengthy time period post-washout (even at 20 min, Figure 3.4K) yet does come back after 2 hours with the dominant negative construct and some repolymerization in CENP-F$^{-/-}$ MEFs after 6 hours (Figure 3.5). This is a remarkable delay, considering the quick recovery seen in untransfected cells in under 5 minutes. Taken together, these data with CENP-F$^{-/-}$cells and NT-CENP-F-expressing cells demonstrate the critical necessity of CENP-F in regulation of MT repolymerization.

CENP-F regulation of MT repolymerization is centrosome specific

To delineate whether the attenuation of MT repolymerization is centrosome-specific, we used two conditions to examine possible MT repolymerization from other subcellular localizations. Human retinal pigment epithelial (RPE) cells, a line recently shown to display abundant Golgi-nucleated MTs (Efimov *et al.*, 2007), and WT and CENP-F$^{-/-}$ MEFs were treated with nocodazole treatment and washout. RPE cells were transfected with NT-CENP-F similar to experiments in Figure 3.4 with COS-7, HeLa, C2C12, and NIH-3T3 cells. RPE cells expressing NT-CENP-F phenocopy the attenuated MT repolymerization seen with other cell lines, with markedly decreased MTOC aster formation (Figure 3.6A). However, MTs can be seen emanating from disassociated Golgi membranes both in experimental and control cells (Figure 3.6A, inset). As noted above, some repolymerization was observed in CENP-F$^{-/-}$

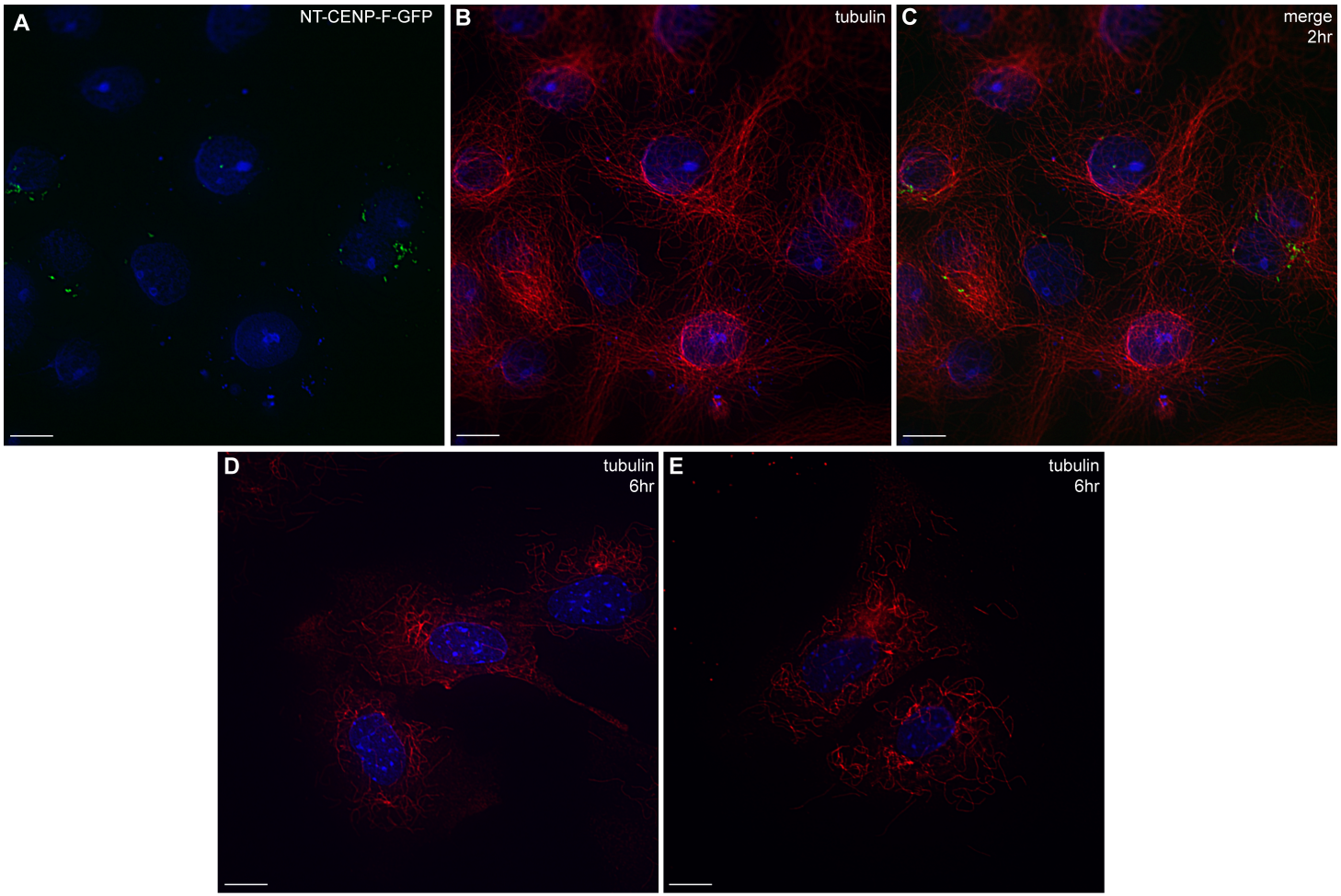

Figure 3.5. Inhibited MT nucleation is not a permanent condition, but significant. (A-C) COS-7 cells transfected with (A) NT-CENP-F-GFP and labeled for (B) tubulin show full MT repolymerization in 2 hours after nocodazole washout. (D, E) CENP-F-/- MEFs show weak MT repolymerization 6 hours after nocodazole washout.

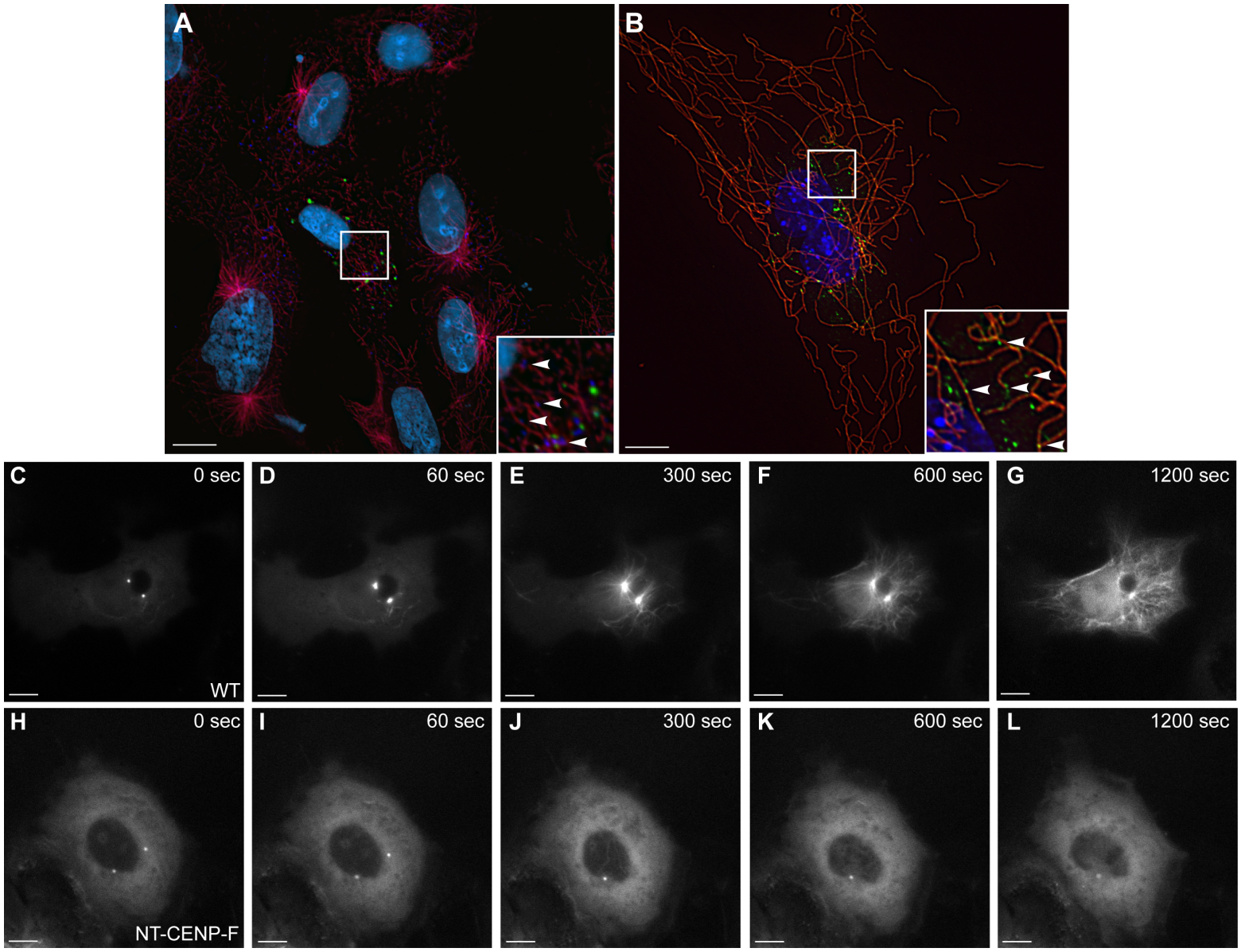
A
B
C
0 sec
WT
D
60 sec
E
300 sec
F
600 sec
G
1200 sec
H
0 sec
NT-CENP-F
I
60 sec
J
300 sec
K
600 sec
L
1200 sec

Figure 3.6. CENP-F disruption of MT repolymerization is centrosome specific and inhibits MT aster nucleation. (A) RPE cells were transfected with NT-CENP-F (green), treated with nocodazole, and labeled for MTs (red), Golgi membrane (dark blue), and nuclei (DAPI, cyan). Transfected cells show attenuated MT aster repolymerization but insets show MTs associated with Golgi membranes in the cytoplasm (arrowheads). (B) CENP-F$^{-/-}$ MEFs were treated with nocodazole and fixed after 5 minutes of recovery. Insets show MTs associated with Golgi membranes (arrowheads). MTs are labeled in red and Golgi marked with green. WT COS-7 cells (C-G) and NT-CENP-F transfected cells (H-L) were both transfected with EMTB-GFP, a MT marker, incubated with nocodazole, washed out, and immediately imaged for 20 minutes at 1 frame/20seconds. (C-G) EMTB-marked MTs emanate from 2 MTOC asters very quickly and MTs repopulate the entire cell within 10 minutes. (H-L) The EMTB-GFP pool remains cytoplasmic throughout the 20 minute period in a cell expressing NT-CENP-F. After imaging, other untransfected cells in the dish were checked and showed full MTOC recovery (not shown). Scale bars 10 μm.

cells, but not asters. In Figure 3.6B, CENP-F$^{-/-}$ MEFs which escape total block of MT repolymerization show a reduced and disorganized MT network and the MTs are associated with the dispersed Golgi membranes. WT MEFs do show a radial array but the images do not discount additional repolymerization from the Golgi membranes (Figure 3.4C). These data using CENP-F$^{-/-}$ MEFs and the RPE cell line with NT-CENP-F demonstrate the robust repolymerization of MTs from non-centrosomal sources, thus confirming that the role of CENP-F in regulating MT repolymerization is centrosome-specific.

CENP-F regulates MT nucleation

To examine in detail the mechanism of the effect of CENP-F on MT repolymerization, a live-imaging approach was employed to capture the entire repolymerization period after nocodazole washout. This strategy provided insight into the mechanism of the delay in MT repolymerization; visualization of the entire period shows concretely whether this delay is either due to lack of nucleation or instead, catastrophe in nascent MTs. Inhibited nucleation would obstruct any MT repolymerization, whereas MT catastrophe, depolymerization at the plus end of the growing MT, would allow initial growth from the centrosome before dispersal. Both control and experimental COS-7 cells were transfected with a MT-coating protein, EMTB-GFP, to visualize MT polymerization. Experimental samples were co-transfected with NT-CENP-F-Cerulean. After nocodazole treatment, both control and experimental cells show a typical cytoplasmic pool of EMTB-GFP before MT repolymerization begins (Figure 3.6C

and 3.6H). Post-nocodazole washout, control MTs clearly nucleate and polymerize from the centrosome into an organized network (Figure 3.6C-G); asters form within 60 seconds and MTs reach the cell periphery in just over 6 minutes. In contrast, expression of NT-CENP-F alteres this process considerably. As shown in Figure 3.6H-L, NT-CENP-F-expressing COS-7 cells are unable to repolymerize the MT network after nocodazole washout, even up to 20 minutes post-washout. No MT repolymerization is seen in the experimental condition and this severe retardation of MT outgrowth with expression of NT-CENP-F demonstrates that CENP-F plays a role in nucleation of the MT network from the centrosome.

CENP-F regulates nucleation and anchoring of MT polymerization from the centrosome

A minority of cells (<10%, Figure 3.4N) escape inhibited MT repolymerization induced by NT-CENP-F and thus provide an additional method of investigating the mechanism of CENP-F function. Live imaging data demonstrated a clear nucleation defect with CENP-F disruption, therefore we next examined experimental NT-CENP-F-expressing cells with an incomplete attenuation phenotype. This population of cells is characterized by significantly diminished MT repolymerization after nocodazole treatment and within this range of phenotypes, three phenotype categories would indicate the spectrum of CENP-F functional mechanism: sparse, disorganized, and short MT asters (Chakravarty et al., 2004; Fumoto et al., 2009; Zhapparova et al., 2007). The presence of full-length but fewer MTs emanating from the centrosome in

expressing cells would further support our previously seen nucleation defects; this category is the sparse phenotype. Alternatively, if MTs are disorganized rather than arrayed as a centrosomal centered aster, there could be additional interference with MT-anchoring; this category is termed disorganized. Whereas shorter, full MT asters with disrupted CENP-F function would suggest an elongation defect – the short phenotype. Using these categories, we classified NT-CENP-F expressing cells that escape inhibition of MT repolymerization post-nocodazole washout (<10% of all NT-CENP-F expressing cells, Figure 3.4N). Figure 3.7 shows a representative example of each condition described. Figure 3.7A shows both a sparse and disorganized aster, which is most common in the cells with an incomplete phenotype (51.1 ±11.4%). Figure 3.7B lacks a MTOC aster but disorganized MTs are present; in this case both nucleation and anchoring could be affected and/or other parts of the cell could be acting as MTOCs (21.8 ±5.3%). Figure 3.7C shows a representative image of a sparsely populated, yet organized radial array of MTs, indicative of inhibited nucleation (16.6 ±5.8%). Figure 3.7D displays a characteristic example of a populated, yet disorganized MTOC with mostly short MTs, characteristic of a potential elongation defect (10.4 ±2.1%). The relative populations of each of these phenotypes within the general category of “incomplete” is shown in Figure 3.7E and show a continuum of disrupted MT nucleation and anchoring, as nearly 90% of all cells counted fall into the sparse and disorganized characterization. Nevertheless, it should be noted that this range of incomplete phenotypes could also be attributed simply to a partial loss-of-function in nucleation with expression

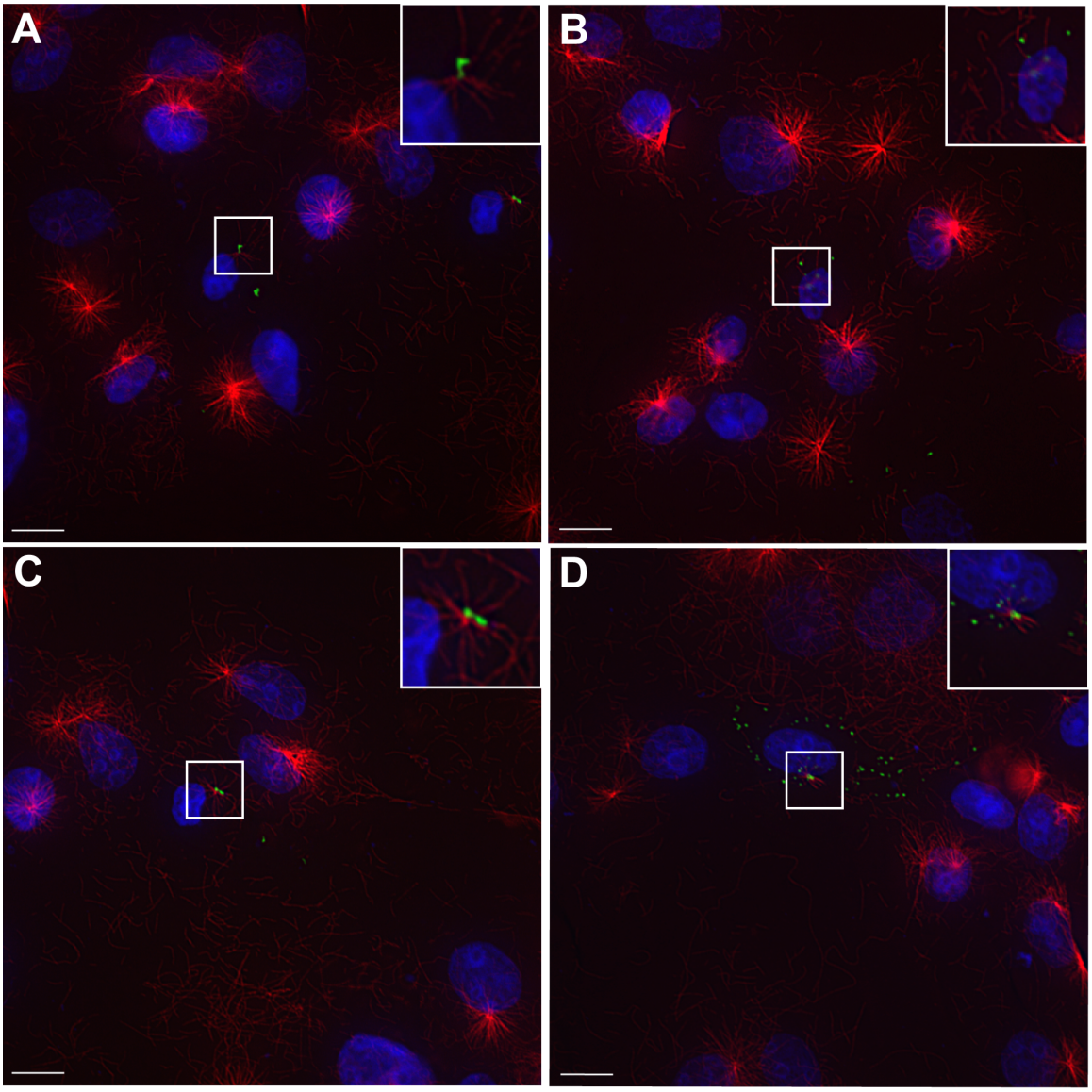
A
B
C
D

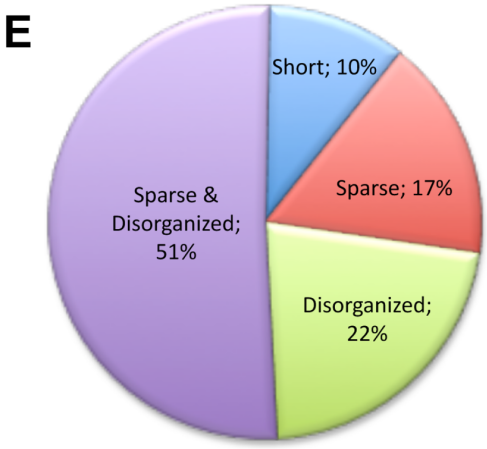
E
Short; 10%
Sparse; 17%
Disorganized; 22%
Sparse & Disorganized; 51%

Figure 3.7. **CENP-F functions in MTOC nucleation and anchoring.** NT-CENP-F expressing COS-7 cells were examined for incomplete inhibition of MT repolymerization. Various phenotypes are shown: (A) sparse and disorganized MTs, most commonly seen with NT-CENP-F expressing cells, (B) sparse aster, (C) disorganized MTs, (D) short, disorganized aster (E) Quantification of each phenotype along spectrum. Scale bars 10 μm.

of NT-CENP-F. Thus, these results reveal a role in MT nucleation and possibly anchoring within CENP-F regulation of MT repolymerization.

Disruption of CENP-F function redistributes centrosomal proteins

Interestingly, after application of nocodazole, the localization of NT-CENP-F scatters into cytoplasmic puncta and remains dispersed even after 10-20 minutes in fresh media. As seen in Figure 3.4, post-nocodazole washout, NT-CENP-F is no longer confined to a centrosomal localization demonstrated in Figure 3.2. Instead, NT-CENP-F is spread out as a cloud of puncta in the cytoplasm. It is possible that these nocodazole-induced puncta harbor proteins normally present at the centrosome that function there in MT organization. As demonstrated above in Figure 3.4, binding partner Hook2 redistributed with NT-CENP-F after nocodazole treatment in this manner. We next examined other centrosomal proteins involved in MT organization. Ninein, a mother centriole, MT-anchoring protein recently shown to also participate in MT nucleation (Bouckson-Castaing et al., 1996; Delgehyr et al., 2005; Mogensen et al., 2000; Ou et al., 2002) shows distinct redistribution to NT-CENP-F puncta (Figure 3.8A-C, arrows). Disruption of ninein causes a delay in MT nucleation as well as anchoring defects, similar to the phenotypes seen in this study (Delgehyr *et al.*, 2005). Overexpression of ninein has been shown to increase γ-tubulin recruitment to the centrosome (Stillwell *et al.*, 2004) and knockdown of human ninein results in reduced expression of γ-tubulin at the centrosome (Lin *et al.*, 2006); both of these studies indicate a link between ninein and the γ-tubulin ring

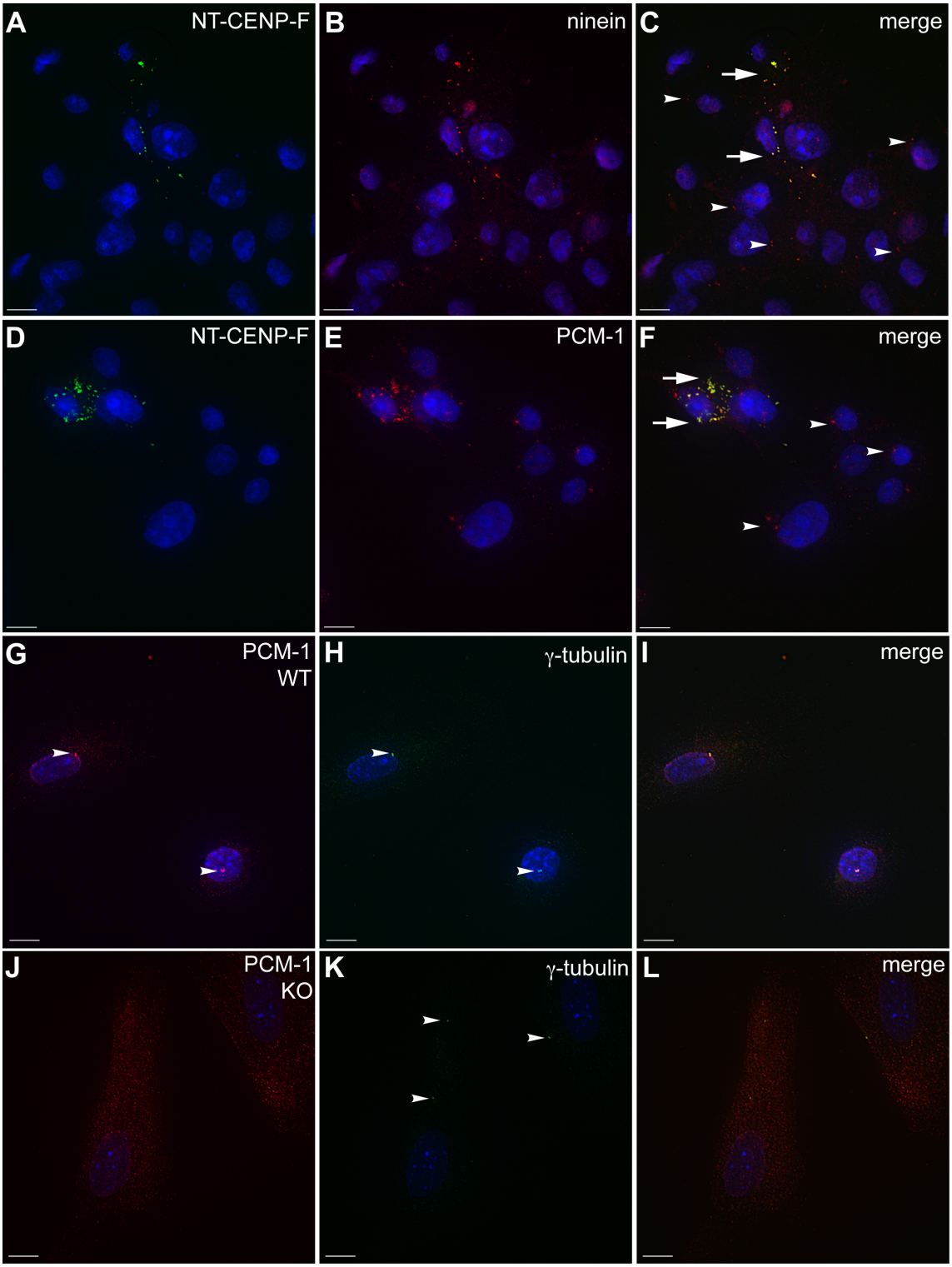
A
NT-CENP-F
B
ninein
C
merge
D
NT-CENP-F
E
PCM-1
F
merge
G
PCM-1
WT
H
γ-tubulin
I
merge
J
PCM-1
KO
K
γ-tubulin
L
merge

Figure 3.8. **Centrosomal proteins are redistributed by CENP-F disruption and deletion**. (A-F) COS-7 cells expressing NT-CENP-F show colocalization of the CENP-F truncation puncta with ninein and PCM-1. An arrowhead indicates normal centrosomal protein expression and aberrant colocalization with NT-CENP-F is labeled with an arrow. (A) NT-CENP-F. (B) ninein. (C) Merge. (D) NT-CENP-F. (E) PCM-1. (F) Merge. (G-L) WT and CENP-F-/- MEFs were labeled for PCM-1 (red) and γ-tubulin (green). (I) PCM-1 clearly localizes with γ-tubulin in WT MEFs, whereas in (L) CENP-F-/- MEFs, PCM-1 is diffusely cytoplasmic. Bars, 10 μm.

complex. Intriguingly, NT-CENP-F does not redistribute γ-tubulin (Figure 3.9A-C), indicating the complex relationship between MT regulatory proteins at the centrosome. Also, pericentrin or centrin1 proteins are not redistributed with expression of NT-CENP-F either (Figure 3.9D-I). However, the anchoring of MTs at the centrosome generates the radial array of the MT aster and another specific centrosomal protein regulates the anchoring process: PCM-1, a protein seen in the centriolar satellites that are required for MT anchoring (Balczon et al., 2002; Dammermann and Merdes, 2002; Mack et al., 1998) (Kubo *et al.*, 1999). PCM-1 also affects the centrosomal proteins ninein, centrin, and pericentrin (Dammermann and Merdes, 2002). The characterization of incomplete attenuated MT repolymerization implicated an anchoring defect with expression of NT-CENP-F and it is possible that the disruption of CENP-F affects other centrosomal proteins in the anchoring process, such as PCM-1. To test whether PCM-1 is sequestered in NT-CENP-F puncta after nocodazole treatment, we used COS-7 cells fixed 5 minutes post-nocodazole washout. Figure 3.8D-F clearly demonstrates that PCM-1 does disperse with NT-CENP-F (arrows), whereas untransfected cells show normal PCM-1 localization (arrowheads). Additionally, in CENP-F$^{-/-}$ MEFs, proper recruitment and/or stabilization of centrosome proteins could be impaired due to lack of CENP-F. Accordingly, we examined PCM-1 localization in both MEF populations after nocodazole challenge and WT MEFs show clear centrosomal PCM-1 localization (Figure 3.8G-I), whereas CENP-F$^{-/-}$ MEFs only exhibit diffuse cytoplasmic PCM-1 labeling (Figure 3.8J-L). Interestingly, Hook2 and ninein localization remained

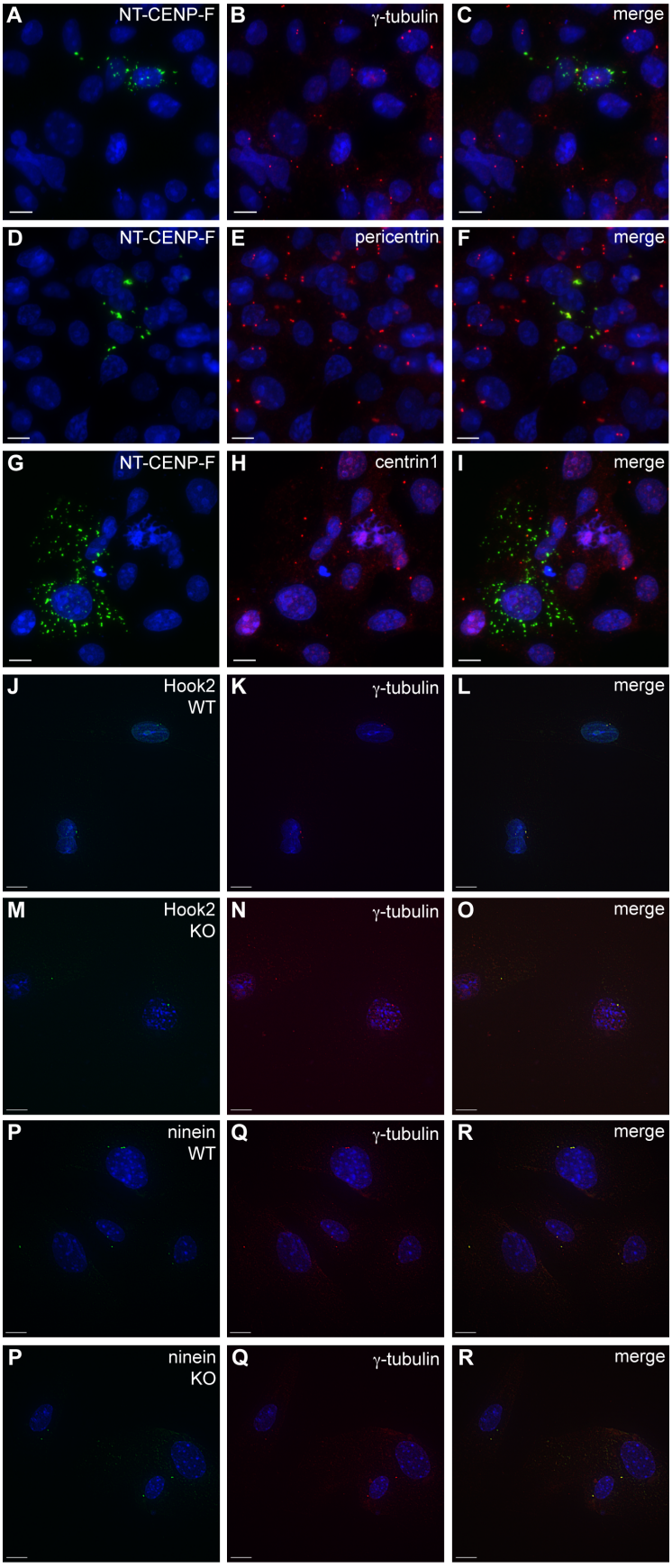

Figure 3.9. Some centrosomal proteins are not redistributed by expression of NT-CENP-F. COS-7 cells expressing NT-CENP-F do not show co-localization of the CENP-F truncation puncta with endogenous γ-tubulin, pericentrin, or centrin1. (A) NT-CENP-F-GFP, (B) γ-tubulin, (C) merge. (D) NT-CENP-F-GFP, (E) pericentrin, (F) merge. (G) NT-CENP-F-GFP, (H) centrin1, (I) merge. (J-R) WT and CENP-F-/- MEFs were labeled for Hook2 and ninein (red) and γ-tubulin (green). (M, O, P, R) Both Hook2 and ninein retain centrosomal localization in CENP-F-/- MEFs. Scale bars 10 μm.

centrosomal in CENP-F$^{-/-}$ MEFs (Figure 3.9J-R), indicating a potential shift in mechanism between expression of truncated CENP-F and ablation of endogenous CENP-F. However, the redistribution of the PCM-1 anchoring protein may explain the inability of CENP-F$^{-/-}$ cells and NT-CENP-F expressing cells to coordinate MT growth from the centrosome and taken together, these data provide a link to the mechanism of CENP-F in MT network regulation.

Discussion

In this study we have shown a previously unrecognized centrosomal localization, binding partner, and function of CENP-F. Hook2, a centrosomal participant in MT regulation, was confirmed as a direct binding partner of CENP-F. Ablation of CENP-F function in newly developed CENP-F$^{-/-}$ cells dramatically attenuates MT repolymerization and overexpression of the N-terminal portion of CENP-F that binds Hook2 phenocopies this event. Our experiments demonstrate that this is due to lack of nucleation, not catastrophe events, and that the Golgi retains MT nucleation activity. Therefore, this phenotype is specific to microtubule repolymerization at the centrosome. Additionally, incomplete phenotype analysis shows that experimentally altered cells that escape inhibited MT repolymerization have fewer and more disorganized MT emanating from the centrosome, indicating a defect in anchoring in addition to nucleation. Expression of NT-CENP-F redistributes localization of centrosomal proteins ninein and PCM-1, and mislocalization of PCM-1 protein is also seen in CENP-F$^{-/-}$ MEFs, an important and additional indicator of CENP-F anchoring function at the centrosome. Taken

together, these data reveal a novel role for CENP-F at the centrosome in MT formation via its interaction with Hook2 and predict a broader role for this protein in regulation of the MT network.

CENP-F displays a novel endogenous localization, binding partner, and function at the centrosome

CENP-F (mitosin) was independently discovered as a cell cycle dependent kinetochore (KT) associated and Rb-binding protein (Rattner *et al.*, 1993; Zhu *et al.*, 1995b). Since those initial discoveries, homologous proteins have been found in other vertebrates, invertebrates, and prokaryotes (Moore *et al.*, 1999; Ortiz *et al.*, 1999, Goodwin et al., 1999; Litvin et al., 1993; Redkar et al., 2002). These are large proteins and have a predicted coiled-coil structure with multiple intervening protein/protein binding domains (Figure 3.1) (Goodwin et al., 1999; Wei et al., 1996; Zhu et al., 1995a) and varying localizations (Ashar et al., 2000; Holt et al., 2005; Hussein and Taylor, 2002; Liao et al., 1995; Rattner et al., 1993; Yang et al., 2005; Zhou et al., 2005; Zhu et al., 1995a; Zhu et al., 1995b, Dees *et al.*, 2000, Ashe et al., 2004; Evans et al., 2007; Pooley et al., 2008; Pooley et al., 2006; Soukoulis et al., 2005). Despite the various localizations seen in the analysis of CENP-F homologs, many well-conserved domains have been shown to function and/or bind similar partners in more than one family member. CENP-F has been widely described as a nuclear, KT-associated protein and the conserved region responsible for this localization is found in the C-terminus (Zhu *et al.*, 1995a). More recently, analysis of CENP-F function has moved beyond the carboxyl terminus into the central and N-terminal

regions of the protein (Pooley et al., 2008; Pooley et al., 2006; Soukoulis et al., 2005). These more recently characterized domains show localization and function of CENP-F in the cytoplasm. In this study, we reveal that CENP-F localizes to the centrosome and regulates MT organizing activity from this organelle.

The interaction of CENP-F with Hook2 reveals additional cytoplasmic function and further substantiates centrosomal localization. Hook2 primarily localizes to the centrosome and binds another centrosomal protein, centriolin (Szebenyi *et al.*, 2007). The Hook2 linker protein participates in MT growth and organization at the centrosome, but the mechanism underlying this activity remains unknown. Our data identify a previously undetermined binding domain within Hook2 in the central coiled-coil region. The interaction with Hook2 is of particular interest as members of the Hook family have been described linker proteins between the MT and specific organelles (Gönczy, 2004; Linstedt, 2004; Malone et al., 2003; Mendoza-Lujambio et al., 2002; Szebenyi et al., 2007; Walenta et al., 2001). Given the established interaction of CENP-F with MT regulators such as Nude/Nudel (Soukoulis *et al.*, 2005; Vergnolle and Taylor, 2007) and tubulin itself (Feng *et al.*, 2006), the newly-identified relationship with the Hook family potentially links CENP-F to a myriad of sub-cellular domains and organelle-specific activities.

CENP-F regulates MT nucleation and anchoring at the centrosome with other centrosomal proteins

In this study, we see an even more dramatic attenuation of MT repolymerization with disruption of CENP-F, as compared to disruption of binding partner Hook2 (Szebenyi *et al.*, 2007). This effect is expansive, as CENP-F$^{-/-}$ MEFs shown a dramatic delay in MT repolymerization, providing essential supportive evidence of this new CENP-F function. It is significant to note that a highly similar phenotype is observed with several cell lines of different species when transfected with NT-CENP-F (Figure 3.4). Given that this role of CENP-F was heretofore unrecognized, we performed several experiments to investigate the mechanism of CENP-F function at the MTOC. First, live imaging data showed that this effect was not due to premature catastrophe and subsequent depolymerization of nascent MT (Figure 3.6). Additionally, this effect is centrosome-specific since Golgi membranes, known to initiate MT nucleation and polymerization (Efimov *et al.*, 2007), retain the capability to nucleate MTs in the presence of NT-CENP-F while the centrosome does not (Figure 3.6). These data further corroborate centrosomal localization of CENP-F and led us to explore the specific function of CENP-F at the centrosome in MT repolymerization.

To determine this mechanism, we closely examined those NT-CENP-F-expressing cells that escaped complete inhibition of MT repolymerization. We reasoned that by characterizing these MTs, we would provide initial evidence of function in one or more of three processes controlling MT network emanation from the centrosome: nucleation, elongation, and/or anchoring. As seen in Figure

3.7, we saw substantially fewer MTs emanating from the centrosome and poor organization in the few that formed throughout the continuum of incomplete phenotypes. These data suggest a role for CENP-F in MT nucleation and possibly anchoring from the centrosome, and constitute an initial step in defining the mechanism of the attenuation phenotype.

Inhibition of MT regrowth through nucleation/anchoring defects at the centrosome is a constant observed with disruption of CENP-F function whether it be by ablation or expression of truncation mutants. With the loss of CENP-F function, it was plausible that specific centrosomal proteins would be displaced from the centrosome where complex interactions are essential for protein targeting (Delgehyr *et al.*, 2005; Hames *et al.*, 2005; Srsen *et al.*, 2006). Therefore, we examined the localization of several diverse centrosomal proteins concurrent with disruption of CENP-F. Our results show definitive dispersal of Hook2 along with endogenous ninein and PCM-1 to NT-CENP-F-positive puncta distal from the centrosome. Both ninein and PCM-1 have well-documented roles in nucleation and anchoring of MT from the centrosome (Azimzadeh and Bornens, 2007; Dammermann and Merdes, 2002; Delgehyr et al., 2005). Critically, dispersal of endogenous PCM-1 is observed in both CENP-F$^{-/-}$ MEFs and NT-CENP-F-expressing cells. PCM-1 has a well-documented role in MT anchoring from the centrosome (Dammermann and Merdes, 2002; Delgehyr et al., 2005; Mogensen et al., 2000; Ou et al., 2002), as both expression of PCM-1 truncations and knockdown results in disorganization of the MT array, both in

steady state and nocodazole challenge (Dammermann and Merdes, 2002). Additionally, with the expression of a C-terminal deletion PCM-1 construct, ectopic granules formed and redistributed endogenous ninein, centrin, and pericentrin, and PCM-1 (Dammermann and Merdes, 2002). Thus, the re-location of this key regulator may a central role in the centrosome-specific inhibition of MT regrowth in both experimental models presented here.

Studies by Delgehy and Stillwell suggest that localization of γ-tubulin to the centrosome is necessary for MT nucleation (Delgehyr et al., 2005; Stillwell et al., 2004). With this in mind, it is interesting to note that γ-tubulin does not appear to redistribute in either experimental model presented here. However, direct disruption of PCM-1 function does not alter γ-tubulin localization at the centrosome yet produces the same inhibition of MT regrowth observed in CENP-$F^{-/-}$ or NT-CENP-F-expressing cells (Figure 3.4 and (Dammermann and Merdes, 2002)). Thus, it appears that γ-tubulin localization in the absence of CENP-F function is not adequate to support MT regrowth from the centrosome and that localization of PCM-1 is dependent on intact CENP-F. Additionally, with expression of NT-CENP-F (the Hook2-binding domain), Hook2 redistributed to the NT-CENP-F-positive puncta and was not observed at the centrosome. However, when the same experiment was conducted with CENP-$F^{-/-}$ cells, Hook2 localized to the centrosome in the absence of its binding partner suggesting that other mechanisms direct its localization. Nevertheless, both NT-CENP-F expression and CENP-F ablation experiments lead to a common phenotype,

attenuated MT repolymerization, and this difference in centrosomal protein localization could indicate different mechanisms in each scenario. While the interactions and relationships of proteins are complex, our data reveal that CENP-F as an essential component critical for the assembly and/or stability of essential MT organizers at the centrosome and disruption of its function results in a loss of centrosomal regulation of the MT network.

CENP-F is a possible master regulator of MT network processes with cellular organelles

The novel role and localization of CENP-F presented here open a new perspective on CENP-F function as a whole. The understanding that CENP-F functions with MTs at the centrosome is reminiscent of the highly regulated nuclear MT association with KTs that is well studied with CENP-F. The KT is a complex organelle that captures plus ends of MTs and links them to the chromosome; the centrosome shows a similar level of complexity in regulating the minus ends of MTs and anchoring them in a radial array. The association between MTs and CENP-F is seen in another cellular process: vesicular transport with SNARE proteins SNAP25 and syntaxin 4 (Pooley et al., 2008; Pooley et al., 2006). Vesicular trafficking is highly dependent on regulated association with MTs (Caviston and Holzbaur, 2006; Hehnly and Stamnes, 2007; Ishiki and Klip, 2005; Soldati and Schliwa, 2006; Vedrenne and Hauri, 2006). In this study, we have identified a third MT-related process regulated by CENP-F: centrosomal MT nucleation and anchoring. Taken together, these roles suggest CENP-F as a global linker protein to the MT network with many different

organelles. Indeed, with so many unexplored motifs on this large protein, there are various other modalities possible within this context of CENP-F function.

Acknowledgements

We thank Dr. Kramer (UT Southwestern) for the Hook2 reagents, Dr. Kilkenny Rocheleau for her microscopy expertise, Samyukta Reddy for her work with the yeast two-hybrid, Dr. Soukoulis for his CENP-F antibody development, and members of the Bader and Dees laboratories for helpful discussions and critical reading of this manuscript. Some experiments and data analysis were performed in part through the use of the VUMC Cell Imaging Shared Resource (supported by NIH grants CA68485, DK20593, DK58404, HD15052, DK59637 and EY08126) and the Imaging Resource of the Epithelial Biology Center. We are thankful for the following support: K.L.M., American Heart Predoctoral grant 09PRE2170006; P.M.M., American Heart Predoctoral grant 09PRE2260729; I.K., NIH NIGMS grant 1R01GM078373-01; and D.M.B., NIH grant R01HL037675

References

Altschul, S. F. and Lipman, D. J. (1990). Protein database searches for multiple alignments. *Proc Natl Acad Sci USA* **87**, 5509-13.

Ashar, H. R., James, L., Gray, K., Carr, D., Black, S., Armstrong, L., Bishop, W. R. and Kirschmeier, P. (2000). Farnesyl transferase inhibitors block the farnesylation of CENP-E and CENP-F and alter the association of CENP-E with the microtubules. *J Biol Chem* **275**, 30451-7.

Ashe, M., Pabon-Peña, L., Dees, E., Price, K. L. and Bader, D. (2004). LEK1 is a potential inhibitor of pocket protein-mediated cellular processes. *J Biol Chem* **279**, 664-76.

Azimzadeh, J. and Bornens, M. (2007). Structure and duplication of the centrosome. *Journal of Cell Science* **120**, 2139-42.

Balczon, R., Simerly, C., Takahashi, D. and Schatten, G. (2002). Arrest of cell cycle progression during first interphase in murine zygotes microinjected with anti-PCM-1 antibodies. *Cell Motil Cytoskeleton* **52**, 183-92.
Bomont, P., Maddox, P., Shah, J. V., Desai, A. B. and Cleveland, D. W. (2005). Unstable microtubule capture at kinetochores depleted of the centromere-associated protein CENP-F. *EMBO J* **24**, 3927-39.
Bouckson-Castaing, V., Moudjou, M., Ferguson, D. J., Mucklow, S., Belkaid, Y., Milon, G. and Crocker, P. R. (1996). Molecular characterisation of ninein, a new coiled-coil protein of the centrosome. *Journal of Cell Science* **109 (Pt 1)**, 179-90.
Caviston, J. P. and Holzbaur, E. L. (2006). Microtubule motors at the intersection of trafficking and transport. *Trends Cell Biol* **16**, 530-7.
Chakravarty, A., Howard, L. and Compton, D. A. (2004). A mechanistic model for the organization of microtubule asters by motor and non-motor proteins in a mammalian mitotic extract. *Mol Biol Cell* **15**, 2116-32.
Clark, I. B. and Meyer, D. I. (1999). Overexpression of normal and mutant Arp1alpha (centractin) differentially affects microtubule organization during mitosis and interphase. *Journal of Cell Science* **112 (Pt 20)**, 3507-18.
Dammermann, A. and Merdes, A. (2002). Assembly of centrosomal proteins and microtubule organization depends on PCM-1. *The Journal of Cell Biology* **159**, 255-66.
Dees, E., Pabón-Peña, L. M., Goodwin, R. L. and Bader, D. (2000). Characterization of CMF1 in avian skeletal muscle. *Dev Dyn* **219**, 169-81.
Delgehyr, N., Sillibourne, J. and Bornens, M. (2005). Microtubule nucleation and anchoring at the centrosome are independent processes linked by ninein function. *Journal of Cell Science* **118**, 1565-75.
Efimov, A., Kharitonov, A., Efimova, N., Loncarek, J., Miller, P. M., Andreyeva, N., Gleeson, P., Galjart, N., Maia, A. R., McLeod, I. X. et al. (2007). Asymmetric CLASP-dependent nucleation of noncentrosomal microtubules at the trans-Golgi network. *Developmental Cell* **12**, 917-30.
Evans, H. J., Edwards, L. and Goodwin, R. L. (2007). Conserved C-terminal domains of mCenp-F (LEK1) regulate subcellular localization and mitotic checkpoint delay. *Experimental Cell Research* **313**, 2427-37.
Feng, J., Huang, H. and Yen, T. J. (2006). CENP-F is a novel microtubule-binding protein that is essential for kinetochore attachments and affects the duration of the mitotic checkpoint delay. *Chromosoma* **115**, 320-9.
Fumoto, K., Kadono, M., Izumi, N. and Kikuchi, A. (2009). Axin localizes to the centrosome and is involved in microtubule nucleation. *EMBO Rep* **10**, 606-13.
Gönczy, P. (2004). Centrosomes: hooked on the nucleus. *Curr Biol* **14**, R268-70.
Goodwin, R. L., Pabón-Peña, L. M., Foster, G. C. and Bader, D. (1999). The cloning and analysis of LEK1 identifies variations in the LEK/centromere protein F/mitosin gene family. *J Biol Chem* **274**, 18597-604.
Hames, R. S., Crookes, R. E., Straatman, K. R., Merdes, A., Hayes, M. J., Faragher, A. J. and Fry, A. M. (2005). Dynamic recruitment of Nek2 kinase to the centrosome involves microtubules, PCM-1, and localized proteasomal degradation. *Mol Biol Cell* **16**, 1711-24.

Hehnly, H. and Stamnes, M. (2007). Regulating cytoskeleton-based vesicle motility. *FEBS Lett* **581**, 2112-8.
Holt, S. V., Vergnolle, M. A., Hussein, D., Wozniak, M. J., Allan, V. J. and Taylor, S. S. (2005). Silencing Cenp-F weakens centromeric cohesion, prevents chromosome alignment and activates the spindle checkpoint. *Journal of Cell Science* **118**, 4889-900.
Hussein, D. and Taylor, S. S. (2002). Farnesylation of Cenp-F is required for G2/M progression and degradation after mitosis. *Journal of Cell Science* **115**, 3403-14.
Ishiki, M. and Klip, A. (2005). Minireview: recent developments in the regulation of glucose transporter-4 traffic: new signals, locations, and partners. *Endocrinology* **146**, 5071-8.
Kubo, A., Sasaki, H., Yuba-Kubo, A., Tsukita, S. and Shiina, N. (1999). Centriolar satellites: molecular characterization, ATP-dependent movement toward centrioles and possible involvement in ciliogenesis. *The Journal of Cell Biology* **147**, 969-80.
Laoukili, J., Kooistra, M. R., Brás, A., Kauw, J., Kerkhoven, R. M., Morrison, A., Clevers, H. and Medema, R. H. (2005). FoxM1 is required for execution of the mitotic programme and chromosome stability. *Nat Cell Biol* **7**, 126-36.
Liao, H., Winkfein, R. J., Mack, G., Rattner, J. B. and Yen, T. J. (1995). CENP-F is a protein of the nuclear matrix that assembles onto kinetochores at late G2 and is rapidly degraded after mitosis. *The Journal of Cell Biology* **130**, 507-18.
Lin, C. C., Cheng, T. S., Hsu, C. M., Wu, C. H., Chang, L. S., Shen, Z. S., Yeh, H. M., Chang, L. K., Howng, S. L. and Hong, Y. R. (2006). Characterization and functional aspects of human ninein isoforms that regulated by centrosomal targeting signals and evidence for docking sites to direct gamma-tubulin. *Cell Cycle* **5**, 2517-27.
Linstedt, A. D. (2004). Positioning the Golgi apparatus. *Cell* **118**, 271-2.
Litvin, J., Montgomery, M. O., Goldhamer, D. J., Emerson, C. P. and Bader, D. M. (1993). Identification of DNA-binding protein(s) in the developing heart. *Developmental Biology* **156**, 409-17.
Mack, G. J., Rees, J., Sandblom, O., Balczon, R., Fritzler, M. J. and Rattner, J. B. (1998). Autoantibodies to a group of centrosomal proteins in human autoimmune sera reactive with the centrosome. *Arthritis Rheum* **41**, 551-8.
Malone, C. J., Misner, L., Le Bot, N., Tsai, M. C., Campbell, J. M., Ahringer, J. and White, J. G. (2003). The C. elegans hook protein, ZYG-12, mediates the essential attachment between the centrosome and nucleus. *Cell* **115**, 825-36.
Mendoza-Lujambio, I., Burfeind, P., Dixkens, C., Meinhardt, A., Hoyer-Fender, S., Engel, W. and Neesen, J. (2002). The Hook1 gene is non-functional in the abnormal spermatozoon head shape (azh) mutant mouse. *Human Molecular Genetics* **11**, 1647-58.
Mogensen, M. M., Malik, A., Piel, M., Bouckson-Castaing, V. and Bornens, M. (2000). Microtubule minus-end anchorage at centrosomal and non-centrosomal sites: the role of ninein. *Journal of Cell Science* **113 (Pt 17)**, 3013-23.

Moore, L. L., Morrison, M. and Roth, M. B. (1999). HCP-1, a protein involved in chromosome segregation, is localized to the centromere of mitotic chromosomes in Caenorhabditis elegans. *The Journal of Cell Biology* **147**, 471-80.
Moynihan, K., Pooley, R., Miller, P., Kaverina, I. and Bader, D. (2009). Murine CENP-F Regulates Centrosomal Microtubule Nucleation and Interacts with Hook2 at the Centrosome. *Mol Biol Cell*.
Ortiz, J., Stemmann, O., Rank, S. and Lechner, J. (1999). A putative protein complex consisting of Ctf19, Mcm21, and Okp1 represents a missing link in the budding yeast kinetochore. *Genes Dev* **13**, 1140-55.
Ou, Y. Y., Mack, G. J., Zhang, M. and Rattner, J. B. (2002). CEP110 and ninein are located in a specific domain of the centrosome associated with centrosome maturation. *Journal of Cell Science* **115**, 1825-35.
Pooley, R. D., Moynihan, K. L., Soukoulis, V. and Reddy, S. (2008). Murine CENPF interacts with syntaxin 4 in the regulation of vesicular transport. *Journal of Cell Science*.
Pooley, R. D., Reddy, S., Soukoulis, V., Roland, J. T., Goldenring, J. R. and Bader, D. M. (2006). CytLEK1 is a regulator of plasma membrane recycling through its interaction with SNAP-25. *Mol Biol Cell* **17**, 3176-86.
Quintyne, N. J., Gill, S. R., Eckley, D. M., Crego, C. L., Compton, D. A. and Schroer, T. A. (1999). Dynactin is required for microtubule anchoring at centrosomes. *The Journal of Cell Biology* **147**, 321-34.
Rattner, J. B., Rao, A., Fritzler, M. J., Valencia, D. W. and Yen, T. J. (1993). CENP-F is a .ca 400 kDa kinetochore protein that exhibits a cell-cycle dependent localization. *Cell Motil Cytoskeleton* **26**, 214-26.
Redkar, A., deRiel, J. K., Xu, Y. S., Montgomery, M., Patwardhan, V. and Litvin, J. (2002). Characterization of cardiac muscle factor 1 sequence motifs: retinoblastoma protein binding and nuclear localization. *Gene* **282**, 53-64.
Robertson, J. B., Zhu, T., Nasreen, S., Kilkenny, D., Bader, D. and Dees, E. (2008). CMF1-Rb interaction promotes myogenesis in avian skeletal myoblasts. *Dev Dyn* **237**, 1424-33.
Soldati, T. and Schliwa, M. (2006). Powering membrane traffic in endocytosis and recycling. *Nat Rev Mol Cell Biol* **7**, 897-908.
Soukoulis, V., Reddy, S., Pooley, R. D., Feng, Y., Walsh, C. A. and Bader, D. M. (2005). Cytoplasmic LEK1 is a regulator of microtubule function through its interaction with the LIS1 pathway. *Proc Natl Acad Sci USA* **102**, 8549-54.
Srsen, V., Gnadt, N., Dammermann, A. and Merdes, A. (2006). Inhibition of centrosome protein assembly leads to p53-dependent exit from the cell cycle. *The Journal of Cell Biology* **174**, 625-30.
Stillwell, E. E., Zhou, J. and Joshi, H. C. (2004). Human ninein is a centrosomal autoantigen recognized by CREST patient sera and plays a regulatory role in microtubule nucleation. *Cell Cycle* **3**, 923-30.
Szebenyi, G., Hall, B., Yu, R., Hashim, A. and Krämer, H. (2007). Hook2 Localizes to the Centrosome, Binds Directly to Centriolin/CEP110 and Contributes to Centrosomal Function. *Traffic* **8**, 32-46.
Vedrenne, C. and Hauri, H. P. (2006). Morphogenesis of the endoplasmic reticulum: beyond active membrane expansion. *Traffic* **7**, 639-46.

Vergnolle, M. A. and Taylor, S. S. (2007). Cenp-F links kinetochores to Ndel1/Nde1/Lis1/dynein microtubule motor complexes. *Curr Biol* **17**, 1173-9.
Walenta, J. H., Didier, A. J., Liu, X. and Krämer, H. (2001). The Golgi-associated hook3 protein is a member of a novel family of microtubule-binding proteins. *The Journal of Cell Biology* **152**, 923-34.
Wei, Y., Bader, D. and Litvin, J. (1996). Identification of a novel cardiac-specific transcript critical for cardiac myocyte differentiation. *Development* **122**, 2779-89.
Yang, Z., Guo, J., Chen, Q., Ding, C., Du, J. and Zhu, X. (2005). Silencing mitosin induces misaligned chromosomes, premature chromosome decondensation before anaphase onset, and mitotic cell death. *Mol Cell Biol* **25**, 4062-74.
Zhapparova, O. N., Burakov, A. V. and Nadezhdina, E. S. (2007). The centrosome keeps nucleating microtubules but looses the ability to anchor them after the inhibition of dynein-dynactin complex. *Biochemistry Mosc* **72**, 1233-40.
Zhou, X., Wang, R., Fan, L., Li, Y., Ma, L., Yang, Z., Yu, W., Jing, N. and Zhu, X. (2005). Mitosin/CENP-F as a negative regulator of activating transcription factor-4. *Journal of Biological Chemistry* **280**, 13973-13977.
Zhu, X., Chang, K. H., He, D., Mancini, M. A., Brinkley, W. R. and Lee, W. H. (1995a). The C terminus of mitosin is essential for its nuclear localization, centromere/kinetochore targeting, and dimerization. *J Biol Chem* **270**, 19545-50.
Zhu, X., Mancini, M. A., Chang, K. H., Liu, C. Y., Chen, C. F., Shan, B., Jones, D., Yang-Feng, T. L. and Lee, W. H. (1995b). Characterization of a novel 350-kilodalton nuclear phosphoprotein that is specifically involved in mitotic-phase progression. *Mol Cell Biol* **15**, 5017-29.
Zuccolo, M., Alves, A., Galy, V., Bolhy, S., Formstecher, E., Racine, V., Sibarita, J. B., Fukagawa, T., Shiekhattar, R., Yen, T. et al. (2007). The human Nup107-160 nuclear pore subcomplex contributes to proper kinetochore functions. *EMBO J* **26**, 1853-64.

CHAPTER IV

AN OVERVIEW OF AVIAN HEART STRUCTURE AND DEVELOPMENT

This chapter is published under the same title in *Heart Development and Regeneration*, 2009 (Moynihan et al., 2009b).

Overview

The avian, and more specifically the chicken, heart has provided a key experimental model for the developmental biologist. Advances in the regulation of cardiac myogenesis using genetic models have provided key insights. Still, the avian heart remains as one of the most accessible models for the manipulation of cardiac, epicardial, and endothelial differentiation in heart development. The avian heart has so many advantages to the experimental zoologist that it seems hard to think of the analysis of cardiac developmental biology without it. We have been asked to provide a chapter on the avian heart in overview. In writing this chapter, we have made a conscious decision to focus solely on the avian, and in most cases, the chicken heart and have focused our attention on the cardiac myocyte and myocardium with reference to the overall differentiation and morphogenesis of the heart. The discussion of the cardiac myocyte is framed in the overall context of the developing heart. For a more in depth discussion of the development of the endo- and epicardium, readers are asked to survey other chapters. Finally, this chapter relies heavily on work that examines avian heart

structure and studies particularly using experimental zoology to understand mechanisms regulating cardiac myogenesis.

Anatomy of the chicken heart

The anatomy of the avian heart is very similar to that of the mammalian heart, yet offers deviations unique to its specific niche. Both of these vertebrate classes demonstrate a significant demand for oxygen while maintaining homiothermy. The highly conserved four-chambered heart separates the pulmonary and systemic circulatory pathways to meet these demands (Proctor and Lynch, 1993). The anterior cardiac chambers, the atria, and the posterior chambers, the ventricles, lie in series between the two circulation paths and serve to repressurize the blood. The entire organ is enclosed in fluid within the thin, fibrous perdicardial sac and is located in the thoracoabdominal cavity (Whittow and Sturkie, 2000). However, the physical act of flight, mostly restricted to birds, is more strenuous than any other activity and requires some basic modification of the heart. The avian heart is significantly heavier in proportion to its body weight than all other vertebrates (Proctor and Lynch, 1993). By combining this larger size with its bigger stroke volume, the output of the avian cardiovascular system can carry enough oxygen to muscular tissue to sustain flight.

Circulation, chambers, and valves

The four-chambered heart moves the blood through the pulmonary and somatic circuits with each contraction. Deoxygenated blood returns from the body and enters anteriorly into the right atrium. This atrium tends to be much larger than its left counterpart but both have relatively thin walls and no inflow valves (Whittow and Sturkie, 2000). The blood then moves through the right atrioventricular (AV) valve and into the right ventricle. This valve is a single spiral plane of myocardium, significantly different from the fibrous flap of the mammalian heart (Lu et al., 1993a; Lu et al., 1993b) (Figure 4.1). It even has a ring of conduction tissue around the aperture, suggesting that muscular contraction may play a role during valve closure (Lu et al., 1993a; Lu et al., 1993b). The right ventricle is the less muscular of the two lower chambers and does not extend to the apex of the heart. It compresses and sends a volume of blood through the pulmonary arteries to the lungs, a route not requiring extensive pressure. The outflow valve here is made up of three semilunar cusps. Once oxygenated, the blood returns to the heart via the pulmonary veins and enters the left atrium. It passes through the left AV valve and into the highly muscular left ventricle. This AV valve is also encircled by conduction fibers, again suggesting deviation from the passive nature of mammalian valve leaflets. The muscular wall of the left ventricle is two to three times thicker than its right counterpart and its cone shape extends all the way to the apex of the heart (Whittow and Sturkie, 2000). This chamber empties with considerable force through the aortic outflow valve, comprised of three rigid cusps linked to the left

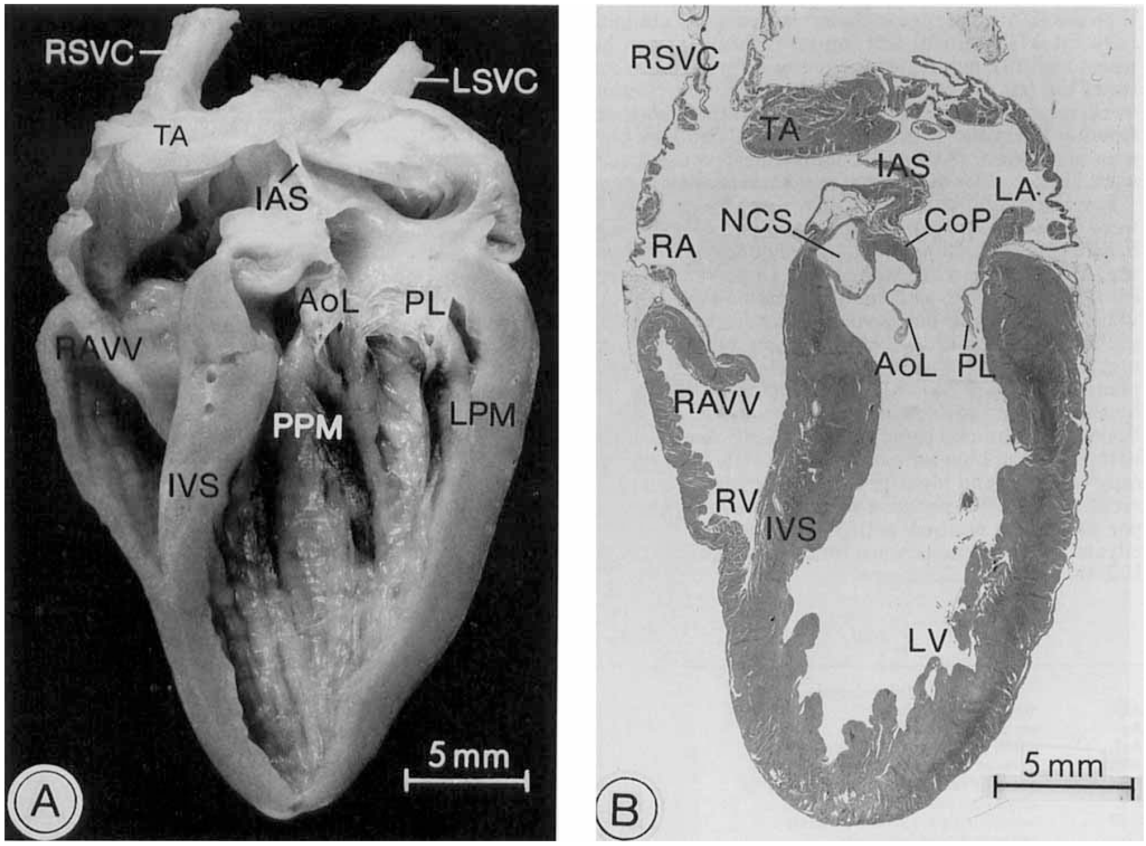

Figure 4.1. Anterior view of adult chicken heart. This diagram shows a longitudinal section from an adult avian heart orginally published by Lu et al. (Lu et al., 1993a). This diagram illustrates the basic structure of the avian heart with the relative thicknesses of atria (RA and LA) and ventricles (RV and LV). The ventricles are relatively thicker than the atria and have significant trabeculation. The interventricular septum is also thick. Note that the right ventricle does not extend to the apex of the heart. The left atrioventricular value leaflets are relatively thin and are linked to the ventricular wall by chordae tendinae and papillary muscles. The right atrioventricular value has only one lateral leaflet (arrowhead). The atria can be very thin. RA, right atrium; LA, left atrium; RV, right ventricle; LV, left ventricle.

AV valve by an arch of cardiac muscle (Lu et al., 1993a). This chamber delivers blood to the rest of the body first as it passes through the aortic arch, which branches to the right in birds unlike mammals.

Coronary circulation and conduction

The coronary vessels originate immediately above the aortic outflow valve as two sinuses leading to the right and left branches. The right coronary artery tends to be the dominant of the two in most species, but both begin with a split into a superficial and deep branch on either side of the heart. The dominant branch supports the left ventricular myocardium, intraventricular septum, the apex, and the dorsal walls of the atria (West, 1981). The arteries form frequent anastomoses en route to capillary beds and venous blood is returned to the heart via five groups of cardiac veins, also prone to anastomoses. Relative to other avian tissues this circulatory system leads to a highly perfused myocardium. Additionally, blood flow increases with reduction in the oxygen supply, allowing high-altitude flight.

Systemic circulation emanating from the heart is dependent on the conduction system prompting chamber contraction. This conduction system relies on electrical impulses initiated by the pacemaker cells of the sinoatrial (SA) node on the anterior side of the right atrium. Cardiac myocytes carry this signal through low-resistance pathways; the intercalated disc uses physical (desmosome) and electrical (nexus) connections between cells to couple many

individual cells to work as a unit. This signal sweeps through both atria, causing depolarization, and thus, contraction. Mathur and Shrivastava demonstrated the presence of distinct bundle branches connecting the SA node with the atrioventricular (AV) node across the atria (Mathur and Shrivastava, 1979). The presence of these structures in mammalian hearts has been a point of debate. Once the signal reaches the AV node, it is then delayed, moving at a rate two to three orders of magnitude slower at the atrioventricular (AV) node to allow the atria to empty. It should be noted that Szabo et al. reported that light and electron microscopic examination of the AV junction in avian species did not reveal a distinct AV node when compared to other classes of vertebrates (Szabo et al., 1986). They determined that myocytes of an AV ring that has contact with working atrial myocytes served as the AV node. Conduction system myocytes represent the only myogenic connection between the adult atria and ventricles.

The His bundle and its three branches extend from the AV node and are invested in connective tissue (Szabo et al., 1986). Two of the bundles branch into subendocardium of the left and right ventricles and follow the pathways of the coronary arteries. The third bundle takes an unusual route up around the aorta and connects to the avian-specific ring around the right AV valve (Lu et al., 1993a; Lu et al., 1993b). These branches disperse as they enter the myocardium and connect with the terminal cells of the conduction system, the Purkinje fibers. These cells are large, elongated cardiac myocytes that conduct electrical impulses to the working myocardium. Their conductivity is much faster

than cardiomyocytes of the atrial and ventricular walls. Many groups have studied the variation in gene expression in avian conduction system myocytes. There are many immunochemical reagents available to identifying these cells within the developing and adult heart (de Groot et al., 1985; Gonzalez-Sanchez and Bader, 1985; Takebayashi-Suzuki et al., 2001; Takebayashi-Suzuki et al., 2000). Gonzalez-Sanchez and Bader suggested that a common myosin heavy chain was expressed in both the atrial and ventricular muscle components of the avian conduction system (Gonzalez-Sanchez and Bader, 1985). However, all of these studies attest to the diversity among these specialized myocytes in the ventricular wall even though they are derived from common working myocytes (see below).

Histology

The histology of the avian heart is very similar to the mammalian heart. The heart tissue is comprised of three layers – the epicardium, myocardium, and endocardium. The epicardium and endocardium are similar in structure: loose connective tissue supporting a simple squamous layer of mesothelium or endothelium. The two layers are separated by myocardium, a layer of striated muscle fibers, which differs within the heart only by its significantly thicker presence in the ventricles. This particular layer does differ in three ways from mammalian cardiac muscle. Avian striated muscle bands lack M-bands, the significance of which is unknown. The muscle bands are also much shorter in diameter than those of mammals, leading to a much higher number of cells/unit

volume within the organ. Avian myocardial cells also lack transverse tubules (T tubules) and instead use junctional processes as “couplings” between the sarcoplasmic reticulum and plasmalemma (Hirakow, 1970; Sommer et al., 1991; Sommer and Johnson, 1969; Whittow and Sturkie, 2000).

Differentiated atrial, ventricular and conduction myocytes express distinct myosin heavy chains, which have been used to trace the embryogenesis of their cell lineages. Interestingly, avian hearts express more than just the alpha and beta-type MyHCs detected in mammalian hearts and antibodies exist for many of these additional myosin isoforms (Evans et al., 1988; Gonzalez-Sanchez and Bader, 1984; Gonzalez-Sanchez and Bader, 1985; Stockdale, 1992; Stockdale et al., 2002; Wang et al., 1996). The regulation of gene expression in developing and adult hearts is explored in depth in other chapters.

Development: an overview

The avian embryo has provided a critical model for the analysis of cardiac development. Aristotle is one of the first scientists to publish on the use of avian embryos to study heart development. More recent publications ((Malpighi, 1672); Rosenthal and Harvey, this scholarly tome) attest to the value of the avian embryo as a model of heart development.

The work of Waddington, Butler, Patton, DeHaan and colleagues in the chick embryo, laid the foundation for molecular approaches to cardiogenic

commitment and differentiation (Manner, 2000). Anyone who has worked with both avian and mammalian embryos knows that mRNA expression boundaries seem to be sharper, that cardiogenic tissue is more easily obtained, and experimental manipulations more easily executed in the embryos of birds. The procurement and availability of the embryo has certainly been a large factor in its use. More importantly, experimental zoologists have long understood that the hardy nature and resilience of this embryo makes it an outstanding model for study of cardiac development even in the absence of genomic manipulation. McCain and McLaughlin give a wonderful compilation of methodologies pertaining to isolation, morphology and analysis of whole chicken hearts of the early embryo at http://www.zoo.utoronto.ca/able/volumes/vol-20/4-mccain.pdf (McCain, 1998). Additionally, advances in lineage marking with viral systems (Mikawa, 1995; Mikawa et al., 1992; Mikawa and Fischman, 1992; Mjaatvedt et al., 2001) and vital dyes (Gonzalez-Sanchez and Bader, 1990; Mjaatvedt et al., 2001; Satin et al., 1988) are particularly amenable to the avian embryo and the heart in particular. In this section of the chapter we will discuss the basic development of the avian heart with reference to the cardiac myocytes and present methods that are particularly useful for experimentation in this system.

Determination and earliest development

The avian epiblast contains cells that will give rise to the embryo proper. The posterior thickening of the epiblast, called Koller's sickle, can be seen at stage 2 (Hamburger and Hamilton, 1992). With its anterior, mid-line movement or

extension, Koller's sickle gives rise to the primitive streak. Cardiomyogenic cells of the heart are some of the first to ingress during formation of the primitive streak. The studies of Garcia-Martinez and Schoenwolf (Garcia-Martinez and Schoenwolf, 1993) established the location of cardiomyogenic progenitors in the pre-gastrulated chicken embryo and are pictured in Figure 4.2. Cells were mapped using vital dyes in the primitive streak (stages 2 and 3) and these studies revealed that progenitors were located in the anterior region of the structure. This domain extends 125-700 microns from the anterior-most tip of the primitive streak. It should be noted that the cells at the very anterior tip of the streak are not cardiogenic but are fated to the notochord (Garcia-Martinez and Schoenwolf, 1993). In addition, cardiac progenitors were shown to be arranged in an anteroposterior fashion within the streak and that the anterior-most cells were destined to form the conus and ventricles. In turn, the more posteriorly positioned cells were fated to the atria and outflow tract.

Experimental manipulation of avian cardiac progenitors *in vitro* is a highly important and continuously employed procedure used by scientists interested in heart development. Identification and isolation of these progenitors is key for further work in this area to elucidate mechanisms regulating cardiogenic commitment and differentiation. Further, because disagreement exists on the position of these progenitors in the lateral plate, we will emphasize recent mapping studies here. Several mapping and extirpation analyses of gastrulating chicken embryos demonstrate the presence of cardiac progenitors in the

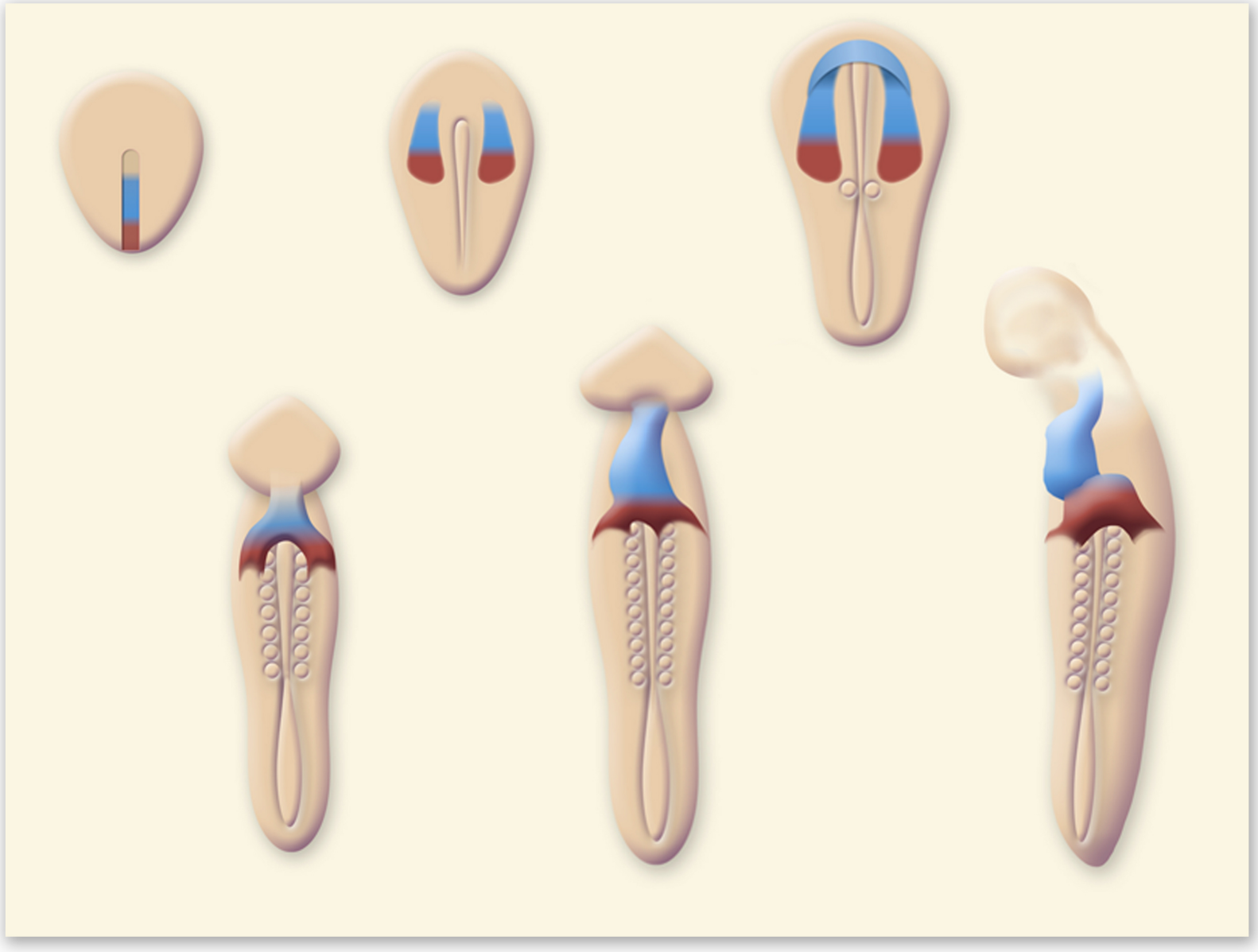

Figure 4.2. Fate maps of cardiogenic progenitors and myocytes in the early avian embryo. The relative position of atrial and ventricular myogenic cells in the primitive streak at stage 3 through 13 (Garcia-Martinez and Schoenwolf, 1993; Yutzey and Bader, 1995; Yutzey et al., 1994) (modified from these three publications). Solid black represents the relative position of atrial progenitors and myocytes while the stippled area depicts the regions occupied by ventriculogenic cells. For precise localization using in situ hybridization in post-gastrulated embryos see (Yutzey et al., 1994).

primitive streak at late stage 3 (Garcia-Martinez and Schoenwolf, 1993) and all agree that progenitors have migrated out of the streak at stage 4. Controversy arises regarding the position of cardiomyogenic cells after they leave the primitive streak. Our goal here is to present a clear picture of the two views concerning the positions of post-gastrulated, pre-differentiated progenitors in the lateral plate. In that way, the investigator should be able to isolate and culture cells and determine the location of progenitors for their experiment. The first issue to consider is the medial-lateral position of cardiac progenitors after gastrulation. Rosenquist and later Redkar et al used radioactive and DiI labeling of stage 5-8 chicken embryos with subsequent differentiation to localize progenitors to mesodermal regions directly ventral to the developing neural plate (Redkar et al., 2001; Rosenquist, 1970b). This is a “very medial” position with reference to the zona pellucida. Conversely, DeHaan (1963), Stahlsberg and DeHaan (1989) and Ehrman and Yutzey (1999) localized cells of cardiomyogenic potential to a much more lateral position (Dehaan, 1963; Ehrman and Yutzey, 1999; Stalsberg and DeHaan, 1969). Indeed, these studies suggested that these progenitors are near to the lateral boundary of the zona pellucida (i.e. at the lateral edge of the embryonic mesoderm). While there is agreement concerning the anterior deposition of progenitors just superior to the anterior intestinal portal (Yutzey et al., 1995), the limits of the posterior (atrial forming domain) boundary are disputed. Surface labeling and time lapse studies of Ehrman and Yutzey (Ehrman and Yutzey, 1999) put the posterior boundary of heart-forming cells at the level of the first condensing somite in the stage 7 embryo. But, radioisotope

and DiI labeling analyses determined that this boundary extended more posteriorly (Redkar et al., 2001; Rosenquist, 1970b). With isolation of stage 4-8 chicken embryos using the methods outlined by Gannon and Bader (Gannon and Bader, 1995), the individual investigator can easily resolve this issue in their own laboratory.

There is little chance for interaction between anterior and posterior progenitors as they leave the streak in a temporally determined fashion (anterior, first; posterior, last) and they apparently move to like-positioned stations in the lateral mesoderm. The lateral mesoderm is first to lose mesenchymal structure quickly forming a definitive epithelium (Osler and Bader, 2004). All cardiomyogenic cells have left the streak by stage 4. Conversely, endocardial cells are still present in the streak at this stage.

Studies on the position of cardiogenic mesoderm in the anterior lateral plate mesoderm of the chicken embryo began over 60 years ago (Rawles, 1952) and have continued to nearly the present day (Dehaan, 1963; DeHaan and Ursprung, 1965; Ehrman and Yutzey, 1999; Gannon and Bader, 1995; Gannon and Bader, 1997; Montgomery et al., 1994; Redkar et al., 2001; Rosenquist, 1970a; Rosenquist, 1970b; Satin et al., 1988; Stalsberg and DeHaan, 1968; Stalsberg and DeHaan, 1969; Yutzey and Bader, 1995; Yutzey et al., 1994). While the precise location of myocyte progenitors is still not completely resolved, it is generally agreed that two regions of anterior splanchnic mesoderm

positioned lateral to midline and separated by 800 microns comprise much of the embryo's native cardiogenic potential (Stalsberg and DeHaan, 1969). When embryos are isolated by a "paper ring" method described below and viewed in a dissecting microscope, cardiac progenitors can be visualized by their greater opacity relative to the adjoining tissue (Gannon and Bader, 1997). This bilaterally positioned tissue has been referred to as the cardiogenic crescent. At stage 6, these cells form an elongated horseshoe that approaches or possibly abuts the midline anterior to the forming anterior intestinal portal (Figure 4.3).

The actual "mechanism of movement" of myogenic cells from the streak to their positions in lateral mesoderm has not been established. It is assumed that single cells or small groups of cells move laterally prior to stage 4 and take up assigned positions in the lateral mesoderm but to our knowledge real-time analysis of cell movement in the avian embryo has not been reported. Interestingly, lineage marking and grafting studies support the idea that anteroposterior mixing of cells does not occur during this or subsequent timeframes (Gonzalez-Sanchez and Bader, 1990; Rosenquist, 1970b; Satin et al., 1988; Stalsberg and DeHaan, 1969). By stage 6 and beginning in the anterior region of the cardiogenic mesoderm, an intact and polarized epithelium is formed (for examples of this situation see (Osler and Bader, 2004)). Cardiogenic mesoderm and resulting cardiac muscle remains polarized throughout formation of the looping heart tube and subsequent chamber formation (Peng et al., 1990). Until trabeculation begins, cardiomyogenic morphogenesis is driven by epithelial

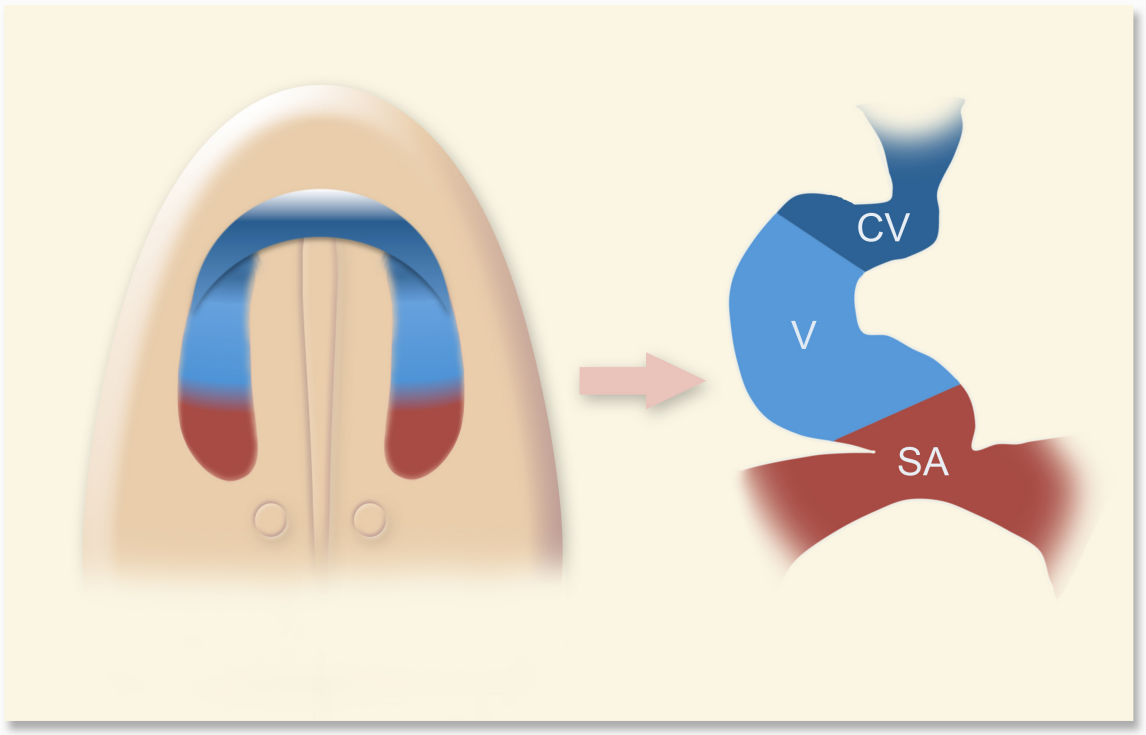

Figure 4.3. Position of cardiogenic cells at stage 6 in the developing chicken embryo. Redrawn from DeHaan (DeHaan and Ursprung, 1965). Fate maps of cells at stage 6 have determined the relative positions of cells that incorporate into the chicken heart tube. Several investigators have used this classic map to isolate cells of ventriculogenic and atriogenic potential and DeHaan's early work remains a reliable departure point for studies in this area. CV, conoventricular tissue; V, ventricles; SA, sinoatrium,

movement, folding and remodeling. The importance of forming a cardiogenic epithelium has not been resolved. Differences in the cardiogenic potential along the anteroposterior axis, with regard to ventricular or atrial differentiation have been noted (Gannon and Bader, 1995; Gannon and Bader, 1997; Yutzey and Bader, 1995; Yutzey et al., 1994).

Cardiogenic determination

Slack defines “specification” as the ability of a cell to express a certain phenotype in a neutral environment (such as cell culture) whereas “determination” is the ability to differentiate within different cellular environments (such as a different locale in the embryo) (Slack, 1991). Gilbert defines “determination” as the cell’s commitment to eventually differentiate into a specific cell type and into no other tissue (Gilbert, 2006). Applying this principal to cardiac myogenesis is difficult and, to our knowledge, has not often been directly tested. Le Douarin conducted heterotopic transplantation of cardiogenic tissue to non-cardiogenic regions of the embryo and reported an early commitment to the lineage (Le Douarin et al., 1965). When epiblast cells of the chicken embryo are isolated and plated at high density in vitro, cardiac myocytes are observed (Montgomery et al., 1994), suggesting that the physical act of gastrulation is not required for cardiac myocyte differentiation. At low density, this differentiation is not observed. Conversely, stage 4 cardiogenic mesoderm can be isolated, dispersed into single cells and cultured at clonal density. The cells within these clones readily expressed markers of cardiac myocytes (Gonzalez-Sanchez and

Bader, 1990), suggesting that no additional signals are needed to propel these cells into their final state of differentiation. In addition, Antin and colleagues have demonstrated the importance of activin in the early commitment of epiblast cells to the cardiogenic cell lineage (Yatskievych et al., 1997). Taken together, these data suggest that pre-gastrulated cells are not as “determined” as post-gastrulated cells. Still, while genetic regulatory networks have been identified that are essential for cardiogenic determination (Firulli and Thattaliyath, 2002), the exact program governing conversion of mesodermal cells into determined cardiac “myoblast” has not been identified for the chicken or any other organism.

Cardiomyogenic potential is not completely restricted to the cardiogenic crescent. As we will see below, conversion of non-cardiogenic mesoderm to this lineage can be accomplished by culturing explants with specific growth factors that promote cardiac differentiation (Barron et al., 2000; Lough et al., 1996; Schultheiss et al., 1995). These conversions were “induced” by application of exogenous factors. Additionally, Mjaatvedt et al. and Waldo et al. have defined an “anterior heart field” that contributes myocytes to the conus and truncus and originates separately from mesoderm located anterior to the initial cardiac heart tube (Mjaatvedt et al., 2001; Waldo et al., 2005). These results are corroborated by studies in the mouse (Kelly et al., 2001; Verzi et al., 2005). Also, Kruithof et al have recently demonstrated that the proepicardium contributes cardiac myocytes to the inflow tract of the heart (Kruithof et al., 2006). Thus, while it is clear that the cardiogenic crescent is the major contributor to the differentiated myocardium,

other cells (the so called anterior heart field) and proepicardium normally differentiate into cardiac myocytes. Additionally, other cells in the embryo can be induced to take on this cellular phenotype.

Inducers of cardiomyogenic determination

A major question in the development of cardiac myocytes is what signals regulate the conversion of mesodermal, or even pre-mesodermal, cells to the cardiomyogenic cell lineage. Obviously, a first step in these analyses is to determine when cells take on cardiogenic potential. Interestingly, few reports exist examining this issue. As stated above, Montgomery et al demonstrated that pre-gastrulated epiblast cells can differentiate into cardiac myocytes when grown at high density in serum-containing medium (Montgomery et al., 1994). This suggests that simple events may govern the conversion of embryonic cells to the cardiogenic lineage. Corroborating this theme are the many reports of mouse ES cells robustly differentiating into cardiac myocytes under simple culture conditions (Bettiol et al., 2006; van Laake et al., 2006). While these studies in avian species supported the notion that embryonic cells are receptive to inducing signals, they did not identify the factors.

Several groups have used the chicken or quail embryo to analyze soluble factors that regulate cardiogenic specification. This specification is driven by inducing signals that might arise from adjacent tissues or from the target cells themselves. The avian heart has been used as a model system to identify factors

inducing cardiogenic determination. BMPs, FGFs and TGF-beta have all been identified as key inducers (Barron et al., 2000; Ladd et al., 1998; Marvin et al., 2001; Pabon-Pena et al., 2000; Schlange et al., 2000; Sugi and Lough, 1994). Ectopic application of these agents can induce cardiogenic differentiation in medial, anterior mesoderm or in posterior mesoderm (Andree et al., 1998; Marvin et al., 2001; Schultheiss et al., 1995). Still, the exact step in specification/determination mediated by these factors is unknown (Gannon and Bader, 1995). In addition, most of these studies do not report a complete elimination of cardiogenic differentiation but cite a decrease or inhibition of differentiation.

It is important to note the relationship of these avian studies of inducing reagents to the literature on other species. While elimination of specific BMPs, FGFs and TGF-beta gene products with knockout technology in mice leads to defects in heart development, no such knockout reported thus far has eliminated cardiac muscle (PubMed search, May 2007). Thus, in strictest terms, it is not clear that a single “magic bullet” of cardiac induction has been identified.

In vitro analysis of cardiogenic mesoderm

It should be noted that in vitro analysis of avian cardiogenic mesoderm can be carried out with relative ease. Several groups have published on these methods (Gannon and Bader, 1995; Gannon and Bader, 1997; Gonzalez-Sanchez and Bader, 1990; Schultheiss et al., 1995; Stalsberg and DeHaan,

1969; Sugi and Lough, 1994; Yutzey and Bader, 1995; Yutzey et al., 1994). One important consideration in the culturing of chicken cardiogenic mesoderm is the ease of explanting the entire embryo, isolation of relatively pure samples of tissue and obtaining large numbers of precisely staged embryos. Importantly, avian cardiogenic mesoderm can be isolated and cultured with or without anterior endoderm as well as with emerging pharmacological and recombinant agents to test effects on cardiogenic determination and differentiation. We refer readers to Gannon and Bader for detailed protocols for these procedures (Gannon and Bader, 1997).

Finally, with the dawn of stem cell biology and its potential for the analysis of cell determination and differentiation, it is important to remember that a clear understanding of cardiogenic cell lineage processes is essential. The avian system remains one of the few experimental models where the embryonic precursors of the myocardium can be identified, isolated, cultured, manipulated and analyzed for its developmental potential.

Early morphogenetic changes in the forming heart tube

The heart tube is formed from the rostral to caudal fusion of the paired lateral primordia beginning at stage 6. These lateral elements are brought medially and ventrally by the action of the lateral body folds. Accompanying endocardial tubes are formed medial to the myocardial mantle of progenitors on both sides of midline. While left and right endocardial progenitors form bilateral

tubes, left and right myocardial mantles do not truly form tube structures. They are epithelial, non-lumenal structures that reside laterally to the endocardial tubes. With progression of the lateral folds, bilateral endocardial tubes fuse (a line can be seen at the interface of the two tubes as this process begins), the two myocardial mantles meet and the foregut is positioned dorsal to the heart tube. Now the myocardium forms a single epithelium of two or three myocytes in thickness. No epicardium is present at this time (Manasek, 1969a; Manasek, 1969b; Manasek, 1970; Nahirney et al., 2003; Reese et al., 2002).

Fusion or meeting of the two bilaterally positioned wings of the cardiogenic crescent has been recently re-examined in the chick (Moreno-Rodriguez et al., 2006). A summary of their studies is given in Figure 4.4. Originally, Stalsberg and DeHaan proposed that the anterior-most region of the cardiogenic crescent fused at the mid-line and zippered down posteriorly bringing the two wings together as a single heart tube (Stalsberg and DeHaan, 1969). More recent vital dye labeling and explant studies have shown that the wings of the cardiogenic crescent actually meet and fuse at a position posterior to the cranial-most heart forming cells. Subsequent zippering shut of the crescent into a single heart tube occurs anteriorly and posteriorly from this point (Figure 4.3). Addition of cells to the forming anterior heart tube from the secondary heart field occurs after the initial fusion event. Thus, the avian heart represents an outstanding experimental model to examine the early stages of crescent fusion and tube formation.

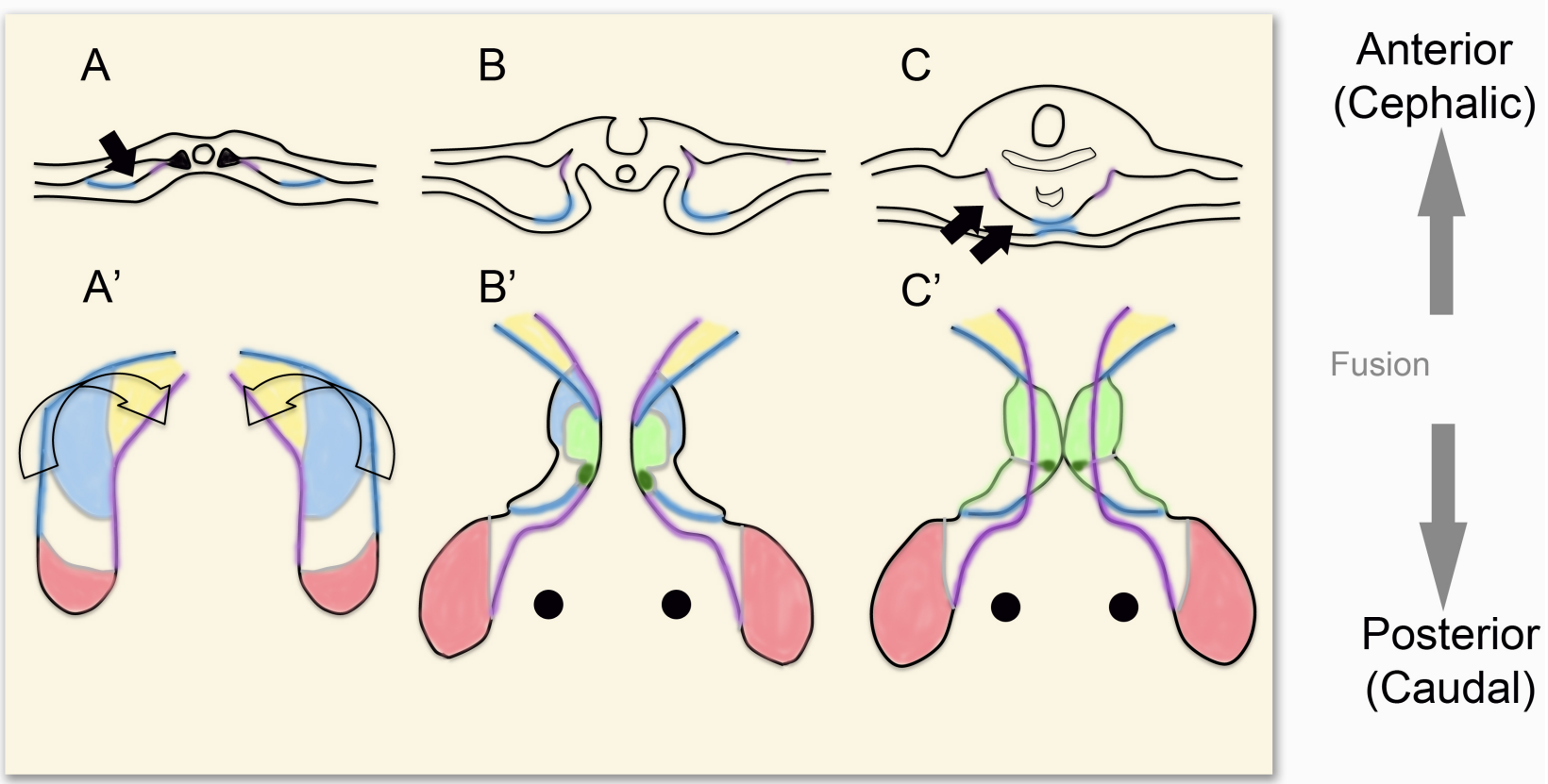

Figure 4.4. Closure of the bilateral wings of the cardiogenic crescent and formation of a heart tube. Modified by permission from Moreno-Rodriguez et al. (Moreno-Rodriguez et al., 2006). A model of fusion and formation of the primitive heart tube is given. Transverse sections through an embryo in the region of the cardiogenic crescent are diagrammed in A-C at stages 6-9. In panel A, the coelom (arrow) is formed when lateral mesoderm cavitates to form somatic and splanchnic layers at approximately stage 6. The two wings of the cardiogenic crescent approach (B) and fuse (C) as the anterior intestinal portal closes. A -C : These are ventral views showing mesoderm only. Moreno-Rodriguez et al. present their theory on the fusion of myocardial mantles via a “zipper complex” that is formed and fuses in a bi-directional fashion (anterior/cephalic vs. posterior/caudal; arrows). The mesoderm turns (seen as twisted arrows in A), and the outer margins (blue) form a ventral fusion line that can be seen through a simple dissecting microscope. This originates in the prospective right ventricle (seen as green horizontal lines in C). The forming pericardial cavity is seen at the same time (two arrowheads). Fusion proceeds in both directions and permits the caudal differentiation of the left ventricle (white area). The future outflow tract is seen as the anterior yellow area. To summarize, the outlet tissue (yellow), right ventricle (horizontal hatch), left ventricle and AV canal (white), sino-atrial tissue (perpendicular hatch), and ventral fusion line (blue) are identified during these stages of development. The green represents differentiating myocytes identified by MF20 staining during several developmental stages (B , C , and D).

Diversification of myogenic cell lineages

Several studies suggest that anterior lateral mesoderm takes on cardiomyogenic potential long before the heart is formed. Moorman and colleagues recognized this in a study of the three-dimensional (3-D) distribution of atrial and ventricular isomyosins during the formation of the tubular chicken heart (HH stage 7 to 12) using antibodies specific for atrial and ventricular myosins. This study demonstrated that both myosins were expressed at stage 8, when the cardiogenic crescent is still two separate plates. The anti-ventricular myosin antibody bound cardiogenic cells adjacent to the anterior intestinal portal. The atrial myosin was identified in regions caudal and lateral to ventricular myosin expression. Regions medial to atrial myosin expression did not express sarcomeric myosin (De Jong et al., 1990). Moorman subsequently has published many studies on this topic in several different species and the reader is encouraged to review those publications for a comprehensive analysis. Later studies have found largely similar, yet specifically variant results at these early stages of heart development in the chicken (Gannon and Bader, 1995; Gannon and Bader, 1997; Gonzalez-Sanchez and Bader, 1990; Schultheiss et al., 1995; Sugi and Lough, 1994; Yatskievych et al., 1997; Yutzey and Bader, 1995).

Interestingly, diversification of ventricular and atrial myocytes appears to occur very early along the anteroposterior axis in the forming heart tube. In the chicken, the straight heart tube is never really “straight” and there is never a stage where anterior is “equal” to posterior. In situ hybridization analyses

demonstrate that anterior progenitors express ventricular myosin heavy chain gene products prior to bilateral myocardial mantle fusion (Yutzey et al., 1994). The same progenitors do not express atrial myosin transcripts at detectable levels at these same times (Figure 4.5). Obviously, variation in probe preparation, and size as well as length of hybridization time and stringency can play a role in the interpretation of in situ experiments (Somi et al., 2006), but general patterns of expression do exhibit consistent results. Expression of the atrial myosin heavy chain is largely confined to the posterior regions of the cardiogenic crescent and forming tube, suggesting that cardiomyogenic differentiation varies along the anteroposterior axis. Isolation of anterior and posterior progenitors followed by culture in standard medium demonstrated that only posterior cells activate the atrial-specific myosin gene further indicating that differentiative potential varies along the anteroposterior axis (Yutzey et al., 1994). These experiments also suggest that expression of atrial-specific genes is not dependent on formation of the definitive atrium as posterior myogenic cells will activate these genes in vitro. Interestingly, this initial diversification of myocytes can be modulated by treatment with retinoic acid (Yutzey et al., 1995; Yutzey and Bader, 1995) and is controlled in the chicken and mouse by the same mechanism (Wang et al., 2001). In this situation, application of retinoic acid results in conversion of anterior ventriculogenic cells to an atrial phenotype. Conversely, mis-expression of the ventricular region-specific iroquois gene product in developing avian embryos is thought to activate the ventricular phenotype along the anterior/posterior axis (Bao et al., 1999). The atrial myosin

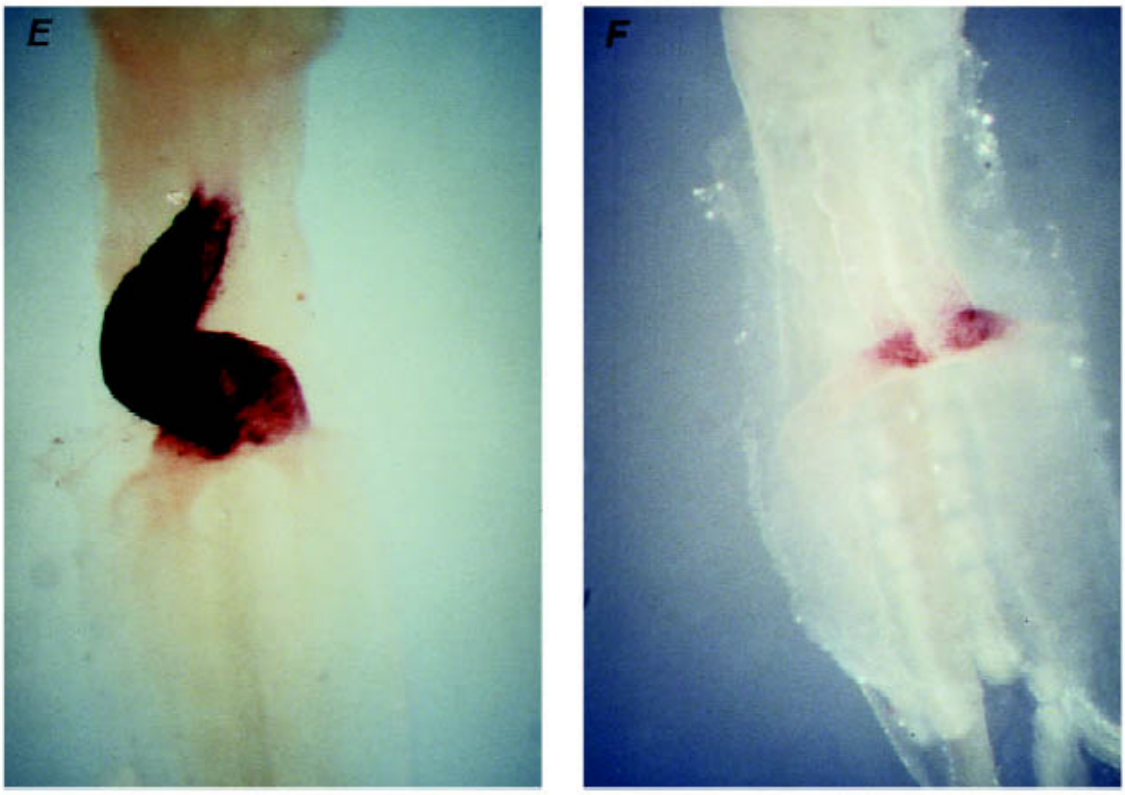

Figure 4.5. Position of ventricular and atrial MHC-expressing cells at stage 10. Modified from Yutzey et al (Yutzey et al., 1994). The region of VMHC1staining depicts the position of all differentiated myocytes as this gene product is expressed in all striated muscle cells (left panel). In the right panel, the regions of AMHC1 staining shows the regions of the forming heart tube that will later incorporate into the embryonic atria. It should be noted that addition of the secondary heart fields and later morphogenesis are not considered in this representation.

heavy chain gene product encoded by AMHC1 has the most highly restricted pattern of gene expression along this axis (Yutzey et al., 1994). Additionally it should be noted that the chicken heart, unlike mammalian hearts, expresses more than two heavy chain genes and one atrial isoform becomes restricted to the atria only much later in development (Evans et al., 1988).

While differences in gene expression have garnered much attention in recent years as a model for myocyte and chamber diversification, simple observation of heart morphology at the time of bilateral fusion demonstrates the initial diversification of the heart in terms of anteroposterior variation. Most anteriorly, the aortic sac, truncus arteriosis, bulbus chordus are restricted in diameter when compared to the ventriculogenic region that bulges to the right. It should be remembered that the aortic outlet (the aortic sac, truncus arteriosis, bulbus chordus) are derived from the secondary heart field (Evans et al., 1988; Mjaatvedt et al., 2001; Waldo et al., 2005). Posteriorly, a restriction is easily seen in the heart tube. This restriction coincides with the line that separates AMHC1-expressing myocytes from anterior myocytes that do not. The right and left posterior cardiac regions of the stage 10 embryo straddle the anterior intestinal portal and look nothing like their anterior counterparts. It is interesting to note that chicken embryos isolated and grown on paper rings develop hearts that undergo these anteroposterior morphogenetic events.

Diversification of atrial and ventricular cells along the anteroposterior axis appears to be a component of the initial differentiative process in chicken heart development (Yutzey and Bader, 1995). This is not to say that the final fully differentiated phenotype of the ventricular or atrial phenotype is established at this early stage (for example, see Evans et al) (Evans et al., 1988). Still, this initially diverse state may play a role in driving differential development of ventricles and atria. As stated above, the avian heart tube is “diverse” along its anteroposterior and left-right axes from the moment it is formed with its specific constrictions and protrusions.

It is also obvious to even the most casual observer that the avian heart is diverse along its left-right axis. The ventricular region of the heart loops to the right. Without doubt, early mechanisms in the establishment of right-left asymmetry in the embryo as a whole drive subsequent asymmetry in the heart (Raya and Belmonte, 2006; Tabin, 2006).

One of the more fascinating aspects of myogenic diversification in the developing avian heart is the generation of the conduction system. Interestingly, the avian heart, like that of the mammal, displays rhythmic posterior-to-anterior contractions very early in development. This topic is extensively reviewed in Moorman and Christoffels (Moorman and Christoffels, 2003a; Moorman and Christoffels, 2003b). While this indicates the presence of a defined conduction system, morphological or molecular characterization of these cells is not

advanced. Moorman and colleagues have proposed that the embryonic heart may be reflective of the hearts of more primitive organisms where every myocyte might be considered a “conduction system” cell (Anderson et al., 2004). For theories on the generation of the central conduction system, see Gourdie et al. and other contributors to the Novartis Foundation Symposium (2003) (Gourdie et al., 2003). Generation of Purkinje cells in the embryonic ventricle has been more firmly established in the avian heart. Mikawa and coworkers have established that working ventricular myocytes give rise to conduction system cells within the developing heart wall (Gourdie et al., 2003; Gourdie et al., 1995; Gourdie et al., 1998; Hyer et al., 1999). Interaction with the developing coronary system is critical in lineage determination of some Purkinje fibers and endothelin appears to be a major signaling factor in this process.

Obviously, morphogenesis and growth of the heart continue long after the initial establishment of the asymmetric tube and primitive chambers. This is exemplified in Figure 4.4. At day three, the heart is seen as a looped structure where atrial and ventricular myocytes are clearly positioned within their developing chambers. While the diversification process is still incomplete (Stockdale, 1992; Stockdale et al., 2002; Wang et al., 1996), atrial and ventricular myocytes are clearly positioned in the heart and express at least one MHC specific to their respective adult chambers (Gonzalez-Sanchez and Bader, 1984). While other chapters focus on the differentiation of the cardiac chambers and their overall structure, it is interesting to consider the atrioventricular canal seen

in Figure 4.6. This is a major structure in the embryonic heart and provides a muscular connection between ventricular and atrial chambers. It is a critical signaling structure for the generation of AV values. Still, this myogenic connection between ventricular and atrial chambers is completely missing in the adult. The mechanisms underlying this morphogenetic process are almost completely unknown. The chicken embryo may be an excellent model for this study.

Thus, the avian system has provided critical data in the examination of myogenic lineage determination and continues to provide a model for these analyses by the experimental zoologist.

Trabeculation and cardiac myocytes

Trabeculation is a complex process whereby the epithelial myocardium expands to produce finger-like projections into the cardiac lumen. A diagram of this overall process is given in Figure 4.6 (modified from Sedmera et al, 1999 (Sedmera et al., 1999)). Depending on the species studied, trabeculae may be retained in the adult heart without subsequent compaction. This is generally true for species with circulatory systems under lower blood pressures. For example, most amphibian species and many fish have non-compacted, trabeculated ventricles. All avian hearts studied thus far have compacted hearts (Hicks, 2002).

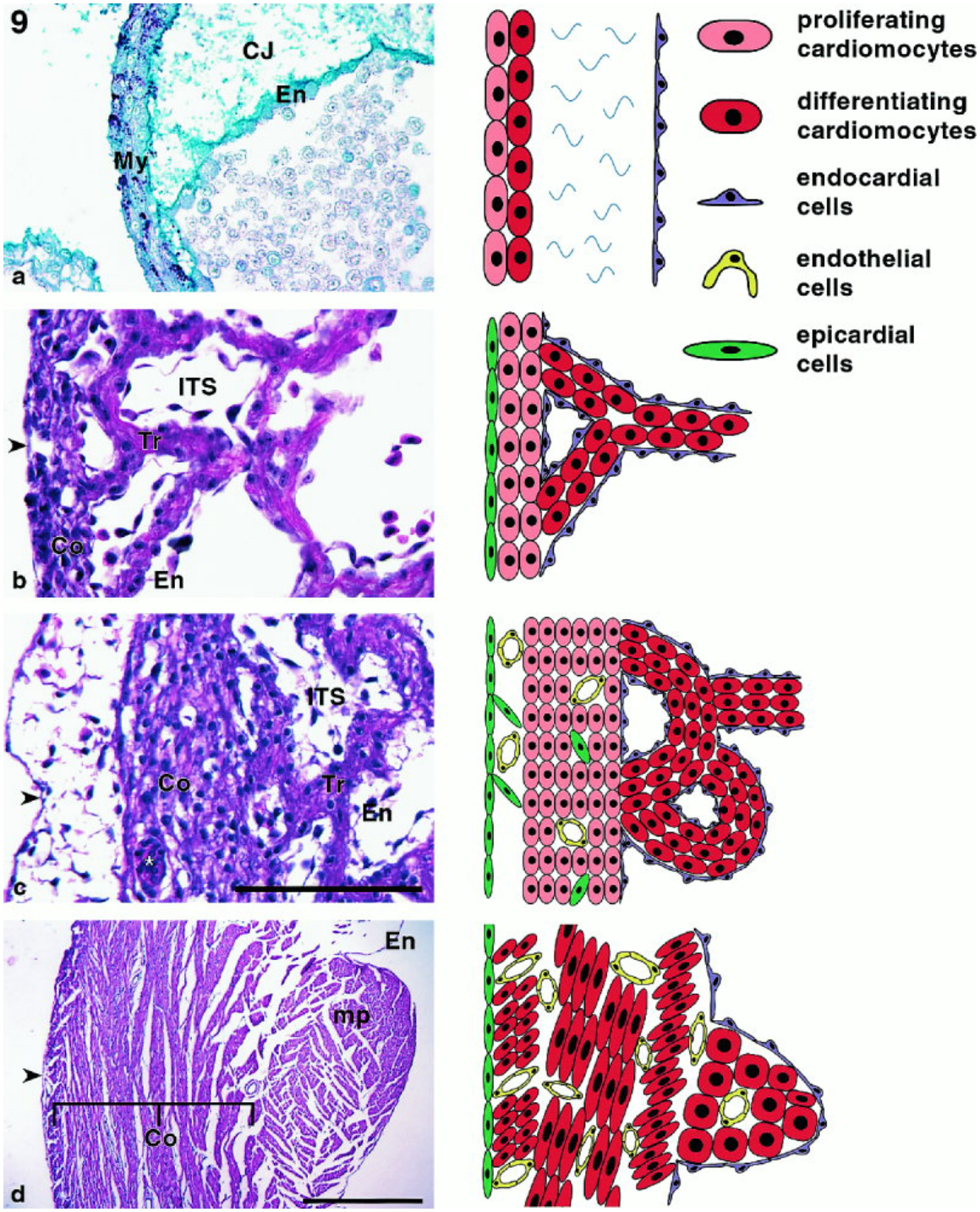

Figure 4.6. Diagram of the morphogenetic events regulating trabeculation and compaction. Modified from Sedmera et al (Sedmera et al., 2000). This diagram from an insightful review by Sedmera and colleagues summarizes the proliferation, growth, movement, and differentiation of cardiac myocytes in the trans-mural axis. Along with this cell type, the position of endocardial and epicardial cells is noted.

As with other classes of vertebrates, there are significant differences in the trabeculating potential of the avian atria and ventricles. While atria undergo trabeculation, most of the literature has focused on the process in the ventricles (Sedmera et al., 1999). In the chicken beginning around stage 13 or 14, the polarized epithelial myocardium is one to three cells thick (Peng et al., 1990). At this time, spaces in the myocardium are seen between myocytes (Nahirney et al., 2003). It should be remembered that cardiac myocytes are the only cell type seen in the myocardium before the arrival of the epicardium ((Reese et al., 2002) see references cited therein). As the outer heart wall expands by proliferation, myocytes change their distribution of adhesion molecules including cadherins, ZO-1 and Bves (Osler and Bader, unpublished results). These myocytes have numerous cell processes that appear to interact with other myocytes (Mikawa and Fischman, 1992; Nahirney et al., 2003). The Fischman and Mikawa laboratories have shown that clones of cardiac myocytes extend from the outer wall transmurally to the lumen. Thus, trabeculae are polyclonal and derived from radial expansion of proliferative myocytes of the outer wall. Butcher et al. has recently generated a new and very sensitive method for analysis of trabeculation in the chicken heart (Butcher et al., 2007).

Proliferation is a key to trabeculation and disruption of many gene products leads to a blunting of growth and extension. For example, Hatcher et al. have determined that Tbx5 is a critical regulator of myocyte proliferation of avian cardiomyogenic cells in vitro and in vivo, potentially regulating trabeculation

(Hatcher et al., 2004; Hatcher and McDermott, 2006). Lee and colleagues have made critical contributions to our understanding of trabeculation using the mouse as a model. In these studies, Erb2, a receptor tyrosine kinase, and its ligand neuregulin-1 were shown to play essential roles in the selective trabeculation of the ventricular wall (Lee et al., 1995; Negro et al., 2004). Loss of Erb2 caused major blunting of ventricular trabeculation and death in embryonic mice (Lee et al., 1995). Other growth factors including FGFs are critical for the progression of myocyte division and expansion of the avian heart wall (Mima et al., 1995a; Mima et al., 1995b).

Thompson and colleagues have provided extensive analysis of myocyte proliferation patterns in the developing avian ventricular wall that have been reviewed (Sedmera et al., 1999; Sedmera et al., 2000). Briefly, myocytes of the outer wall remain proliferative and addition of new myocytes is appositional (Figure 4.6). Proliferation of myocytes at the tips of forming trabeculae is modest. It is of interest to question when the last mesodermal cells are added to the ventricular wall and when addition of new myocytes is strictly from the division of pre-exiting myocytes. No stem cells have been identified in avian hearts as claimed in mammalian counterparts (Anversa et al., 2007). During this phase of wall growth, spaces in the myocardium are observed and cells of the developing coronary system move to form the vascular system of the heart (Reese et al., 2002). The mechanisms whereby spaces in the proliferating, differentiating myocardium are eliminated and intervening endocardial cells are moved or

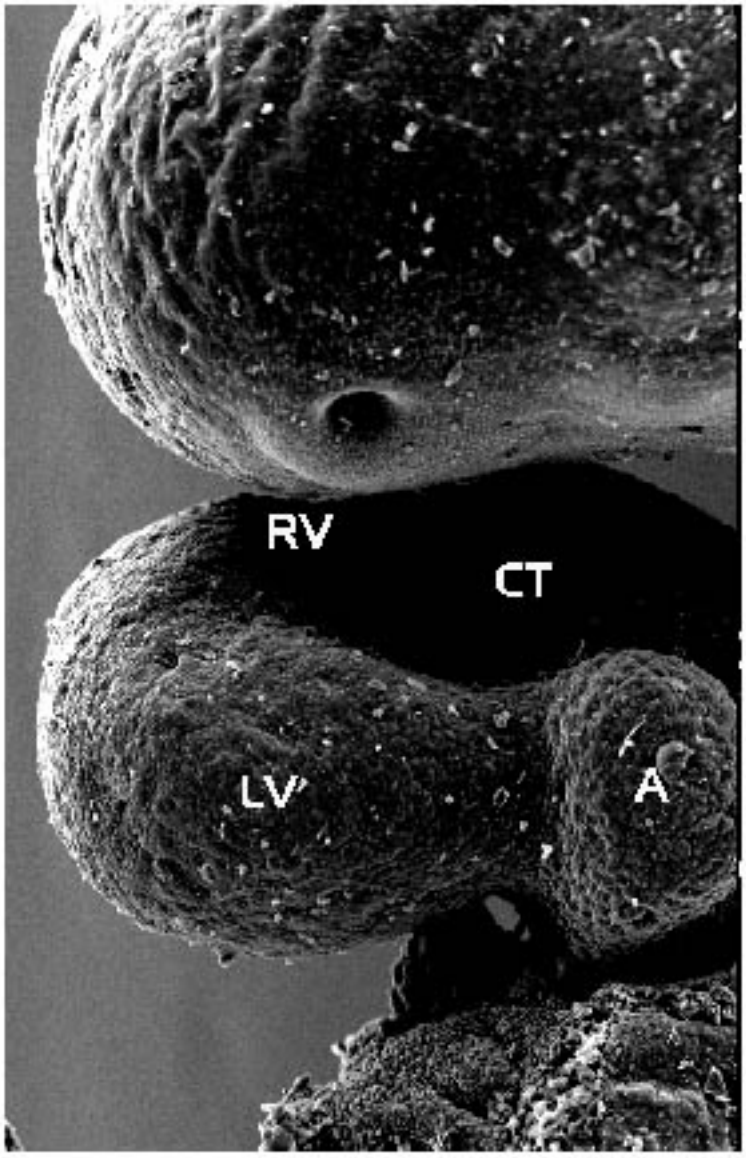

Figure 4.7. Prominence of the atrioventricular canal in the early chicken heart. This scanning EM modified from McCain and McLaughin 1998 (McCain, 1998) demonstrates the atrioventricular canal that is prominently seen from day 3 through 5 (between LV and A). This is an important signaling center for generation of the atrioventricular valves. Interestingly, this structure and its muscular band is absent in the adult heart. LV; left ventricle; A, atria, CT; conotruncus; RV, right ventricle.

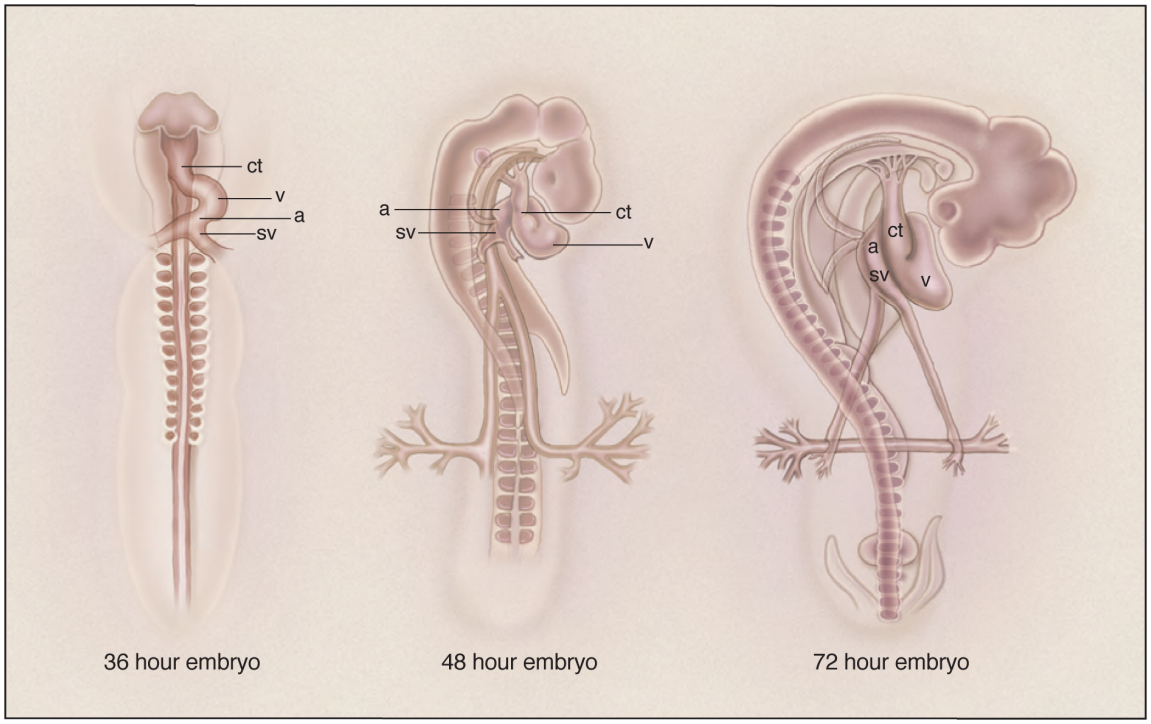

Figure 4.8. Early morphogenetic moments of the heart tube. Changes in the relative positions of the conotruncus (ct), ventricles (v), atria (a) and sinoatrium (sa) in the developing chicken heart is seen in these illustrations modified from McCain and MacLaughin (McCain, 1998) (by permission).

removed are not well understand. Species of birds with non-compacted heart walls have not been reported.

Summary

The avian heart remains an important component in the analysis of heart development. While not yet easily manipulated at the genomic level, descriptive embryology, experimental manipulation, lineage tracing, in vitro analysis of cardiomyogenesis as well as determination of endothelial and epicardial differentiation are often best approached in this class of vertebrates. With the recent sequencing of the chicken genome along with the many advances in non-genomic manipulation of gene product expression, the avian heart will continue to play an essential role in discovering the mechanistic basis of cardiac morphogenesis.

References

Anderson, R. H., Christoffels, V. M. and Moorman, A. F. (2004). Controversies concerning the anatomical definition of the conduction tissues. *Anat Rec B New Anat* **280**, 8-14.

Andree, B., Duprez, D., Vorbusch, B., Arnold, H. H. and Brand, T. (1998). BMP-2 induces ectopic expression of cardiac lineage markers and interferes with somite formation in chicken embryos. *Mech Dev* **70**, 119-31.

Anversa, P., Leri, A., Rota, M., Hosoda, T., Bearzi, C., Urbanek, K., Kajstura, J. and Bolli, R. (2007). Concise review: stem cells, myocardial regeneration, and methodological artifacts. *Stem Cells* **25**, 589-601.

Bao, Z. Z., Bruneau, B. G., Seidman, J. G., Seidman, C. E. and Cepko, C. L. (1999). Regulation of chamber-specific gene expression in the developing heart by Irx4. *Science* **283**, 1161-4.

Barron, M., Gao, M. and Lough, J. (2000). Requirement for BMP and FGF signaling during cardiogenic induction in non-precardiac mesoderm is specific, transient, and cooperative. *Dev Dyn* **218**, 383-93.

Bettiol, E., Clement, S., Krause, K. H. and Jaconi, M. E. (2006). Embryonic and adult stem cell-derived cardiomyocytes: lessons from in vitro models. *Rev Physiol Biochem Pharmacol* **157**, 1-30.
Butcher, J. T., Norris, R. A., Hoffman, S., Mjaatvedt, C. H. and Markwald, R. R. (2007). Periostin promotes atrioventricular mesenchyme matrix invasion and remodeling mediated by integrin signaling through Rho/PI 3-kinase. *Dev Biol* **302**, 256-66.
de Groot, I. J., Hardy, G. P., Sanders, E., Los, J. A. and Moorman, A. F. (1985). The conducting tissue in the adult chicken atria. A histological and immunohistochemical analysis. *Anat Embryol (Berl)* **172**, 239-45.
De Jong, F., Geerts, W. J., Lamers, W. H., Los, J. A. and Moorman, A. F. (1990). Isomyosin expression pattern during formation of the tubular chicken heart: a three-dimensional immunohistochemical analysis. *Anat Rec* **226**, 213-27.
Dehaan, R. L. (1963). Migration patterns of the precardiac mesoderm in the early chick embrvo. *Exp Cell Res* **29**, 544-60.
DeHaan, R. L. and Ursprung, H. (1965). Organogenesis. New York,: Holt.
Ehrman, L. A. and Yutzey, K. E. (1999). Lack of regulation in the heart forming region of avian embryos. *Dev Biol* **207**, 163-75.
Evans, D., Miller, J. B. and Stockdale, F. E. (1988). Developmental patterns of expression and coexpression of myosin heavy chains in atria and ventricles of the avian heart. *Dev Biol* **127**, 376-83.
Firulli, A. B. and Thattaliyath, B. D. (2002). Transcription factors in cardiogenesis: the combinations that unlock the mysteries of the heart. *Int Rev Cytol* **214**, 1-62.
Gannon, M. and Bader, D. (1995). Initiation of cardiac differentiation occurs in the absence of anterior endoderm. *Development* **121**, 2439-50.
Gannon, M. and Bader, D. (1997). Avian cardiac progenitors: methods for isolation, culture, and analysis of differentiation. *Methods Cell Biol* **52**, 117-32.
Garcia-Martinez, V. and Schoenwolf, G. C. (1993). Primitive-streak origin of the cardiovascular system in avian embryos. *Dev Biol* **159**, 706-19.
Gilbert, S. F. (2006). Developmental biology. Sunderland, Mass.: Sinauer Associates, Inc. Publishers.
Gonzalez-Sanchez, A. and Bader, D. (1984). Immunochemical analysis of myosin heavy chains in the developing chicken heart. *Dev Biol* **103**, 151-8.
Gonzalez-Sanchez, A. and Bader, D. (1985). Characterization of a myosin heavy chain in the conductive system of the adult and developing chicken heart. *J Cell Biol* **100**, 270-5.
Gonzalez-Sanchez, A. and Bader, D. (1990). In vitro analysis of cardiac progenitor cell differentiation. *Dev Biol* **139**, 197-209.
Gourdie, R. G., Harris, B. S., Bond, J., Edmondson, A. M., Cheng, G., Sedmera, D., O'Brien, T. X., Mikawa, T. and Thompson, R. P. (2003). His-Purkinje lineages and development. *Novartis Found Symp* **250**, 110-22; discussion 122-4, 276-9.
Gourdie, R. G., Mima, T., Thompson, R. P. and Mikawa, T. (1995). Terminal diversification of the myocyte lineage generates Purkinje fibers of the cardiac conduction system. *Development* **121**, 1423-31.

Gourdie, R. G., Wei, Y., Kim, D., Klatt, S. C. and Mikawa, T. (1998). Endothelin-induced conversion of embryonic heart muscle cells into impulse-conducting Purkinje fibers. *Proc Natl Acad Sci U S A* **95**, 6815-8.
Hamburger, V. and Hamilton, H. L. (1992). A series of normal stages in the development of the chick embryo. 1951. *Dev Dyn* **195**, 231-72.
Hatcher, C. J., Diman, N. Y., Kim, M. S., Pennisi, D., Song, Y., Goldstein, M. M., Mikawa, T. and Basson, C. T. (2004). A role for Tbx5 in proepicardial cell migration during cardiogenesis. *Physiol Genomics* **18**, 129-40.
Hatcher, C. J. and McDermott, D. A. (2006). Using the TBX5 transcription factor to grow and sculpt the heart. *Am J Med Genet A* **140**, 1414-8.
Hicks, J. W. (2002). The physiological and evolutionary significance of cardiovascular shunting patterns in reptiles. *News Physiol Sci* **17**, 241-5.
Hirakow, R. (1970). Ultrastructural characteristics of the mammalian and sauropsidan heart. *Am J Cardiol* **25**, 195-203.
Hyer, J., Johansen, M., Prasad, A., Wessels, A., Kirby, M. L., Gourdie, R. G. and Mikawa, T. (1999). Induction of Purkinje fiber differentiation by coronary arterialization. *Proc Natl Acad Sci U S A* **96**, 13214-8.
Kelly, R. G., Brown, N. A. and Buckingham, M. E. (2001). The arterial pole of the mouse heart forms from Fgf10-expressing cells in pharyngeal mesoderm. *Dev Cell* **1**, 435-40.
Kruithof, B. P., van Wijk, B., Somi, S., Kruithof-de Julio, M., Perez Pomares, J. M., Weesie, F., Wessels, A., Moorman, A. F. and van den Hoff, M. J. (2006). BMP and FGF regulate the differentiation of multipotential pericardial mesoderm into the myocardial or epicardial lineage. *Dev Biol* **295**, 507-22.
Ladd, A. N., Yatskievych, T. A. and Antin, P. B. (1998). Regulation of avian cardiac myogenesis by activin/TGFbeta and bone morphogenetic proteins. *Dev Biol* **204**, 407-19.
Le Douarin, G., Le Douarin, N. and Cuminge, D. (1965). [Ultrastructural study of the autodifferentiation capabilities of the mesoderm of the cardiac area in the chick embryo]. *C R Acad Sci Hebd Seances Acad Sci D* **260**, 6998-7001.
Lee, K. F., Simon, H., Chen, H., Bates, B., Hung, M. C. and Hauser, C. (1995). Requirement for neuregulin receptor erbB2 in neural and cardiac development. *Nature* **378**, 394-8.
Lough, J., Barron, M., Brogley, M., Sugi, Y., Bolender, D. L. and Zhu, X. (1996). Combined BMP-2 and FGF-4, but neither factor alone, induces cardiogenesis in non-precardiac embryonic mesoderm. *Dev Biol* **178**, 198-202.
Lu, Y., James, T. N., Bootsma, M. and Terasaki, F. (1993a). Histological organization of the right and left atrioventricular valves of the chicken heart and their relationship to the atrioventricular Purkinje ring and the middle bundle branch. *Anat Rec* **235**, 74-86.
Lu, Y., James, T. N., Yamamoto, S. and Terasaki, F. (1993b). Cardiac conduction system in the chicken: gross anatomy plus light and electron microscopy. *Anat Rec* **236**, 493-510.
Malpighi, M. (1672). De formatione pulli in ovo. *London: Royal Society*.
Manasek, F. J. (1969a). Embryonic development of the heart. II. Formation of the epicardium. *J Embryol Exp Morphol* **22**, 333-48.

Manasek, F. J. (1969b). The appearance of granules in the Golgi complex of embryonic cardiac myocytes. *J Cell Biol* **43**, 605-10.
Manasek, F. J. (1970). Histogenesis of the embryonic myocardium. *Am J Cardiol* **25**, 149-68.
Manner, J. (2000). Cardiac looping in the chick embryo: a morphological review with special reference to terminological and biomechanical aspects of the looping process. *Anat Rec* **259**, 248-62.
Marvin, M. J., Di Rocco, G., Gardiner, A., Bush, S. M. and Lassar, A. B. (2001). Inhibition of Wnt activity induces heart formation from posterior mesoderm. *Genes Dev* **15**, 316-27.
Mathur, R. and Shrivastava, A. (1979). Cardiac conducting system of Gallus domesticus with special reference to the atrial bundles. *Acta Morphol Neerl Scand* **17**, 181-9.
McCain, E. a. M., Jacqueline. (1998). Developmental and physiological aspects of the
chicken embryonic heart. *Proceedings of the 20th Workshop/Conference of the Association for Biology Laboratory Education* **20**, 1-15.
Mikawa, T. (1995). Retroviral targeting of FGF and FGFR in cardiomyocytes and coronary vascular cells during heart development. *Ann N Y Acad Sci* **752**, 506-16.
Mikawa, T., Borisov, A., Brown, A. M. and Fischman, D. A. (1992). Clonal analysis of cardiac morphogenesis in the chicken embryo using a replication-defective retrovirus: I. Formation of the ventricular myocardium. *Dev Dyn* **193**, 11-23.
Mikawa, T. and Fischman, D. A. (1992). Retroviral analysis of cardiac morphogenesis: discontinuous formation of coronary vessels. *Proc Natl Acad Sci U S A* **89**, 9504-8.
Mima, T., Ohuchi, H., Noji, S. and Mikawa, T. (1995a). FGF can induce outgrowth of somatic mesoderm both inside and outside of limb-forming regions. *Dev Biol* **167**, 617-20.
Mima, T., Ueno, H., Fischman, D. A., Williams, L. T. and Mikawa, T. (1995b). Fibroblast growth factor receptor is required for in vivo cardiac myocyte proliferation at early embryonic stages of heart development. *Proc Natl Acad Sci U S A* **92**, 467-71.
Mjaatvedt, C. H., Nakaoka, T., Moreno-Rodriguez, R., Norris, R. A., Kern, M. J., Eisenberg, C. A., Turner, D. and Markwald, R. R. (2001). The outflow tract of the heart is recruited from a novel heart-forming field. *Dev Biol* **238**, 97-109.
Montgomery, M. O., Litvin, J., Gonzalez-Sanchez, A. and Bader, D. (1994). Staging of commitment and differentiation of avian cardiac myocytes. *Dev Biol* **164**, 63-71.
Moorman, A. F. and Christoffels, V. M. (2003a). Cardiac chamber formation: development, genes, and evolution. *Physiol Rev* **83**, 1223-67.
Moorman, A. F. and Christoffels, V. M. (2003b). Development of the cardiac conduction system: a matter of chamber development. *Novartis Found Symp* **250**, 25-34; discussion 34-43, 276-9.

Moreno-Rodriguez, R. A., Krug, E. L., Reyes, L., Villavicencio, L., Mjaatvedt, C. H. and Markwald, R. R. (2006). Bidirectional fusion of the heart-forming fields in the developing chick embryo. *Dev Dyn* **235**, 191-202.
Nahirney, P. C., Mikawa, T. and Fischman, D. A. (2003). Evidence for an extracellular matrix bridge guiding proepicardial cell migration to the myocardium of chick embryos. *Dev Dyn* **227**, 511-23.
Negro, A., Brar, B. K. and Lee, K. F. (2004). Essential roles of Her2/erbB2 in cardiac development and function. *Recent Prog Horm Res* **59**, 1-12.
Osler, M. E. and Bader, D. M. (2004). Bves expression during avian embryogenesis. *Dev Dyn* **229**, 658-67.
Pabon-Pena, L. M., Goodwin, R. L., Cise, L. J. and Bader, D. (2000). Analysis of CMF1 reveals a bone morphogenetic protein-independent component of the cardiomyogenic pathway. *J Biol Chem* **275**, 21453-9.
Peng, I., Dennis, J. E., Rodriguez-Boulan, E. and Fischman, D. A. (1990). Polarized release of enveloped viruses in the embryonic chick heart: demonstration of epithelial polarity in the presumptive myocardium. *Dev Biol* **141**, 164-72.
Proctor, N. S. and Lynch, P. J. (1993). Manual of ornithology : avian structure & function. New Haven: Yale University Press.
Rawles, M. E. (1952). Transplantation of normal embryonic tissues. *Ann N Y Acad Sci* **55**, 302-12.
Raya, A. and Belmonte, J. C. (2006). Left-right asymmetry in the vertebrate embryo: from early information to higher-level integration. *Nat Rev Genet* **7**, 283-93.
Redkar, A., Montgomery, M. and Litvin, J. (2001). Fate map of early avian cardiac progenitor cells. *Development* **128**, 2269-79.
Reese, D. E., Mikawa, T. and Bader, D. M. (2002). Development of the coronary vessel system. *Circ Res* **91**, 761-8.
Rosenquist, G. C. (1970a). Cardia bifida in chick embryos: anterior and posterior defects produced by transplanting tritiated thymidine-labeled grafts medial to the heart-forming regions. *Teratology* **3**, 135-42.
Rosenquist, G. C. (1970b). Location and movements of cardiogenic cells in the chick embryo: the heart-forming portion of the primitive streak. *Dev Biol* **22**, 461-75.
Satin, J., Fujii, S. and DeHaan, R. L. (1988). Development of cardiac beat rate in early chick embryos is regulated by regional cues. *Dev Biol* **129**, 103-13.
Schlange, T., Andree, B., Arnold, H. and Brand, T. (2000). Expression analysis of the chicken homologue of CITED2 during early stages of embryonic development. *Mech Dev* **98**, 157-60.
Schultheiss, T. M., Xydas, S. and Lassar, A. B. (1995). Induction of avian cardiac myogenesis by anterior endoderm. *Development* **121**, 4203-14.
Sedmera, D., Pexieder, T., Rychterova, V., Hu, N. and Clark, E. B. (1999). Remodeling of chick embryonic ventricular myoarchitecture under experimentally changed loading conditions. *Anat Rec* **254**, 238-52.
Sedmera, D., Pexieder, T., Vuillemin, M., Thompson, R. P. and Anderson, R. H. (2000). Developmental patterning of the myocardium. *Anat Rec* **258**, 319-37.

Slack, J. M. W. (1991). From egg to embryo : regional specification in early development. Cambridge [England] ; New York: Cambridge University Press.
Somi, S., Klein, A. T., Houweling, A. C., Ruijter, J. M., Buffing, A. A., Moorman, A. F. and van den Hoff, M. J. (2006). Atrial and ventricular myosin heavy-chain expression in the developing chicken heart: strengths and limitations of non-radioactive in situ hybridization. *J Histochem Cytochem* **54**, 649-64.
Sommer, J. R., Bossen, E., Dalen, H., Dolber, P., High, T., Jewett, P., Johnson, E. A., Junker, J., Leonard, S., Nassar, R. et al. (1991). To excite a heart: a bird's view. *Acta Physiol Scand Suppl* **599**, 5-21.
Sommer, J. R. and Johnson, E. A. (1969). Cardiac muscle. A comparative ultrastructural study with special reference to frog and chicken hearts. *Z Zellforsch Mikrosk Anat* **98**, 437-68.
Stalsberg, H. and DeHaan, R. L. (1968). Endodermal movements during foregut formation in the chick embryo. *Dev Biol* **18**, 198-215.
Stalsberg, H. and DeHaan, R. L. (1969). The precardiac areas and formation of the tubular heart in the chick embryo. *Dev Biol* **19**, 128-59.
Stockdale, F. E. (1992). Myogenic cell lineages. *Dev Biol* **154**, 284-98.
Stockdale, F. E., Nikovits, W., Jr. and Espinoza, N. R. (2002). Slow myosins in muscle development. *Results Probl Cell Differ* **38**, 199-214.
Sugi, Y. and Lough, J. (1994). Anterior endoderm is a specific effector of terminal cardiac myocyte differentiation of cells from the embryonic heart forming region. *Dev Dyn* **200**, 155-62.
Szabo, E., Viragh, S. and Challice, C. E. (1986). The structure of the atrioventricular conducting system in the avian heart. *Anat Rec* **215**, 1-9.
Tabin, C. J. (2006). The key to left-right asymmetry. *Cell* **127**, 27-32.
Takebayashi-Suzuki, K., Pauliks, L. B., Eltsefon, Y. and Mikawa, T. (2001). Purkinje fibers of the avian heart express a myogenic transcription factor program distinct from cardiac and skeletal muscle. *Dev Biol* **234**, 390-401.
Takebayashi-Suzuki, K., Yanagisawa, M., Gourdie, R. G., Kanzawa, N. and Mikawa, T. (2000). In vivo induction of cardiac Purkinje fiber differentiation by coexpression of preproendothelin-1 and endothelin converting enzyme-1. *Development* **127**, 3523-32.
van Laake, L. W., Hassink, R., Doevendans, P. A. and Mummery, C. (2006). Heart repair and stem cells. *J Physiol* **577**, 467-78.
Verzi, M. P., McCulley, D. J., De Val, S., Dodou, E. and Black, B. L. (2005). The right ventricle, outflow tract, and ventricular septum comprise a restricted expression domain within the secondary/anterior heart field. *Dev Biol* **287**, 134-45.
Waldo, K. L., Hutson, M. R., Ward, C. C., Zdanowicz, M., Stadt, H. A., Kumiski, D., Abu-Issa, R. and Kirby, M. L. (2005). Secondary heart field contributes myocardium and smooth muscle to the arterial pole of the developing heart. *Dev Biol* **281**, 78-90.
Wang, G. F., Nikovits, W., Jr., Bao, Z. Z. and Stockdale, F. E. (2001). Irx4 forms an inhibitory complex with the vitamin D and retinoic X receptors to regulate cardiac chamber-specific slow MyHC3 expression. *J Biol Chem* **276**, 28835-41.

Wang, G. F., Nikovits, W., Schleinitz, M. and Stockdale, F. E. (1996). Atrial chamber-specific expression of the slow myosin heavy chain 3 gene in the embryonic heart. *J Biol Chem* **271**, 19836-45.
West, N. H., Langille B.L., and Jones, D.R. (1981). Cadiovascular system. *Form and Function in Birds* **2**, 235-339.
Whittow, G. C. and Sturkie, P. D. (2000). Sturkie's avian physiology. San Diego: Academic.
Yatskievych, T. A., Ladd, A. N. and Antin, P. B. (1997). Induction of cardiac myogenesis in avian pregastrula epiblast: the role of the hypoblast and activin. *Development* **124**, 2561-70.
Yutzey, K., Gannon, M. and Bader, D. (1995). Diversification of cardiomyogenic cell lineages in vitro. *Dev Biol* **170**, 531-41.
Yutzey, K. E. and Bader, D. (1995). Diversification of cardiomyogenic cell lineages during early heart development. *Circ Res* **77**, 216-9.
Yutzey, K. E., Rhee, J. T. and Bader, D. (1994). Expression of the atrial-specific myosin heavy chain AMHC1 and the establishment of anteroposterior polarity in the developing chicken heart. *Development* **120**, 871-83.

CHAPTER V

THE ROLE OF CENP-F IN MURINE HEART DEVELOPMENT

Introduction

Organogenesis is undeniably a complicated process within the global development of the vertebrate embryo; cells must specify, pattern, proliferate, migrate, differentiate, and grow in a specific and coordinated manner in response to their microenvironment and embryo as a whole. The vertebrate heart is an excellent model with which to monitor these complex developmental events, especially in reference to the heart wall. As the heart fields move to form the heart tube, migrating cells form an epithelial sheet later to become the myocardium. The endocardium is formed from delaminated cells from this epithelia. The tube closes and loops upon itself as cells begin differentiation and synchronized contraction (Refer to Moynihan et al., 2009b). The heart then undergoes a major growth and remodeling phase for expansion and chamber formation. This dynamic remodeling of the heart tube is especially apparent in formation of the ventricular myocardium through trabeculation, when cardiomyocytes develop the thick muscular wall necessary for proper heart function (Sedmera et al., 2000). The early myocardium must be highly proliferative to generate the sufficient number of myocytes to build the thick heart wall, while individual myogenic cells are repositioned to their correct location and eventually differentiate into mature myocytes. For the proper morphogenesis of

the heart wall, cells must secrete necessary extracellular matrix components and transport membrane proteins such as adhesion molecules, channels, and receptors to the cell surface for proper integration with the developing tissue (Kostetskii et al., 2005; Perriard et al., 2003). The formation of the intercalated disc (ID) relies heavily on this integration. As they differentiate, cardiomyocytes form specialized contacts with their neighbors via an extensively intertwined network of gap junctions and desmosomes; this allows direct electrical connectivity between cells (Kostetskii et al., 2005; Severs, 1990; Shimada et al., 2004). These junctions are formed by specific proteins trafficked to the junctional membrane and allow electrical conduction to spread very quickly (Rohr, 2004). In turn, this rapid spread of depolarization facilitates synchronized contraction. The contraction mechanism relies on the connections between myocytes and the cytoarchitecture to give support and tension. As the cardiac conduction system arises, further myocyte diversification occurs to form an uninterrupted network of these specialized cells. Clearly, indentifying novel genes that regulate the developmental process in the heart is highly significant: congenital heart defects occur in 12 of 1000 live births (Hoffman et al., 2004).

In sum, the genetic profiles of cell populations within this developing organ shift considerably as these different processes occur. In fact, many crucial proteins in organogenesis are upregulated during various developmental stages, yet are absent in the adult organism after maturation. Apoptotic regulators Bim, Apaf-1, and caspase-3 fall into this category in the murine heart (Madden et al.,

2007), as well as many cell cycle regulators (Chen et al., 2004). Murine CENP-F is also one such protein; expression is highest in the heart and brain during mouse embryonic development and is abruptly down-regulated in the heart after neonatal day 4 (Goodwin et al., 1999). This timing coincides with cessation of myocyte cell division and the final stages of terminal differentiation of cardiac myocytes (Dees et al., 2005; Goodwin et al., 1999; Soonpaa and Field, 1998; Soonpaa et al., 1996). Thus, the expression of CENP-F directly correlates to the highly proliferative and morphogenetic period of myocyte development. The link between developmental disruption of basic cellular processes – MT organization, cell division, and vesicular transport – and resulting impairment of function would demonstrate the importance of temporally expressed protein far beyond the time period of actual expression.

Thus far, all investigations into the functions of CENP-F family members have been confined to disruption of the endogenous protein in culture. From these studies, we do know that CENP-F functions in a broad swatch of roles within the cell including those regulating processes important to the development of the heart described above. However, differing methods of disruption leave many unanswered questions. While RNAi and Morpholino treatments are absolutely valid methods of protein knockdown and are extensively used, it is critical to investigate the *in vivo* effect of CENP-F deletion, and given the temporal expression pattern of this protein, particularly with reference to organogenesis. For these studies, we have generated a new mouse model

utilizing the Cre/lox system to ablate CENP-F protein expression. Using a cardiomyocyte-specific Cre mouse line, we have shown successful excision of the CENP-F gene in the developing heart. This deletion leads to a generally small heart phenotype, without a change in body mass, and though most heart structures retain their proper development, chamber walls are thinner and trabeculation is blunted in the CENP-F$^{-/-}$ heart. Cardiac TNT-Cre$^{Tg/WT}$;CENP-F$^{loxP/loxP}$ animals also display physiological phenotypes, including progressive dilated cardiomyopathy and heart block. The characterization of this novel mouse model will illuminate the role(s) of CENP-F in the dynamics of heart development and bring further clarification to the field.

Materials and Methods

Developing the CENP-F$^{-/-}$ mouse

For complete details of the generation of the CENP-F$^{loxP/loxP}$ mouse, please see the thesis document of Ryan Pooley, PhD, (http://etd.library.vanderbilt.edu/available/etd-11302006-131209/) (Pooley, 2006).

Genotyping

We used a PCR strategy to determine genotype based on three characteristics of the mouse genome: presence of the 5' loxP site upstream of CENP-F, generation of a DNA band only possible with recombination after Cre-

mediated excision, and the presence of the cTNT-Cre gene. The primers are listed below.

Across 5’ loxP site:

5’ AATAATGAAGCTGACACCAAAAACT,

3’ GAACCTACCGTCTGAGAACCACTG;

Recombination band:

5’ AATAATGAAGCTGACACCAAAAACT,

3’ GAGGAGCACAGGAGGGAAATG

cTNT-Cre:

5’ TCC GGG CTG CCA CGA CCA A,

3’ GGC GCG GCA ACA CCA TTT TT

Organ and tissue preparation for histochemical analysis

Mouse hearts, both embryonic and adult, were isolated from the animal, imaged on a Zeiss Stemi 2000-C steromicroscope with an Olympus camera (model no. 60806, Optronics) for gross anatomical analysis, fixed with methanol, and washed in PBS prior to placement in O.C.T compound (Sakura). The hearts were positioned for proper sectioning orientation within the O.C.T. in the block, frozen in a methanol/dry ice bath, and stored at –20°C until sectioning. Frozen tissues were cryosectioned on a Jung CM 3000 cryostat (Leica) with a thickness of 7 µm. Successive sections were collected on glass slides and stored at –20°C until immunohistochemical analysis. Frozen tissues slides were washed briefly in 1xPBS, permeabilized for 10 min with 0.25% Triton X-100 in 1xPBS, and blocked

in 2% BSA in PBS for 1 h. Primary antibodies in 1% BSA in PBS were applied overnight at 4°C. After three PBS washes, secondary antibodies were applied for 1 h at room temperature. The slides were washed three times with PBS and twice with water before coverslips were attached with Aqua Poly/Mount (PolySciences). Cells were visualized by fluorescence microscopy on an AX70 (Olympus) and digital images were captured and processed using Magnafire (Optronics) and Photoshop (Adobe) software. CENP-F labeling was conducted with a polyclonal antibody Spec1 to CENP-F peptide (aa 1826-45) that was generated in rabbits (Biosynthesis) and affinity purified using the injected peptide (Backstrom and Sanders-Bush, 1997, Soukoulis et al., 2005). DAPI was used to visualize nucleic material (Boehringer Mannheim). For histological analysis, specimens were dehydrated and subsequently embedded in paraffin. Hematoxylin and Eosin staining (H&E) of sections from unstained tissues was performed following standard protocols.

Echocardiography

In the Vanderbilt University Murine Cardiovascular Core, mice were maintained at 37°C prior to imaging and Redux crème used to adhere electrodes to help with conductivity. Imaging was performed using a standoff generated with Aquasonic gel and placed in the tip of a latex glove finger pulled over the tip. A transducer of at least 12 MHz was used and pressed gently against the mouse while the mouse was in a left lateral decubitus position. Mice were imaged in a parasternal long axis view to study the septum, posterior wall, apex and left

ventricular outflow tract and in a short axis views at the chordal level to study symmetry of wall thickness and contraction. From these studies, M-mode images were recorded on a strip chart at a speed of 100 mm/sec. Dimensions from the M-mode tracings and the summary interpretation were entered in the database after review of the data quality, raw data, and interpretation by a trained echocardiographer.

Electrocardiography (ECG)

In our studies we used a commercially-available system for recording ECG data in unanesthetized, unrestrained WT and cTNT-Cre$^{Tg/WT}$;CENP-F$^{loxP/loxP}$ animals available through the Vanderbilt University Murine Cardiovascular Core. Small (< 4 gm) telemetry devices (Data Sciences, Inc.) were implanted under anesthesia in the peritoneum and the wires tunneled to the left shoulder and right leg. Recovery occurred within a day, and, via a telemetry receiver placed under the cage, ECG data were obtained for 30 minutes. Again, a trained electrophysiologist examined all data (raw and analyzed) and insured quality control.

Results

CENP-F is successfully excised by cTNT-Cre to generate a heart-specific knockout model

Given the lack of any *in vivo* studies of CENP-F function, our laboratory developed a mouse model to delete the CENP-F gene. Ryan Pooley, PhD, used

BAC clones to analyze the 5' region of the CENP-F gene and subsequently, clone the gene segment into the pFRT.loxP vector (a generous gift from Dr. Mark Magnuson, Vanderbilt University). This vector contains the loxP sites, the thymidine kinase negative selection marker utilized for random vector integration events, and FRT sites used to delete the neomycin resistance cassette. The cloning strategy successfully isolated the first five exons of CENP-F with loxP sites within this vector (Figure 5.1A-B, (Pooley, 2006)) and this region contains the functional domains previously characterized with binding partners syntaxin 4, Hook2, and SNAP25 (Moynihan et al., 2009a; Pooley et al., 2008b; Pooley et al., 2006). This process is spelled out in great detail in the final dissertation of Ryan Pooley, PhD, but I will summarize it here. The Vanderbilt Transgenic Mouse/Embryonic Stem Cell Shared Core Resource Facility electroporated this targeting construct into embryonic stem (ES) cells and screened the resulting clones for recombination at the CENP-F locus. Two ES clones were positive for all sections of the screened locus and were injected into blastocysts and then, placed in foster mothers. One founder pup was chosen due to successful transmission in the germline and this line was then backcrossed to the ICR background and maintained in this manner (Pooley, 2006). Currently, these mice are genotyped by PCR analysis with primers bordering the 5' loxP site to identify WT by the shorter band (572bp) and floxed mice by the larger band (606bp) (Figure 5.1C, Lanes 1-3).

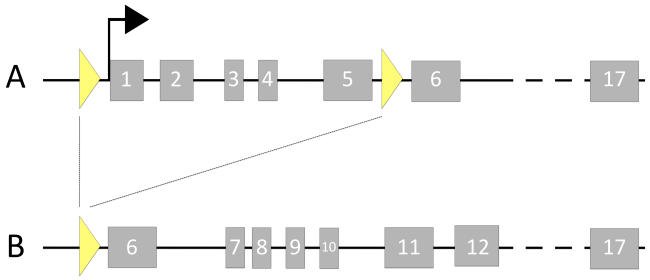
A
1
2
3
4
5
6
17
B
6
7
8
9
10
11
12
17

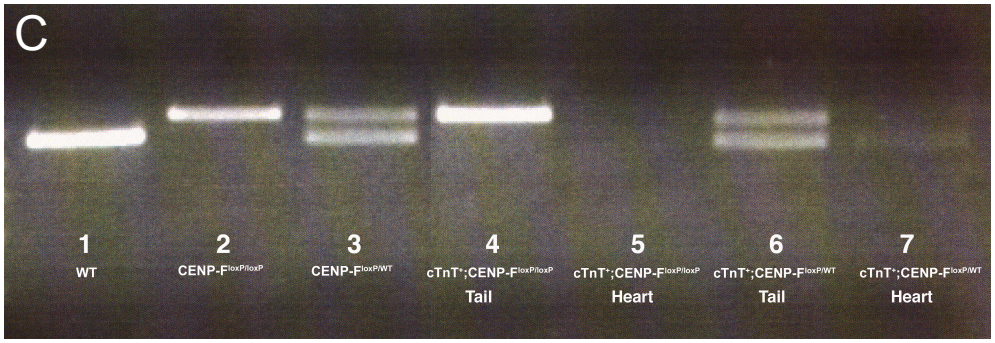
C
1
WT
2
CENP-F loxP/loxP
3
CENP-F loxP/WT
4
cTnT+;CENP-F loxP/loxP
Tail
5
cTnT+;CENP-F loxP/loxP
Heart
6
cTnT+;CENP-F loxP/WT
Tail
7
cTnT+;CENP-F loxP/WT
Heart

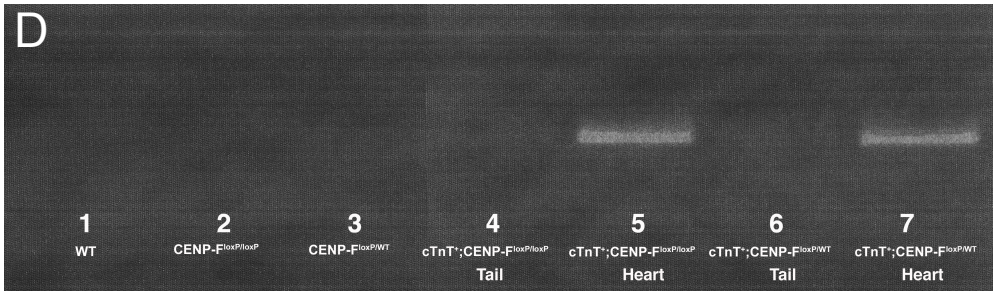
D
1
WT
2
CENP-F loxP/loxP
3
CENP-F loxP/WT
4
cTnT+;CENP-F loxP/loxP
Tail
5
cTnT+;CENP-F loxP/loxP
Heart
6
cTnT+;CENP-F loxP/WT
Tail
7
cTnT+;CENP-F loxP/WT
Heart

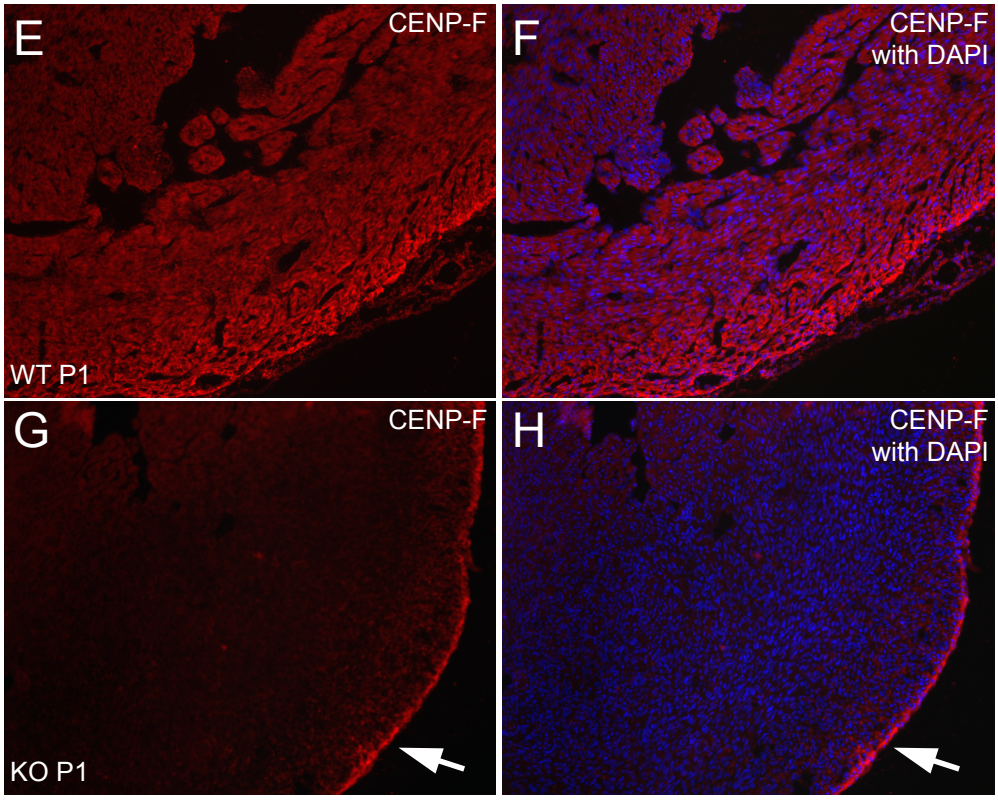
E
CENP-F
WT P1
F
CENP-F
with DAPI
G
CENP-F
KO P1
H
CENP-F
with DAPI

Figure 5.1. Deletion of the CENP-F gene with Cre-lox technology
A. Schematic of CENP-F gene with location of loxP sites marked by yellow arrowheads. Gray boxes indicate CENP-F exons. B. Results post-Cre-expression. The first 5 exons of CENP-F are removed when crossed with the cTnT-Cre mouse line, a generous gift from Dr. Scott Baldwin. This line expresses Cre recombinase in cardiomyocytes beginning at E7.5. (C-D) Genomic PCR confirms Cre-mediated excision of floxed CENP-F gene segment. Lane 1: WT, 2: CENP-$F^{loxP/loxP}$, 3: $CENPF^{loxP/WT}$, 4: Tail sample $cTnT^{+}$; CENP-$F^{loxP/loxP}$, 5: Heart sample $cTnT^{+}$;CENP-$F^{loxP/loxP}$, 6: Tail sample $cTnT^{+}$; CENP-$F^{loxP/WT}$, 7: Heart sample $cTnT^{+}$; CENP-$F^{loxP/WT}$. C. Primers flanking 5' loxP site, D. Opposing primers flanking both loxP sites to show recombination. (E) Loss of CENP-F protein in CENP-$F^{-/-}$ hearts after cross with cTnT-Cre line. α-CENP-F antibodies are negative $cTnT^{+}$;CENP-$F^{loxP/loxP}$ myocytes. Arrows show the retention of protein expression in overlying epicardium.

Using Cre/lox technology, a cross with a Cre-expressing mouse model would excise the region of CENP-F flanked by the inserted loxP sites, thus removing the translational start site of the protein, as well as much of the functional protein, if transcribed at all. The sheer size of the CENP-F gene rendered the process of floxing the entire gene unfeasible at the time the project was initiated. Given the high expression of CENP-F in the developing heart, we crossed the CENP-F$^{loxP/loxP}$ mouse model with the cTNT-Cre mouse line (a generous gift from Dr. Scott Baldwin, Vanderbilt University) to remove CENP-F expression from the developing cardiomyocytes. CENP-F ablation is specific to the heart, as shown by Figure 5.1C-D. Figure 5.1C shows PCR analysis with primers flanking the 5' loxP site. Lanes 4-7 show the disappearance of the flox band with the expression of Cre in the heart, whereas tail samples from the same mice still generate DNA bands of floxed size similar to those in Figure 5.1A. However, after Cre-mediated excision, a DNA band indicative of recombination appears when primers flanking both loxP sites are used with the same DNA samples. Figure 5.1D shows these bands in the heart samples of CENP-F$^{loxP/loxP}$ and CENP-F$^{loxP/WT}$ mice. From this point onward, cTNT-Cre^{Tg}; CENP-F$^{loxP/loxP}$ hearts will be referred to with the CENP-F$^{-/-}$ nomenclature.

Considering the successful deletion of the CENP-F gene, we then pursued confirmation of protein ablation. Figure 5.1E-H demonstrates the difference in CENP-F protein expression when comparing P1 WT and CENP-F$^{-/-}$ heart sections via immunofluorescence. Figure 5.1E-F shows widespread CENP-F

expression throughout the myocardium, whereas panels G and H indicate the absence of CENP-F in the myocardium. However, as an internal positive control, expression is retained and can be visualized in the epicardium of the CENP-F$^{-/-}$ heart. The cTNT-Cre does not recombine DNA in the epicardium. Taken together, these data all demonstrate the effective development and evaluation of the heart specific CENP-F$^{-/-}$ mouse model.

CENP-F$^{-/-}$ hearts display morphological differences in size and chamber wall thickness

After confirmation of CENP-F ablation, we initially analyzed the gross anatomy of the resulting hearts. CENP-F$^{-/-}$ hearts demonstrate a markedly smaller size from before birth through to adulthood. Figure 5.2A-B shows representative examples of E17.5 hearts from WT (Figure 5.2A) and CENP-F$^{-/-}$ (Figure 5.2B) hearts and the tracing of the ventricles shows a distinct size difference between the two. Even at 7 weeks after birth, Figure 5.2C shows a consistently 30-40% larger WT (left) heart than CENP-F$^{-/-}$ heart (right). However, despite the smaller overall size, specific heart structures appear to develop normally, including valves, endocardium, and vessels. There is a modest reduction in the coronary vasculature and epicardium in the CENP-F$^{-/-}$ hearts, but this has not yet been quantified. Additionally, cTNT-Cre^{Tg}; CENP-F$^{loxP/loxP}$ animals show no difference in overall body size, therefore this effect is putatively heart-specific thus far in our analyses.

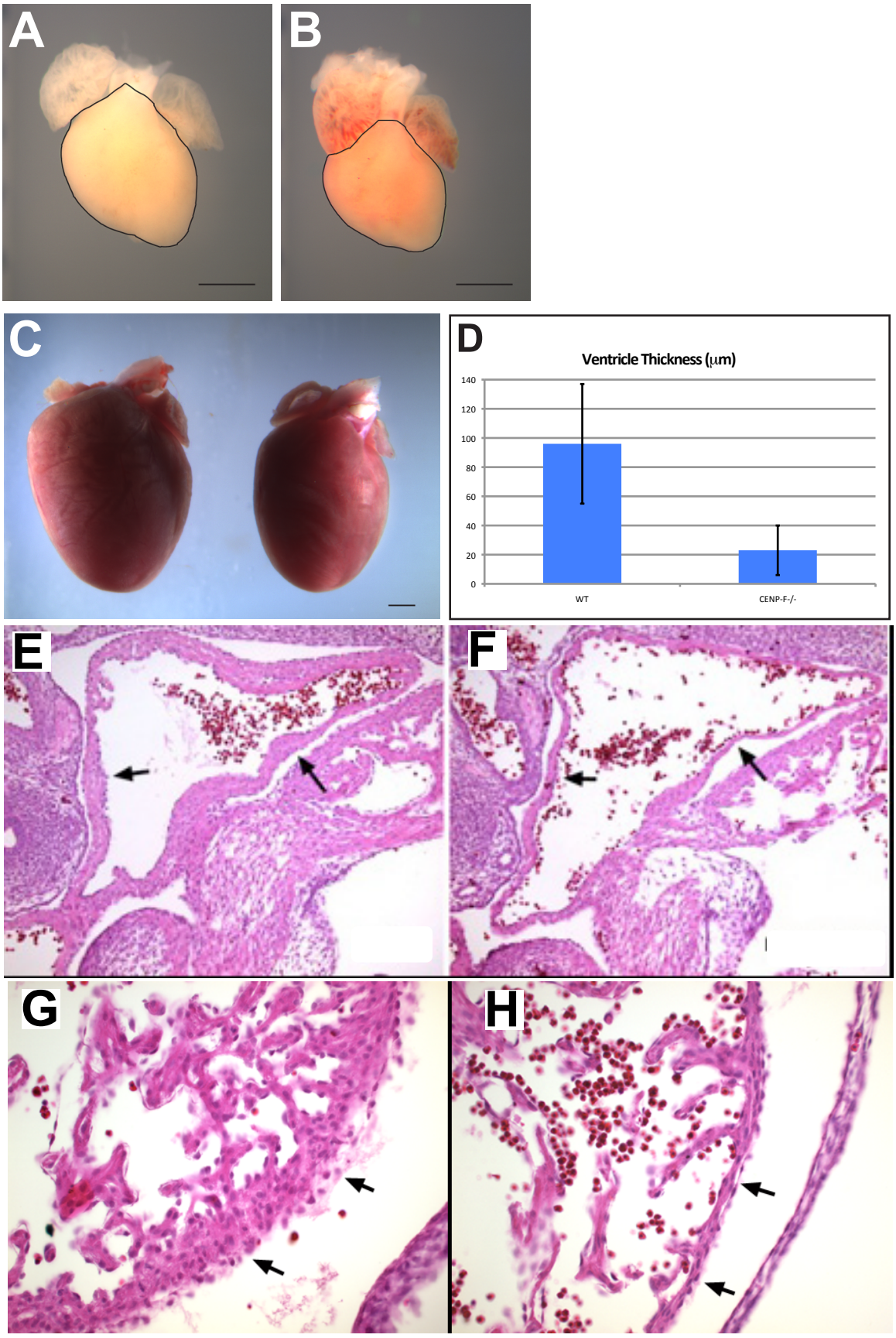
A
B
C
D
Ventricle Thickness (μm)
140
120
100
80
60
40
20
0
WT
CENP-F-/-
E
F
G
H

Figure 5.2. CENP-F$^{-/-}$ hearts display morphological differences in size and chamber wall thickness.
(A) E17.5 CENP-F$^{-/-}$ and (B) WT hearts display a 25-35% difference in overall size when compared. Scale bar 1mm. (C) CENP-F$^{-/-}$ hearts (right) are 30-40% smaller in ventricular mass/size (N = 12; all males) yet no difference in animal size is observed when compare to WT hearts (left). Scale bar 1mm. (E-F) Clear differences in atrial wall thickness are observed in low power view of E12.5 (E) WT and (F) CENP-F$^{-/-}$ hearts. Arrows show regions of marked disparity in atria. (G-H) Cross sections through the widest point in both ventricles show that the (G) WT ventricle has thicker outer walls and greater trabeculation. (H) The CENP-F$^{-/-}$ ventricle has much thinner walls and blunted trabeculae. (D) Non-trabeculated regions of WT and CENP-F$^{-/-}$ ventricular outer wall were measured (n=20) and significant differences in thickness (CENP-F$^{-/-}$: 23μm ±17; WT: 96μm ±4; mean±sd. $p<0.05$) were observed in the myocardium. Arrows demonstrate equivalent regions where variation in wall thickness is readily observed.

Since the heart undergoes much of its proliferative period between stages E11.5 and E14 (Erokhina, 1968; Kirby, 2007; Savolainen et al., 2009), our next step was to examine heart sections during this time period. From our preliminary investigation, it appears that both atrial and ventricular heart walls are thinner in the CENP-F$^{-/-}$ heart than in the WT heart at E12.5. The difference between controls and experimental models is significant upon measurement of the thickest transverse section of the ventricle (Figure 5.2D). Atrial walls are thinner at several points indicated by arrows in representative H&E transverse sections of WT (Figure 5.2E) and CENP-F$^{-/-}$ (Figure 5.2F) hearts. In addition, not only are CENP-F$^{-/-}$ ventricle walls thinner, as shown by the arrows in Figure 5.2H, but their trabeculae are also thin and blunted compared to those in the developing chamber of the WT heart in Figure 5.2G. This pronounced difference in heart wall thickness in the embryo could explain the overall size difference in the mutant hearts, though other stages need to be examined.

CENP-F$^{-/-}$ hearts show impaired function

Continuing our preliminary characterization of the heart specific knockout, CENP-F$^{-/-}$ and WT littermates were analyzed for cardiac function from four to 26 weeks old. Experimental and control mice did not show significant variation in either body weight or heart rate at 12 weeks of age. The Vanderbilt University Murine Cardiovascular Core carried out left ventricular dimensional and contractility analyses with serial conscious transthoracic echocardiography. This technique can detect the presence of local or general hypertrophy or myocardial

thinning in the left ventricle as well as the presence of regional or global chamber wall motion abnormalities (Jeff Rottman, personal communication). An example of the visual image gathered by the technique is pictured in Figure 5.3A-B. Figure 5.3, Panel A shows a reading of a WT left ventricle and Panel B details a representative example of a CENP-F$^{-/-}$ left ventricle. The diastolic and systolic dimensions of the heart can be seen and accurately quantified as shown by the thick (systolic) and thin (diastolic) lines to the right of each image. Precise measurements throughout the length of the study established a trend toward increased diastolic and systolic left ventricular dimension, indicative of progressive dilated cardiomyopathy and decreased contractile capacity (Figure 5.3C). Accordingly, the CENP-F$^{-/-}$ hearts showed diminishing function within this time frame, as evidenced by the waning shortening fraction (Figure 5.3D). This measurement is representative of the output function of the heart by virtue of contractility. Together, these longitudinal studies confirm a functional phenotype of the CENP-F$^{-/-}$ heart model, a progressively enlarged heart and impaired in terms of contractile properties.

In light of the size and contractility deficiencies observed in aging CENP-F$^{-/-}$ hearts, additional functional studies were performed assessing conduction through the heart. Again, the Vanderbilt University Murine Cardiovascular Core performed these techniques, specifically long-term electrocardiographic (ECG) recordings. Within the PQRST conduction wave throughout the heart, the PR interval is readily measured, quantified, and

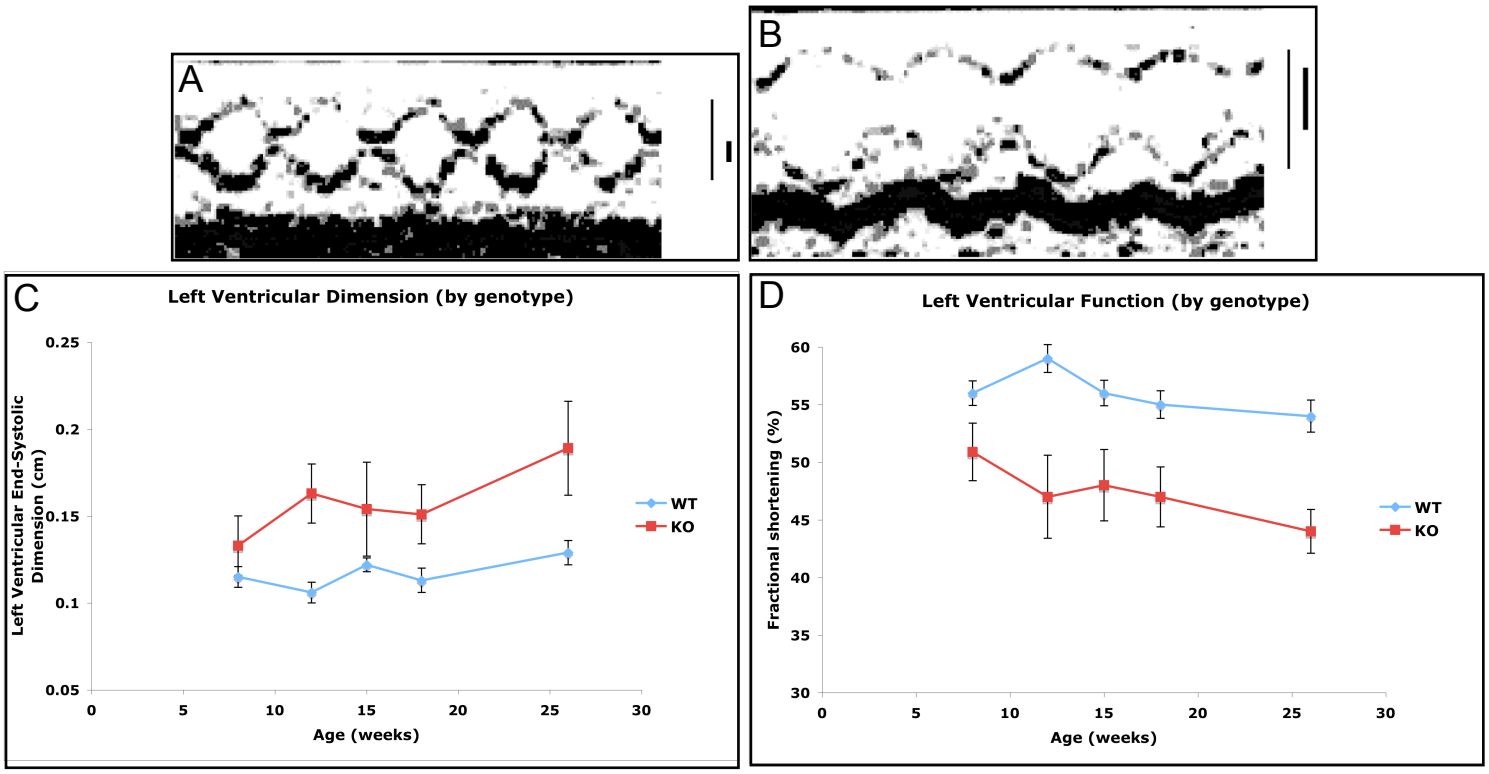
A
B
C
Left Ventricular Dimension (by genotype)
Left Ventricular End-Systolic Dimension (cm)
0.25
0.2
0.15
0.1
0.05
0
5
10
15
20
25
30
Age (weeks)
WT
KO
D
Left Ventricular Function (by genotype)
Fractional shortening (%)
60
55
50
45
40
35
30
0
5
10
15
20
25
30
Age (weeks)
WT
KO
E

Figure 5.3. CENP-F$^{-/-}$ mice show enlarged ventricles and impaired function.
(A-D) Longitudinal echocardiography with M-mode echocardiograph was used to measure ventricle size and contractility. Representative images of the left ventricle of (A) WT and (B) CENP-F$^{-/-}$ hearts at the mid-papillary level. To the right of each panel are a thin line (diastolic) and thick line (systolic) to demonstrate measurement. CENP-F$^{-/-}$ hearts show ~2x ventricular dilation in diastole and moderate ventricular systolic dysfunction (decreased FS% at comparable afterload). This increased dimension worsens with time as seen in Panel C. At 12 weeks, WT (n=11) and CENP-F$^{-/-}$ mice (n=5) did not differ in terms of body weight (WT: 21.1±1.9g; CENP-F$^{-/-}$: 22.8±2.4g, mean±sd, p>.05,not significant) or heart rate during echocardiography (WT: 678±46 bpm; CENP-F$^{-/-}$: 654±61 bpm, mean±sd, p>.05, not significant). (C) However, by 26 weeks, left ventricular dimension was distinctly increased in CENP-F$^{-/-}$ mice: LVIDs 0.19±0.03cm (WT); 0.13±0.01cm (CENP-F$^{-/-}$), p<0.01. (D) Dysfunction is observed at all time points during the study and CENP-F$^{-/-}$ hearts developed major differences in cardiac function. The shortening fraction of the knockout was substantially less (FS% 44±1.9) compared to the WT (54±1.9, mean±sd,), p< 0.001. Additionally, irregular ECG intervals are seen in CENP-F$^{-/-}$ mice with ambulatory echocardiograms. Panel E shows erratic sinus node function through irregular and extended P-P intervals (110–410ms). Further deficiencies are observed with analysis of long-term electrocardiographic recordings, including persistently prolonged PR intervals, low QRS complex amplitude and prolonged duration, and evidence of sinus node dysfunction or sino-atrial exit block.

represents a measure of cardiac conduction. In our studies, CENP-F$^{-/-}$ hearts displayed prolonged PR intervals, which is indicative of primary heart block, also known as sinus node dysfunction (Figure 5.3E, Ellen Dees, MD, personal communication). Additionally, Figure 5.3E also shows irregularly dropped beats, often evidence of secondary heart block and sino-atrial exit block. Moreover, there is some evidence of low QRS complex amplitude and prolonged duration in the cTNT-Cre$^{Tg/WT}$;CENP-F$^{loxP/loxP}$ animals. In humans, the QRS duration represents a measure of ventricular conduction but in mice the QRS often fuses with the ST segment, and hence QRS duration cannot be as reliably measured (Jeff Rottman, MD, personal communication). In view of the significant dilated cardiomyopathy developed in the CENP-F$^{-/-}$ hearts, these observed conduction flaws could be a result of the terminally enlarged heart or a primary result and we will explore these possibilities further (Kozlov et al., 2005). If the disrupted conduction pattern is not a direct result of the dilated cardiomyopathy, it is possible that the intercalated discs (IDs) connecting the CENP-F$^{-/-}$ cardiomyocytes could be affected on a cellular level and thus globally impacting conduction. Furthermore, in a nine month time period of analysis, the experimental animal population had a 20% mortality rate, with no deaths of WT animals. Therefore, from morphological, functional, and survival standpoints, CENP-F is required for proper heart development and function.

Discussion and Future Directions

In this first examination of CENP-F function *in vivo*, we used Cre-mediated excision to specifically delete the CENP-F gene in the developing cardiomyocytes. After crossing the CENP-F$^{loxP/loxP}$ mouse model with the cTNT-Cre mouse model, we confirmed the heart-specific absence of the floxed portion of CENP-F via PCR and immunofluorescence. The resulting CENP-F$^{-/-}$ mice had the same body size as their WT littermates, but demonstrated a significantly smaller heart both during development and up to seven weeks of age. Upon examination of the interior of the organ, we determined that the chamber walls were thinner in cTNT-Cre$^{Tg/WT}$;CENP-F$^{loxP/loxP}$ animals. In addition to the morphological differences between WT and CENP-F$^{-/-}$ hearts, cTNT-Cre$^{Tg/WT}$;CENP-F$^{loxP/loxP}$ animals also displayed physiological deficiencies. Long-term echocardiography analyses revealed dilation of the left ventricle and diminishing contractile function of CENP-F$^{-/-}$ hearts. Furthermore, electrocardiography showed primary and potentially secondary heart block in cTNT-Cre$^{Tg/WT}$;CENP-F$^{loxP/loxP}$ animals. Finally, to this point in our analyses, 100% of adult CENP-F$^{-/-}$ hearts exhibit progressive dilated cardiomyopathy. From these studies, ablation of CENP-F in developing cardiomyocytes clearly has detrimental effects on the morphology and function of the heart.

Despite the notable phenotypes seen with the deletion of CENP-F in the heart, we have not yet addressed the underlying mechanism. Further studies are ongoing to delineate which role(s) of CENP-F are involved in the developmental

defects seen here. First, the smaller size of the heart seen with the ablation of CENP-F immediately suggests a decreased level of proliferation, especially considering the work in the field characterizing the importance of CENP-F family member CMF1 in the balance of proliferation and differentiation (Dees et al., 2006; Robertson et al., 2008). Moreover, Dees et al. have also shown that CENP-F expression in the heart matches the high level of proliferation occurring up until postnatal day 7, after which both CENP-F expression and proliferation is down-regulated (Dees et al., 2005). Disruption of CENP-F has been shown to disturb the progression of mitosis and this delay could be the mechanism leading to the observed phenotype (Bomont et al., 2005; Cheeseman et al., 2005; Evans et al., 2007; Feng et al., 2006; Holt et al., 2005; Laoukili et al., 2005; Yang et al., 2005). The balance joining proliferation, apoptosis, and differentiation is critical in producing trabeculae of cardiomyocytes to eventually compact and form the heart wall (Savolainen et al., 2009). Disrupting this time-sensitive process impacts adult function, as the heart is not an organ that can remodel easily (Ahuja et al., 2007). Therefore, BrdU and TUNEL analyses will be performed to assess the effect of CENP-F deletion on levels of proliferation and apoptosis within the developing heart.

Wall formation through trabeculation relies heavily on proliferating myocytes migrating to form “finger-like” projections into the ventricular space (Sedmera et al., 2000). In our preliminary studies, we have observed shorter, less extensive trabeculae in the ventricular wall. CENP-F$^{-/-}$ and WT sections will

be examined for potential changes in myocyte proliferation by BrdU analysis at specific stages of development (Dees et al., 2005; Dees et al., 2006). Cross-sections of CENP-F$^{-/-}$, CENP-F$^{+/-}$, and WT hearts at E8.5, E11.5, E14.5, E18.5, P4, P7, and P14 will be analyzed in randomly selected samples at comparable ventricular, atrial, and outflow tract levels. To determine whether labeled cells are myocytes, anti-myosin (MF20) staining will be coupled with BrdU analysis. Additional proliferation markers such as K167, phosphorylated histone 3, and PCNA can also be quantified (Dees et al., 2005). From previous work showing CENP-F involvement in myocyte division (Dees et al., 2005), I expect to see a significant decrease in proliferation in CENP-F$^{-/-}$ myocardium. Given that a heart wall forms despite lack of CENP-F, it is possible that proliferation is affected, but not blocked completely, or that the rate of division is reduced. Sections at sequential stages will show the effects of CENP-F ablation on different stages of myocardial development. If a reduction in BrdU incorporation is observed at all or specific stages, this may explain the reduction in wall thickness and reduction in trabecular outgrowth and these data would fit with the documented role of CENP-F in proliferation. It is also possible that reduction in myocyte number is the result of abnormal MT array structure as well as disruption of mitosis. This may be better analyzed in the following section describing experiments at the single cell level. Disruption of CENP-F function has also increased apoptosis in culture (Ashe et al., 2004), thus giving credence to expected results showing increased apoptotic cells in the CENP-F$^{-/-}$ myocardium. Using antibodies to cleaved Caspase 9, the potential increase in apoptotic myocytes and their distribution in

developing CENP-F$^{-/-}$ hearts will be compared to WT controls (Goldspink et al., 2004). An increase in apoptosis in the presence or absence of reduced mitotic activity may provide a mechanistic understanding of the cellular functions disrupted in CENP-F gene ablation, leading to the observed phenotype and supporting the overall hypothesis.

If proliferation or apoptosis anomalies do not contribute to this phenotype as demonstrated by statistical analysis (Dees et al., 2005; Gonzalez-Sanchez and Bader, 1990), smaller cell size could be a potential factor in explaining the small heart phenotype. In situ investigation of myocyte diameter using anti-Bves antibodies to mark the sarcolemma of myocytes will provide quantified morphological data at various stages (Smith and Bader, 2006). Confocal microscopy allows accurate measurement of cardiac myocyte dimensions, and thus, cell volume (Blaser et al., 2006; Bullard et al., 2005; Fotos et al., 2006). Moreover, confocal microscopy will also be used to quantify potential changes in the cytoskeleton as well as its associated proteins with antibodies against tubulins, Hook2, NudE, Lis1, and centrosomal markers.

Additionally, cell division is reliant on centrosome function and the MT network to ensure proper mitotic activity. Given the role of CENP-F in regulation of the MT network, cytoskeleton, and cell shape, I anticipate that CENP-F$^{-/-}$ hearts will demonstrate disordered MTs and thus, variable cell shape and size compared to control animals. The appearance of the “rod-like” structure in

coincidence with MF20 labeling will constitute a WT shape. This disruption will likely show mistargeted proteins of the MTOC, including Hook2. Loss of Hook2 localization and/or MT disruption could lead to potential changes in cardiac myocyte structure and contractile activity as well as loss of proliferative behavior. I defer much of this discussion the next section, where I describe cell shape and cytoarchitecture experiments more easily studied at the subcellular level in isolated cardiomyocytes.

CENP-F has been shown to regulate several cytoplasmic cellular processes as described previously and in this document (Feng et al., 2006; Moynihan et al., 2009a; Pooley et al., 2008b; Pooley et al., 2006; Soukoulis et al., 2005). Therefore, to examine the potential contribution of these processes to the emergence of the small heart phenotype and resulting physiological problems, we will examine isolated cardiomyocytes in culture. This will provide the background for analysis of molecular function in the complex environment of *in vivo* development, since the stress of cell culture conditions may intensify any defects in cellular or developmental processes.

Immunofluorescence will be used to examine cytoskeletal organization in conjunction with appropriate antibodies such as α, β, and tyrosinated tubulin markers, MTOC markers γ tubulin and centrin, and both α-skeletal and α-cardiac actin markers. These studies will be carried out in consultation with Dr. Irina Kaverina's laboratory to gather additional live imaging and quantitative

microtubule data after being statistically verified according to published work (Gonzalez-Sanchez and Bader, 1990; Yutzey et al., 1995; Yutzey et al., 1994). In particular, Hook2 and other CENP-F binding partner distributions will be examined, as well as specific centrosomal proteins.

Similar to expectations with Hook2 interference, I predict disrupted MT network organization after CENP-F ablation. These data would provide confirmation of cell line data demonstrating the role of CENP-F in MT organization. If MT organization is disrupted, the literature suggests Ca2+ signaling and channel trafficking could be disrupted (Gómez et al., 2004; Gómez et al., 2000; Leach et al., 2005). Accordingly, I would investigate vesicular trafficking as described in previous publications (Pooley et al., 2008b; Pooley et al., 2006) and cell coupling in CENP-F-ablated myocytes as described below. From previous Hook2 and CENP-F studies, I predict disruption of centrosomal proteins involved in MT nucleation and anchoring. If this is observed, potential interaction/collaboration of the mislocalized proteins with CENP-F will be pursued.

Immunolabeling and western blots will be used to determine the localization and expression level of various connexin proteins (Cx43, 40, 46) to determine the viability of cell coupling in vitro. Additionally, Dr. Cecilia Lo, in collaboration with our laboratory, has provided instruction in microelectrode impalement of cultured cells with carboxyfluorescein dye spread by gap junction

interaction (Huang et al., 1998). One cultured ablated cell will be impaled with dye and time-lapse imaging provides quantitative measurement of coupling via dye spread from one tier of cells to the next tier removed from the original cell. This method, quantification, statistical analysis, and resulting data are shown in a recent publication (Pooley et al., 2008b) and this technique can be used to assay gap junction viability. I would expect to see a lack of connexin protein(s) at the intercalated disc, thus indicating improper gap junction formation. As seen in preliminary studies with NT-CENP-F, cell coupling is compromised in transfected 3T3 cells (Pooley, 2006). This is likely to be more evident with ablated primary cultures programmed to form gap junctions and provides a correlation to those connections necessary in the electrical conduction of the heart via the ID. It should be noted that the irregularities in ECG tracings, particularly low QRS complex amplitude and prolonged duration, are observed in *in vivo* CENP-F preliminary studies. Additionally, synchronization of membrane potential or calcium transients could also be used to assay gap junction function. Thus, it is possible that malformation or disruption of the gap junction is the underlying mechanism to explain this phenotype.

Myocyte shape is important in cardiac wall formation; therefore irregularities could contribute to thinner walls and blunted trabeculae. The cytoskeleton is a primary factor in determining cell shape, and thus is the focus of these studies. Knockdown of CENP-F expression has clearly shown effects on the cytoskeleton in previous studies (Soukoulis et al., 2005), thus ablation would

likely produce a similar, if not more dramatic, phenotype. Myocytes will be monitored to determine whether they change shape and maintain cell-cell contact and IDs as shown by Barker, et al (Barker et al., 2002). Time-lapse imaging microscopy will quantify cell shape and motility as described by McDevitt, Eppenberger, and Pantos in their respective publications (Eppenberger and Zuppinger, 1999; McDevitt et al., 2002; Pantos et al., 2007). If a change in cell shape or migration is observed as expected, then it is likely that the cytoskeleton is affected by the loss of CENP-F protein. This cytoskeletal disruption could then be further investigated by examining the MTOC function to determine if the phenotype originates with MT nucleation and retention.

To this point, we have very promising and consistent results demonstrating a readily apparent phenotype in the cTNT-Cre$^{Tg/WT}$;CENP-F$^{loxP/loxP}$ animals. Our published work performed in culture establishing several functions of CENP-F shows good potential in explaining the mechanism underlying the small heart phenotype. The additional studies outlined above should be able to elucidate the cellular basis for the observed developmental defects by analyzing these functions separately. My ongoing examinations, as well as those of laboratory members to come after me, will be submitted for publication in conjunction with the results summarized here.

CHAPTER VI

CONCLUSIONS AND FUTURE DIRECTIONS

Conclusions

The studies presented here result from two big picture approaches to characterizing CENP-F function: identification of new binding partners and thus, cellular processes in which CENP-F plays a role, and analysis of phenotypes generated by genetic deletion of the CENP-F gene. These analyses establish further definitive links between CENP-F and MT network function and serve as a novel perspective on the general theme of CENP-F function at many diverse locations of MT function. Additionally, this work demonstrates the essential function of CENP-F in murine heart development. Previous investigation of CENP-F function provided a framework of CENP-F participation in vesicular recycling and the LIS1 pathway, and from that point, this thesis identifies another role in vesicular transport and at the centrosome in MT nucleation. Chapter II outlines our data identifying syntaxin 4, a t-SNARE, as a binding partner for CENP-F, determined in a yeast two-hybrid screen. The binding of these two proteins was confirmed by co-immunoprecipitation and colocalization visualized with immunofluorescence. Expression of the syntaxin-binding domain of CENP-F shows accumulation of syntaxin 4, as well as SNAP-25 and VAMP2, in the TGN as indicated by golgin-97 labeling. Additionally, expression of truncated CENP-F with either SNARE binding partner (syntaxin 4 or SNAP-25) inhibited cell

coupling as evidenced by the decrease in dye spreading from an impaled and transfected cell. Furthermore, additional corroboration of impaired vesicular trafficking was shown with depletion of CENP-F. Differentiated adipocytes were treated with CENP-F morpholino and stimulated with insulin to facilitate GLUT4 vesicular trafficking. This exocytotic pathway was impaired in those cells with CENP-F knockdown despite constant levels of other involved proteins. These studies, in combination with previous work demonstrating the binding of CENP-F and SNAP-25, definitively show cytoplasmic localization and function of CENP-F in vesicular trafficking.

In chapter III, I further explore the function of CENP-F in the context of a newly identified binding partner, Hook2. The Hook2 linker protein localizes to the centrosome and regulates MT network organization (Szebenyi et al., 2007). Again, after initial discovery via Y2H, interaction was confirmed in mammalian cells by co-immunoprecipitation and established at the centrosome by immunofluorescence. In addition to transient tagged protein constructs, experiments were also conducted endogenously and the data show both Hook2 and CENP-F at the centrosome. This work is the first documentation of endogenous CENP-F protein localization to this organelle. This report also introduces the first CENP-$F^{-/-}$ cells used in the field, as isolated MEFs from a CMV-Cre; CENP-$F^{loxP/loxP}$ cross. Given the role of binding partner Hook2 at the centrosome in MT organization, WT and CENP-$F^{-/-}$ cells were treated with nocodazole to depolymerize MTs and then allowed to recover. While WT cells

regained a robust MT network quickly, CENP-F$^{-/-}$ cells showed a definitive block in MT repolymerization. In addition, cells transfected with NT-CENP-F, the domain of CENP-F responsible for binding Hook2, and subjected to nocodazole treatment and washout also demonstrated significant repolymerization inhibition. However, both CENP-F$^{-/-}$ and transfected RPE cells showed some MT polymerization in the cytoplasm, presumably from minor MTOCs such as the Golgi (Efimov et al., 2007); therefore, the phenotype seen with CENP-F disruption is centrosome specific. Disruption of CENP-F also disturbs localization of other centrosomal proteins involved in nucleation and anchoring: ninein and PCM-1. Thus, these data demonstrate a novel localization, binding partner, and function at the centrosome for CENP-F. Taken together, chapters II and III begin to outline the comprehensive role of CENP-F within the context of the MT network.

To build upon the CENP-F$^{loxP/loxP}$ mouse model recently developed by our laboratory and explore the function of CENP-F in organogenesis, I turned to the first organ to function in the embryo: the heart. CENP-F expression is especially high in the developing heart in both the mouse and the chicken. In fact, the avian homolog (termed CMF1) is restricted to developing striated muscle, though other family members are ubiquitous in the embryo (Dees et al., 2000; Goodwin et al., 1999; Wei et al., 1996). Therefore, chapter IV serves as a thorough introduction to heart development, with an avian focus. The first section centers on the anatomy of the heart, including the circulatory chambers, valves, coronary

circulation, conduction system, and histology. I then move into heart development, covering very early development, cardiogenic determination and its inducers, the morphogenesis of the developing heart tube, the diversification of the heart lineages, and trabeculation of the heart wall. These themes are discussed in terms of the easily manipulated avian embryo, but can be broadly applied to mammalian heart development in most circumstances.

Chapter V begins the examination of CENP-F function in heart development. Again utilizing the CENP-F$^{loxP/loxP}$ mouse model generated by Ryan Pooley, PhD, crosses were performed with the cTNT-Cre line to excise CENP-F in the cardiomyocytes lineage beginning at E7.5. Successful excision was observed and the resulting offspring survive through birth. However, CENP-F$^{-/-}$ animals display a definite phenotype, even in embryonic stages. The hearts of these KO animals are smaller than those of littermate controls, beginning at E12.5 and continuing in post-natal development. Gross morphology of the heart is relatively unaffected, but upon close examination of the heart wall, CENP-F$^{-/-}$ animals show significant thinning of the developing myocardium. The small hearts eventually develop progressive dilated cardiomyopathy throughout postnatal life and show decreased ventricular functional output. Electrical conduction is also affected in the CENP-F$^{-/-}$ animals, with erratic sinus node function and other abnormalities. Studies are ongoing to determine the mechanism underlying these phenotypes; we are pursuing potential shifts in the proliferation/apoptosis balance and cytoskeletal defects during remodeling.

Nevertheless, it is clear that CENP-F plays an important role in heart development, as its genomic deletion negatively impacts the heart on several levels.

In sum, these chapters demonstrate our characterization of CENP-F by means of binding partner identification and protein-depletion induced phenotypes. These two broad strategies have allowed us to identify two cytoplasmic cellular processes in which CENP-F functions: vesicular trafficking and centrosomal MT regulation. The participation of CENP-F in these processes is mediated by the N-terminus, but does not rule out cooperation with the functions of the C-terminus. In fact, the domains along the entirety of the CENP-F protein have now been shown to function with the MT network in some capacity. As discussed in the introduction, C-terminal CENP-F localizes to the MT-insertion site on the KT and regulates the sustained activation of the spindle checkpoint. Depletion of CENP-F adversely affects chromosome segregation and interferes with the accumulation of spindle checkpoint proteins Mad1, Mad2, hBUBR1, hBUB1, and hMps1 (Bomont et al., 2005; Feng et al., 2006; Holt et al., 2005; Laoukili et al., 2005; Yang et al., 2005). Importantly, depletion of CENP-F also prevents normal oscillation after new K-fiber formation and decreases the distance between KTs (Holt et al., 2005). Additionally, CENP-F binding partner Nde1 is dependent on CENP-F for KT localization and is necessary for chromosome alignment and dynein at the KT (Vergnolle and Taylor, 2007). Also, N-terminal and central CENP-F domains have now both been shown to be

involved along the length of the MTs – either again through Nde1 and the LIS1 pathway or via vesicular trafficking and SNARE proteins (Pooley et al., 2008b; Pooley et al., 2006; Soukoulis et al., 2005). The cytoskeleton is the basis of motor protein-directed vesicular transport; MTs form the intrinsically polar array fundamental in protein and organelle trafficking throughout the cell (Bornens, 2008; Kamal and Goldstein, 2000; Müsch, 2004; Rogers and Gelfand, 2000). SNARE proteins are a very important part of these processes as they facilitate the membrane fusion necessary for vesicle delivery (Jahn and Scheller, 2006) and the interaction of CENP-F with syntaxin 4 and SNAP-25 demonstrates that CENP-F also plays a role in this aspect of the MT network (Pooley et al., 2008b; Pooley et al., 2006). Most recently, our work has established a role for CENP-F in centrosomal MT nucleation, thus ultimately encompassing the entire length of the MT from the minus-end to the plus-end. These associations with MT network functions, as well as the ability to bind tubulin (Feng et al., 2006), provide a novel perspective of CENP-F function on a broader, yet tightly related, scale.

Moreover, we have the tools to further pursue the effect of CENP-F deletion *in vivo* and determine the mechanism of resulting effects on heart development. These ongoing studies are the first examination of CENP-F function in the developing animal, and with the application of cellular studies, could prove very informative in integrating the various roles of CENP-F into an organogenesis model.

Taken together, these studies and those conducted previously have identified a role for CENP-F in the KT assembly and perpetuation of the spindle checkpoint during mitosis, in the balance of proliferation and differentiation, in vesicular trafficking via recycling endosomes and plasma membrane recycling, and finally, in centrosomal MT nucleation. Given the high CENP-F expression during development, CENP-F is positioned as a vital regulator of MT processes during this dynamic period of growth, remodeling, and differentiation. Its unique positioning at both the minus- and plus-end, as well as the length of the microtubule, suggest a bridging mechanism between the MT network and its many functions, as demonstrated by the many cellular processes CENP-F affects. The tubulin-binding domains at the CENP-F termini also support this putative responsibility. Overall, the intersection of CENP-F studies at a cellular level *in vitro* and during organogenesis *in vivo* suggest broad significance in cytoskeletal regulation of development.

Future Directions

Determine the mechanism underlying the heart-specific CENP-F$^{-/-}$ phenotype

The first task at hand is to complete the characterization of the heart-specific CENP-F$^{-/-}$ mouse model. As described in Chapter V, these mice show consistently small hearts that develop dilated cardiomyopathy. Additionally, there are significant conduction defects. Thus, the next step is to identify the

mechanism responsible for this phenotype. Given the many characterized functions of CENP-F, the heart phenotype could be caused by deficiencies in any number of cellular processes. The primary route of investigation will be changes in the balance between proliferation and apoptosis in the developing myocardium. This interpretation is the most straightforward, and as discussed in Chapter I, CENP-F family members have been shown to regulate mitosis through both the spindle checkpoint and the balance between proliferation and differentiation (Bomont et al., 2005; Dees et al., 2005; Encalada et al., 2005; Feng et al., 2006; Holt et al., 2005; Laoukili et al., 2005; Robertson et al., 2008; Yang et al., 2005). Therefore, deletion of CENP-F could quite easily inhibit the high levels of proliferation necessary for myocardial expansion and trabeculation. Examination of BrdU incorporation and TUNEL staining between stages E9.5 and E15.5 would illuminate the potential effect of this heart-specific KO model on this balance.

However, as shown in Chapters II and III, CENP-F regulates other processes such as vesicular trafficking and centrosomal MT nucleation. These processes would be vital during such dynamic remodeling that occurs during myocardial development. Thus, in addition to exploring potential changes in proliferation levels, I also propose examination for cytoskeletal defects and flaws in vesicular transport. While MTs have not been the focus of intense scrutiny in myocardial cells, there is evidence that MTs influence channel expression at the membrane, mRNA transport, and contractile mechanics in differentiated

cardiomyocytes (Cheng et al., 2008; Cooper, 2006; Loewen et al., 2009; Nishimura et al., 2006; Scholz et al., 2008; Shiels et al., 2007). Also, paramount to the functional heart is the development of the interacalated disc (ID) at the borders of coupled cardiomyocytes. This specialized structure is made up of three types of junctions (gap, adherens, and desmosomal) and is integral to the coordinated contraction and conduction between cardiomyocytes. Therefore, the trafficking of proteins specific to the ID, such as potassium channels and junctional proteins, is essential to proper heart function. Given the function of CENP-F in vesicular trafficking as shown with SNARE proteins syntaxin 4 and SNAP-25 (Pooley et al., 2008b; Pooley et al., 2006), it is possible that CENP-F deletion would affect the formation and maintenance of the ID. This effect would fit with the disrupted electrical conduction seen in the CENP-$F^{-/-}$ animals. While *in vivo* analysis with antibody labeling of markers related to both the cytoskeleton and ID would be helpful, it is probable that isolation of embryonic and neonatal cardiomyocytes would be the most revealing. The stresses of cell culture could bring to light those deficiencies unseen in the animal and this type of experimentation would afford manageable observation and manipulation of cell processes separately.

Characterize potential mitotic and migration phenotypes of CENP-$F^{-/-}$ MEFs

As discussed throughout this document, CENP-F has many roles that are governed by domains throughout the considerable length of the protein. Nearly all of these roles relate in some way to the MT network, either on the end or

along the length of the radial array. Therefore, the next logical stop would be to examine the effect of CENP-F disruption on those cellular processes that incorporate major dynamic remodeling of the MT network. For example, mitosis and migration are excellent models. Preliminary data have been gathered using the NT-CENP-F construct generated in Chapter III to disrupt CENP-F protein function during mitosis. Dr. Kevin Vaughan has worked extensively on the role of cytoplasmic dynein regulation in organelle transport and chromosome segregation, and his laboratory used their techniques to examine the effect of transfected NT-CENP-F on mitotic cells. Figure 6.1 shows that NT-CENP-F expression can cause spindle pole fragmentation, but the spindle fragments can still recruit cytoplasmic dynein. This spindle pole fragmentation could potentially affect mitosis overall and we hope to pursue this further with the help of Dr. Vaughan. Additionally, our newly developed CENP-F$^{-/-}$ MEFs could prove to be another helpful tool in examining CENP-F function throughout mitosis; flow cytometry coupled with cell cycle analysis could give us initial clues in whether CENP-F deletion causes a delay or block in the cell cycle.

Furthermore, migration is another major cellular process mediated by the microtubule network. The cytoskeleton as a whole must undergo major shifts as filapodia, lamellipodia, and focal adhesions are in flux during cell movement. To this end, we used live-imaging to analyze MEF migration over six hours, comparing WT and CENP-F$^{-/-}$ cells. While these composite images are preliminary, they do show unusually unregulated lamellipodial extension and a

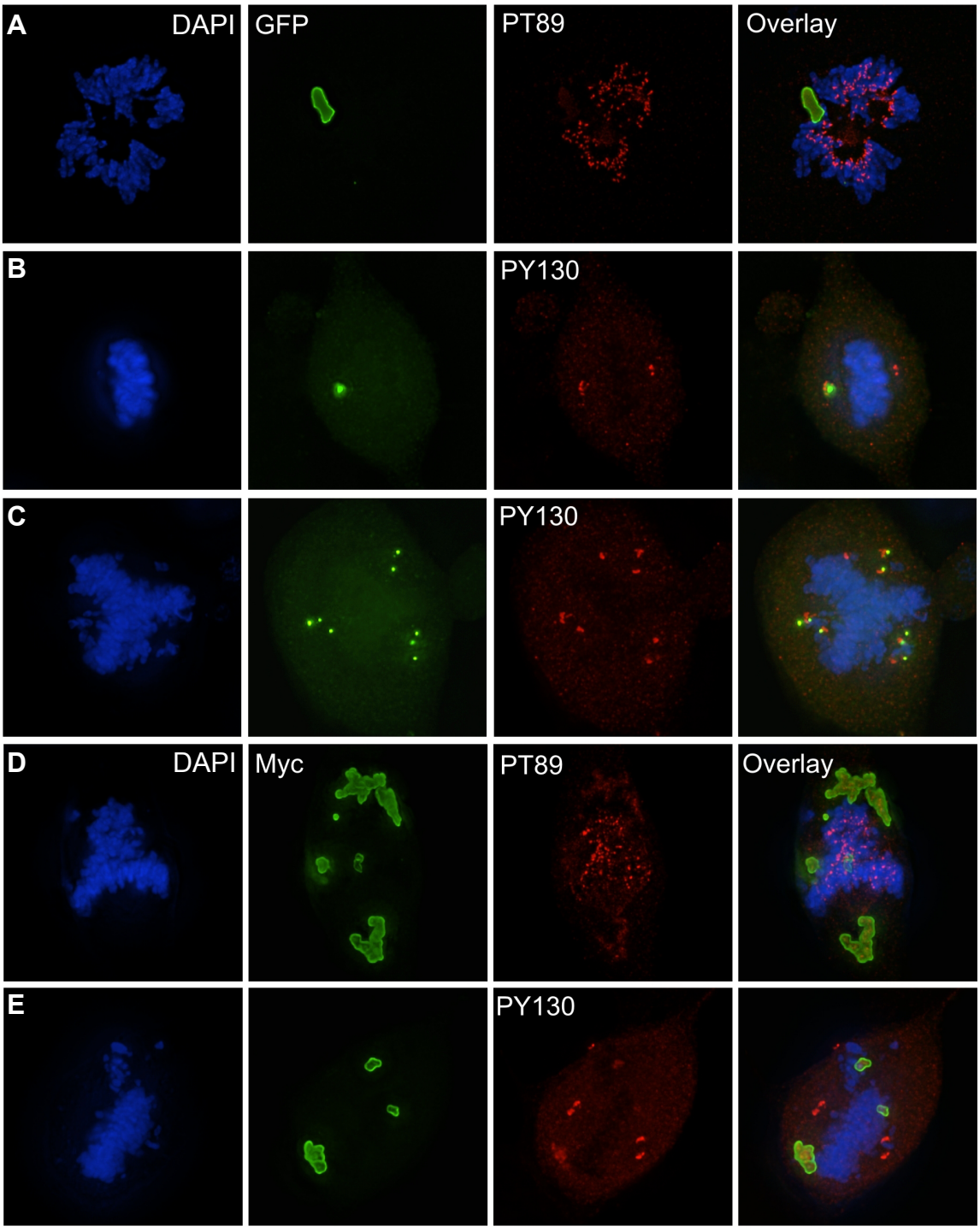
A
DAPI
GFP
PT89
Overlay
B
PY130
C
PY130
D
DAPI
Myc
PT89
Overlay
E
PY130

Figure 6.1. CENP-F disruption induces spindle pole fragmentation but does not affect dynein localization to KTs. Cells were transfected with NT-CENP-F tagged with GFP (Rows A-C) or myc (Rows D and E). Rows A and D demonstrate that NT-CENP-F expression does not affect dynein localization to the KTs (dynein labeled with phospho-T89). Rows B, C, and E show spindle pole fragmentation with expression of NT-CENP-F, but those fragments can still recruit spindle pole dynein (labeled with phospho-Y130).

lack of directed movement. Figure 6.2 shows a representative example of time lapse imaging of both a WT and CENP-F$^{-/-}$ MEF and the extended lamellipodia in the KO cell is very apparent. These studies need to be pursued further, beginning with directional persistence analysis and immunofluorescence to determine the lamellipodial protein composition. It would also be interesting and informative to use our newly acquired full-length human CENP-F construct to look at potential cleavage of N- and C-terminal peptides and utilize different peptide sequences to attempt rescue of any observed phenotype.

Develop and characterize global CENP-F$^{-/-}$ murine model

Finally, it would be very beneficial to use our existing tool, the CENP-F$^{loxP/loxP}$ mouse model, to further explore global CENP-F function. Preliminary matings of the floxed animal with the CMV-Cre used for MEF isolation yields offspring viability, but potential mosaicism of this Cre could throw doubt on potential results (Guoqiang Gu, personal communication). Accordingly, we plan to also employ E2F-Cre in our global CENP-F deletion. It would be very interesting to explore the resulting effect on the brain, as along with the heart, it is a site of high CENP-F expression and substantial MT activity through axonal extension. As we have done in the heart and plan to do with cardiomyocytes, following a similar path in investigating CENP-F function in the brain and in neurons would be another application of CENP-F regulation of MTs and vesicular trafficking. In conjunction with these studies, it would also be advisable to re-examine expression of CENP-F throughout development. With all of the

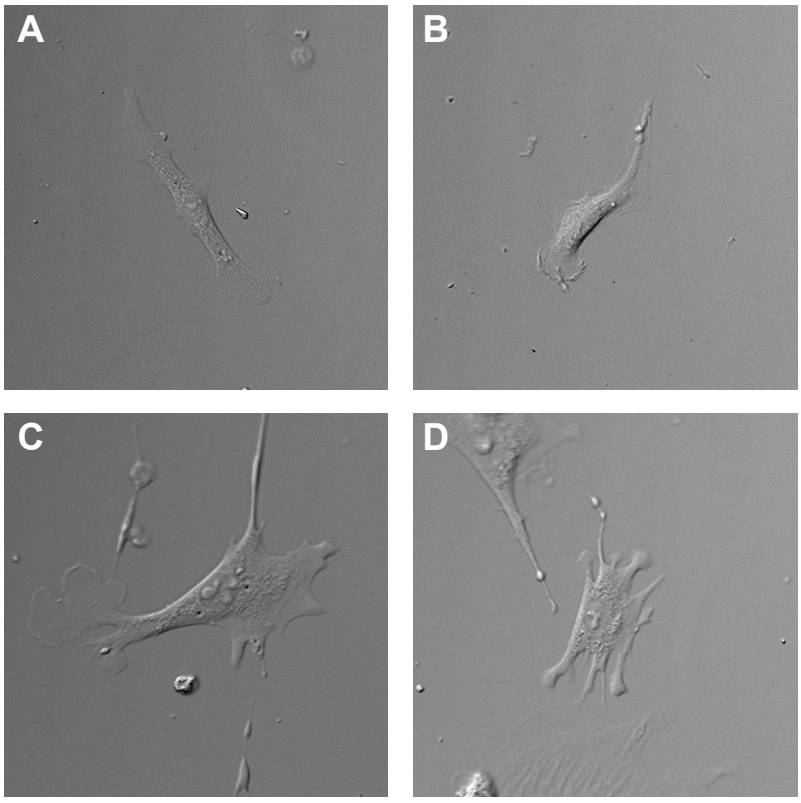

Figure 6.2. CENP-F-/- MEFs display aberrant lamellipodia. MEFs were plated and imaged 1x/2min for 6 hours. (A-B) WT MEFs displayed normal cellular shape and lamellipodial extensions, with putative directional migration. However, (C-D) CENP-F-/- MEFs did not show directional movement and displayed aberrant and uncontrolled lamellipodia.

advances we have made since the initial discovery of the murine homolog, previously unnoticed indications of new CENP-F functions could surface. Specifically, stem cells could be a very interesting source of information. We have seen how CENP-F is used as a cancer marker in a variety of tissues and how the protein functions in the proliferation and differentiation balance; it is possible that CENP-F could play a pivotal role in the earliest decisions in the embryo.

REFERENCES

Ahuja, P., Sdek, P. and MacLellan, W. R. (2007). Cardiac myocyte cell cycle control in development, disease, and regeneration. *Physiol Rev* **87**, 521-44.

Allan, V. J. and Schroer, T. A. (1999). Membrane motors. *Current Opinion in Cell Biology* **11**, 476-82.

Ashar, H. R., James, L., Gray, K., Carr, D., Black, S., Armstrong, L., Bishop, W. R. and Kirschmeier, P. (2000). Farnesyl transferase inhibitors block the farnesylation of CENP-E and CENP-F and alter the association of CENP-E with the microtubules. *J Biol Chem* **275**, 30451-7.

Ashe, M., Pabon-Peña, L., Dees, E., Price, K. L. and Bader, D. (2004). LEK1 is a potential inhibitor of pocket protein-mediated cellular processes. *J Biol Chem* **279**, 664-76.

Barker, R. J., Price, R. L. and Gourdie, R. G. (2002). Increased association of ZO-1 with connexin43 during remodeling of cardiac gap junctions. *Circ Res* **90**, 317-24.

Biggins, S. and Walczak, C. E. (2003). Captivating capture: how microtubules attach to kinetochores. *Curr Biol* **13**, R449-60.

Blaser, H., Reichman-Fried, M., Castanon, I., Dumstrei, K., Marlow, F. L., Kawakami, K., Solnica-Krezel, L., Heisenberg, C.-P. and Raz, E. (2006). Migration of zebrafish primordial germ cells: a role for myosin contraction and cytoplasmic flow. *Developmental Cell* **11**, 613-27.

Bock, J. B., Matern, H. T., Peden, A. A. and Scheller, R. H. (2001). A genomic perspective on membrane compartment organization. *Nature* **409**, 839-41.

Bomont, P., Maddox, P., Shah, J. V., Desai, A. B. and Cleveland, D. W. (2005). Unstable microtubule capture at kinetochores depleted of the centromere-associated protein CENP-F. *EMBO J* **24**, 3927-39.

Bornens, M. (2008). Organelle positioning and cell polarity. *Nat Rev Mol Cell Biol* **9**, 874-86.

Bullard, T. A., Borg, T. K. and Price, R. L. (2005). The expression and role of protein kinase C in neonatal cardiac myocyte attachment, cell volume, and myofibril formation is dependent on the composition of the extracellular matrix. *Microsc Microanal* **11**, 224-34.

Cheeseman, I. M., MacLeod, I., Yates, J. R., Oegema, K. and Desai, A. (2005). The CENP-F-like proteins HCP-1 and HCP-2 target CLASP to kinetochores to mediate chromosome segregation. *Curr Biol* **15**, 771-7.

Chen, H.-W., Yu, S.-L., Chen, W.-J., Yang, P.-C., Chien, C.-T., Chou, H.-Y., Li, H.-N., Peck, K., Huang, C.-H., Lin, F.-Y. et al. (2004). Dynamic changes of gene expression profiles during postnatal development of the heart in mice. *Heart* **90**, 927-34.

Cheng, G., Zile, M. R., Takahashi, M., Baicu, C. F., Bonnema, D. D., Cabral, F., Menick, D. R. and Cooper, G. (2008). A direct test of the hypothesis that increased microtubule network density contributes to contractile dysfunction of the hypertrophied heart. *Am J Physiol Heart Circ Physiol* **294**, H2231-41.

Classon, M., Salama, S., Gorka, C., Mulloy, R., Braun, P. and Harlow, E. (2000). Combinatorial roles for pRB, p107, and p130 in E2F-mediated cell cycle control. *Proc Natl Acad Sci USA* **97**, 10820-5.
Cooper, G. (2006). Cytoskeletal networks and the regulation of cardiac contractility: microtubules, hypertrophy, and cardiac dysfunction. *Am J Physiol Heart Circ Physiol* **291**, H1003-14.
de la Guardia, C., Casiano, C. A., Trinidad-Pinedo, J. and Báez, A. (2001). CENP-F gene amplification and overexpression in head and neck squamous cell carcinomas. *Head Neck* **23**, 104-12.
Dees, E., Pabón-Peña, L. M., Goodwin, R. L. and Bader, D. (2000). Characterization of CMF1 in avian skeletal muscle. *Dev Dyn* **219**, 169-81.
Dees, E., Robertson, J. B., Ashe, M., Pabón-Peña, L. M., Bader, D. and Goodwin, R. L. (2005). LEK1 protein expression in normal and dysregulated cardiomyocyte mitosis. *The anatomical record Part A, Discoveries in molecular, cellular, and evolutionary biology* **286**, 823-32.
Dees, E., Robertson, J. B., Zhu, T. and Bader, D. (2006). Specific deletion of CMF1 nuclear localization domain causes incomplete cell cycle withdrawal and impaired differentiation in avian skeletal myoblasts. *Experimental Cell Research* **312**, 3000-14.
Djinovic-Carugo, K., Gautel, M., Ylänne, J. and Young, P. (2002). The spectrin repeat: a structural platform for cytoskeletal protein assemblies. *FEBS Lett* **513**, 119-23.
Efimov, A., Kharitonov, A., Efimova, N., Loncarek, J., Miller, P. M., Andreyeva, N., Gleeson, P., Galjart, N., Maia, A. R., McLeod, I. X. et al. (2007). Asymmetric CLASP-dependent nucleation of noncentrosomal microtubules at the trans-Golgi network. *Developmental Cell* **12**, 917-30.
Encalada, S. E., Willis, J., Lyczak, R. and Bowerman, B. (2005). A spindle checkpoint functions during mitosis in the early Caenorhabditis elegans embryo. *Mol Biol Cell* **16**, 1056-70.
Eppenberger, H. M. and Zuppinger, C. (1999). In vitro reestablishment of cell-cell contacts in adult rat cardiomyocytes. Functional role of transmembrane components in the formation of new intercalated disk-like cell contacts. *FASEB J* **13 Suppl**, S83-9.
Erlanson, M., Casiano, C. A., Tan, E. M., Lindh, J., Roos, G. and Landberg, G. (1999). Immunohistochemical analysis of the proliferation associated nuclear antigen CENP-F in non-Hodgkin's lymphoma. *Mod Pathol* **12**, 69-74.
Erokhina, E. L. (1968). [Proliferation dynamics of cellular elements in the differentiating mouse myocardium]. *Tsitologiia* **10**, 1391-409.
Esguerra, R. L., Jia, L., Kaneko, T., Sakamoto, K., Okada, N. and Takagi, M. (2004). Immunohistochemical analysis of centromere protein F expression in buccal and gingival squamous cell carcinoma. *Pathol Int* **54**, 82-9.
Evans, H. J., Edwards, L. and Goodwin, R. L. (2007). Conserved C-terminal domains of mCenp-F (LEK1) regulate subcellular localization and mitotic checkpoint delay. *Experimental Cell Research* **313**, 2427-37.

Feng, J., Huang, H. and Yen, T. J. (2006). CENP-F is a novel microtubule-binding protein that is essential for kinetochore attachments and affects the duration of the mitotic checkpoint delay. *Chromosoma* **115**, 320-9.
Fotos, J. S., Patel, V. P., Karin, N. J., Temburni, M. K., Koh, J. T. and Galileo, D. S. (2006). Automated time-lapse microscopy and high-resolution tracking of cell migration. *Cytotechnology* **51**, 7-19.
Frederick, R. L. and Shaw, J. M. (2007). Moving mitochondria: establishing distribution of an essential organelle. *Traffic* **8**, 1668-75.
Goldspink, D. F., Burniston, J. G., Ellison, G. M., Clark, W. A. and Tan, L.-B. (2004). Catecholamine-induced apoptosis and necrosis in cardiac and skeletal myocytes of the rat in vivo: the same or separate death pathways? *Exp Physiol* **89**, 407-16.
Gómez, A. M., Kerfant, B.-G., Vassort, G. and Pappano, A. J. (2004). Autonomic regulation of calcium and potassium channels is oppositely modulated by microtubules in cardiac myocytes. *Am J Physiol Heart Circ Physiol* **286**, H2065-71.
Gómez, A. M., Kerfant, B. G. and Vassort, G. (2000). Microtubule disruption modulates Ca(2+) signaling in rat cardiac myocytes. *Circ Res* **86**, 30-6.
Gonzalez-Sanchez, A. and Bader, D. (1990). In vitro analysis of cardiac progenitor cell differentiation. *Developmental Biology* **139**, 197-209.
Goodwin, R. L., Pabón-Peña, L. M., Foster, G. C. and Bader, D. (1999). The cloning and analysis of LEK1 identifies variations in the LEK/centromere protein F/mitosin gene family. *J Biol Chem* **274**, 18597-604.
Hill, T. L. (1985). Theoretical problems related to the attachment of microtubules to kinetochores. *Proc Natl Acad Sci U S A* **82**, 4404-8.
Hoffman, J. I. E., Kaplan, S. and Liberthson, R. R. (2004). Prevalence of congenital heart disease. *Am Heart J* **147**, 425-39.
Holt, S. V., Vergnolle, M. A., Hussein, D., Wozniak, M. J., Allan, V. J. and Taylor, S. S. (2005). Silencing Cenp-F weakens centromeric cohesion, prevents chromosome alignment and activates the spindle checkpoint. *Journal of Cell Science* **118**, 4889-900.
Holy, T. E. and Leibler, S. (1994). Dynamic instability of microtubules as an efficient way to search in space. *Proc Natl Acad Sci U S A* **91**, 5682-5.
Höök, P. and Vallee, R. B. (2006). The dynein family at a glance. *Journal of Cell Science* **119**, 4369-71.
Huang, G. Y., Cooper, E. S., Waldo, K., Kirby, M. L., Gilula, N. B. and Lo, C. W. (1998). Gap junction-mediated cell-cell communication modulates mouse neural crest migration. *The Journal of Cell Biology* **143**, 1725-34.
Hussein, D. and Taylor, S. S. (2002). Farnesylation of Cenp-F is required for G2/M progression and degradation after mitosis. *Journal of Cell Science* **115**, 3403-14.
Jablonski, S. A., Chan, G. K., Cooke, C. A., Earnshaw, W. C. and Yen, T. J. (1998). The hBUB1 and hBUBR1 kinases sequentially assemble onto kinetochores during prophase with hBUBR1 concentrating at the kinetochore plates in mitosis. *Chromosoma* **107**, 386-96.

Jahn, R. and Scheller, R. H. (2006). SNAREs--engines for membrane fusion. *Nat Rev Mol Cell Biol* **7**, 631-43.
Jena, B. P. (2009). Membrane fusion: role of SNAREs and calcium. *Protein Pept Lett* **16**, 712-7.
Johnson, V. L., Scott, M. I., Holt, S. V., Hussein, D. and Taylor, S. S. (2004). Bub1 is required for kinetochore localization of BubR1, Cenp-E, Cenp-F and Mad2, and chromosome congression. *Journal of Cell Science* **117**, 1577-89.
Kamal, A. and Goldstein, L. S. (2000). Connecting vesicle transport to the cytoskeleton. *Current Opinion in Cell Biology* **12**, 503-8.
Kirby, M. L. (2007). Cardiac development. Oxford ; New York: Oxford University Press.
Kirschner, M. W. and Mitchison, T. (1986). Microtubule dynamics. *Nature* **324**, 621.
Kostetskii, I., Li, J., Xiong, Y., Zhou, R., Ferrari, V. A., Patel, V. V., Molkentin, J. D. and Radice, G. L. (2005). Induced deletion of the N-cadherin gene in the heart leads to dissolution of the intercalated disc structure. *Circ Res* **96**, 346-54.
Kozlov, S., Mounkes, L., Cutler, D., Sullivan, T., Hernandez, L., Levy, N., Rottman, J. and Stewart, C. L. (2005). Mutations in the mouse Lmna gene causing progeria, muscular dystrophy and cardiomyopathy. *Novartis Found Symp* **264**, 246-58; discussion 258-63.
Krämer, H. and Phistry, M. (1996). Mutations in the Drosophila hook gene inhibit endocytosis of the boss transmembrane ligand into multivesicular bodies. *The Journal of Cell Biology* **133**, 1205-15.
Krämer, H. and Phistry, M. (1999). Genetic analysis of hook, a gene required for endocytic trafficking in drosophila. *Genetics* **151**, 675-84.
Laoukili, J., Kooistra, M. R., Brás, A., Kauw, J., Kerkhoven, R. M., Morrison, A., Clevers, H. and Medema, R. H. (2005). FoxM1 is required for execution of the mitotic programme and chromosome stability. *Nat Cell Biol* **7**, 126-36.
Leach, R. N., Desai, J. C. and Orchard, C. H. (2005). Effect of cytoskeleton disruptors on L-type Ca channel distribution in rat ventricular myocytes. *Cell Calcium* **38**, 515-26.
Liao, H., Winkfein, R. J., Mack, G., Rattner, J. B. and Yen, T. J. (1995). CENP-F is a protein of the nuclear matrix that assembles onto kinetochores at late G2 and is rapidly degraded after mitosis. *The Journal of Cell Biology* **130**, 507-18.
Litvin, J., Montgomery, M. O., Goldhamer, D. J., Emerson, C. P. and Bader, D. M. (1993). Identification of DNA-binding protein(s) in the developing heart. *Developmental Biology* **156**, 409-17.
Liu, Z., Steward, R., and Luo, L. (2000). *Drosophila Lis1* is required for neuroblast proliferation, dendritic elaboration and axonal transport. *Nat Cell Biol* **2**, 767–775.
Liu, S., Hittle, J., Jablonski, S., Campbell, M., Yoda, K. and Yen, T. (2003). Human CENP-I specifies localization of CENP-F, MAD1 and MAD2 to kinetochores and is essential for mitosis. *Nat Cell Biol* **5**, 341-5.
Loewen, M. E., Wang, Z., Eldstrom, J., Dehghani Zadeh, A., Khurana, A., Steele, D. F. and Fedida, D. (2009). Shared requirement for dynein function and

intact microtubule cytoskeleton for normal surface expression of cardiac potassium channels. *Am J Physiol Heart Circ Physiol* **296**, H71-83.
Madden, S. D., Donovan, M. and Cotter, T. G. (2007). Key apoptosis regulating proteins are down-regulated during postnatal tissue development. *Int J Dev Biol* **51**, 415-23.
Maiato, H., DeLuca, J., Salmon, E. D. and Earnshaw, W. C. (2004). The dynamic kinetochore-microtubule interface. *Journal of Cell Science* **117**, 5461-77.
Malone, C. J., Misner, L., Le Bot, N., Tsai, M.-C., Campbell, J. M., Ahringer, J. and White, J. G. (2003). The C. elegans hook protein, ZYG-12, mediates the essential attachment between the centrosome and nucleus. *Cell* **115**, 825-36.
McDevitt, T. C., Angello, J. C., Whitney, M. L., Reinecke, H., Hauschka, S. D., Murry, C. E. and Stayton, P. S. (2002). In vitro generation of differentiated cardiac myofibers on micropatterned laminin surfaces. *J Biomed Mater Res* **60**, 472-9.
Mendoza-Lujambio, I., Burfeind, P., Dixkens, C., Meinhardt, A., Hoyer-Fender, S., Engel, W. and Neesen, J. (2002). The Hook1 gene is non-functional in the abnormal spermatozoon head shape (azh) mutant mouse. *Human Molecular Genetics* **11**, 1647-58.
Moore, L. L., Morrison, M. and Roth, M. B. (1999). HCP-1, a protein involved in chromosome segregation, is localized to the centromere of mitotic chromosomes in Caenorhabditis elegans. *The Journal of Cell Biology* **147**, 471-80.
Moynihan, K., Pooley, R., Miller, P., Kaverina, I. and Bader, D. (2009a). Murine CENP-F Regulates Centrosomal Microtubule Nucleation and Interacts with Hook2 at the Centrosome. *Mol Biol Cell* **22**, 4790-803.
Moynihan, K., Stockdale, F. and Bader, D. (2009b). Development of the Avian Heart, in Heart Development and Regeneration.
Müsch, A. (2004). Microtubule organization and function in epithelial cells. *Traffic* **5**, 1-9.
Nishimura, S., Nagai, S., Katoh, M., Yamashita, H., Saeki, Y., Okada, J.-i., Hisada, T., Nagai, R. and Sugiura, S. (2006). Microtubules modulate the stiffness of cardiomyocytes against shear stress. *Circ Res* **98**, 81-7.
O'Brien, S. L., Fagan, A., Fox, E. J., Millikan, R. C., Culhane, A. C., Brennan, D. J., McCann, A. H., Hegarty, S., Moyna, S., Duffy, M. J. et al. (2007). CENP-F expression is associated with poor prognosis and chromosomal instability in patients with primary breast cancer. *Int J Cancer* **120**, 1434-43.
O'Shea, E. K., Rutkowski, R. and Kim, P. S. (1989). Evidence that the leucine zipper is a coiled coil. *Science* **243**, 538-42.
Ortiz, J., Stemmann, O., Rank, S. and Lechner, J. (1999). A putative protein complex consisting of Ctf19, Mcm21, and Okp1 represents a missing link in the budding yeast kinetochore. *Genes Dev* **13**, 1140-55.
Pabón-Peña, L. M., Goodwin, R. L., Cise, L. J. and Bader, D. (2000). Analysis of CMF1 reveals a bone morphogenetic protein-independent component of the cardiomyogenic pathway. *J Biol Chem* **275**, 21453-9.
Pantos, C., Xinaris, C., Mourouzis, I., Malliopoulou, V., Kardami, E. and Cokkinos, D. V. (2007). Thyroid hormone changes cardiomyocyte shape and

geometry via ERK signaling pathway: potential therapeutic implications in reversing cardiac remodeling? *Mol Cell Biochem* **297**, 65-72.
Perriard, J.-C., Hirschy, A. and Ehler, E. (2003). Dilated cardiomyopathy: a disease of the intercalated disc? *Trends Cardiovasc Med* **13**, 30-8.
Pooley, R. D. (2006). THE ROLE OF LEK1 IN RECYCLING ENDOSOME TRAFFICKING AND ITS FUNCTION IN HEART DEVELOPMENT. *etd.library.vanderbilt.edu*.
Pooley, R. D., Moynihan, K. L., Soukoulis, V. and Reddy, S. (2008a). Murine CENPF interacts with syntaxin 4 in the regulation of vesicular transport. *Journal of Cell Science*, **121**, 3413-21.
Pooley, R. D., Moynihan, K. L., Soukoulis, V., Reddy, S., Francis, R., Lo, C., Ma, L.-J. and Bader, D. M. (2008b). Murine CENPF interacts with syntaxin 4 in the regulation of vesicular transport. *Journal of Cell Science* **121**, 3413-21.
Pooley, R. D., Reddy, S., Soukoulis, V., Roland, J. T., Goldenring, J. R. and Bader, D. M. (2006). CytLEK1 is a regulator of plasma membrane recycling through its interaction with SNAP-25. *Mol Biol Cell* **17**, 3176-86.
Rattner, J. B., Rao, A., Fritzler, M. J., Valencia, D. W. and Yen, T. J. (1993). CENP-F is a .ca 400 kDa kinetochore protein that exhibits a cell-cycle dependent localization. *Cell Motil Cytoskeleton* **26**, 214-26.
Rattner, J. B., Rees, J., Whitehead, C. M., Casiano, C. A., Tan, E. M., Humbel, R. L., Conrad, K. and Fritzler, M. J. (1997). High frequency of neoplasia in patients with autoantibodies to centromere protein CENP-F. *Clinical and investigative medicine Médecine clinique et experimentale* **20**, 308-19.
Redkar, A., deRiel, J. K., Xu, Y.-S., Montgomery, M., Patwardhan, V. and Litvin, J. (2002). Characterization of cardiac muscle factor 1 sequence motifs: retinoblastoma protein binding and nuclear localization. *Gene* **282**, 53-64.
Robertson, J. B., Zhu, T., Nasreen, S., Kilkenny, D., Bader, D. and Dees, E. (2008). CMF1-Rb interaction promotes myogenesis in avian skeletal myoblasts. *Dev Dyn* **237**, 1424-33.
Rodionov, V., Nadezhdina, E. and Borisy, G. (1999). Centrosomal control of microtubule dynamics. *Proc Natl Acad Sci USA* **96**, 115-20.
Rodriguez-Boulan, E., Kreitzer, G. and Müsch, A. (2005). Organization of vesicular trafficking in epithelia. *Nat Rev Mol Cell Biol* **6**, 233-47.
Rogers, S. L. and Gelfand, V. I. (2000). Membrane trafficking, organelle transport, and the cytoskeleton. *Current Opinion in Cell Biology* **12**, 57-62.
Rohr, S. (2004). Role of gap junctions in the propagation of the cardiac action potential. *Cardiovasc Res* **62**, 309-22.
Salic, A., Waters, J. C. and Mitchison, T. J. (2004). Vertebrate shugoshin links sister centromere cohesion and kinetochore microtubule stability in mitosis. *Cell* **118**, 567-78.
Sano, H., Ishino, M., Krämer, H., Shimizu, T., Mitsuzawa, H., Nishitani, C. and Kuroki, Y. (2007). The microtubule-binding protein Hook3 interacts with a cytoplasmic domain of scavenger receptor A. *J Biol Chem* **282**, 7973-81.
Santaguida, S. and Musacchio, A. (2009). The life and miracles of kinetochores. *EMBO J* **28**, 2511-31.

Savolainen, S. M., Foley, J. F. and Elmore, S. A. (2009). Histology atlas of the developing mouse heart with emphasis on E11.5 to E18.5. *Toxicol Pathol* **37**, 395-414.
Scholz, D., Baicu, C. F., Tuxworth, W. J., Xu, L., Kasiganesan, H., Menick, D. R. and Cooper, G. (2008). Microtubule-dependent distribution of mRNA in adult cardiocytes. *Am J Physiol Heart Circ Physiol* **294**, H1135-44.
Sedmera, D., Pexieder, T., Vuillemin, M., Thompson, R. P. and Anderson, R. H. (2000). Developmental patterning of the myocardium. *Anat Rec* **258**, 319-37.
Severs, N. J. (1990). The cardiac gap junction and intercalated disc. *Int J Cardiol* **26**, 137-73.
Shiels, H., O'Connell, A., Qureshi, M. A., Howarth, F. C., White, E. and Calaghan, S. (2007). Stable microtubules contribute to cardiac dysfunction in the streptozotocin-induced model of type 1 diabetes in the rat. *Mol Cell Biochem* **294**, 173-80.
Shigeishi, H., Mizuta, K., Higashikawa, K., Yoneda, S., Ono, S. and Kamata, N. (2005). Correlation of CENP-F gene expression with tumor-proliferating activity in human salivary gland tumors. *Oral Oncol* **41**, 716-22.
Shimada, T., Kawazato, H., Yasuda, A., Ono, N. and Sueda, K. (2004). Cytoarchitecture and intercalated disks of the working myocardium and the conduction system in the mammalian heart. *The anatomical record Part A, Discoveries in molecular, cellular, and evolutionary biology* **280**, 940-51.
Smith, T. K. and Bader, D. M. (2006). Characterization of Bves expression during mouse development using newly generated immunoreagents. *Dev Dyn* **235**, 1701-8.
Soonpaa, M. H. and Field, L. J. (1998). Survey of studies examining mammalian cardiomyocyte DNA synthesis. *Circ Res* **83**, 15-26.
Soonpaa, M. H., Kim, K. K., Pajak, L., Franklin, M. and Field, L. J. (1996). Cardiomyocyte DNA synthesis and binucleation during murine development. *Am J Physiol* **271**, H2183-9.
Soukoulis, V., Reddy, S., Pooley, R. D., Feng, Y., Walsh, C. A. and Bader, D. M. (2005). Cytoplasmic LEK1 is a regulator of microtubule function through its interaction with the LIS1 pathway. *Proc Natl Acad Sci USA* **102**, 8549-54.
Steensgaard, P., Garrè, M., Muradore, I., Transidico, P., Nigg, E. A., Kitagawa, K., Earnshaw, W. C., Faretta, M. and Musacchio, A. (2004). Sgt1 is required for human kinetochore assembly. *EMBO Rep* **5**, 626-31.
Sunio, A., Metcalf, A. B. and Krämer, H. (1999). Genetic dissection of endocytic trafficking in Drosophila using a horseradish peroxidase-bride of sevenless chimera: hook is required for normal maturation of multivesicular endosomes. *Mol Biol Cell* **10**, 847-59.
Szebenyi, G., Hall, B., Yu, R., Hashim, A. and Krämer, H. (2007). Hook2 Localizes to the Centrosome, Binds Directly to Centriolin/CEP110 and Contributes to Centrosomal Function. *Traffic* **8**, 32-46.
Taylor, S. S., Ha, E. and McKeon, F. (1998). The human homologue of Bub3 is required for kinetochore localization of Bub1 and a Mad3/Bub1-related protein kinase. *The Journal of Cell Biology* **142**, 1-11.

Taylor, S. S., Hussein, D., Wang, Y., Elderkin, S. and Morrow, C. J. (2001). Kinetochore localisation and phosphorylation of the mitotic checkpoint components Bub1 and BubR1 are differentially regulated by spindle events in human cells. *Journal of Cell Science* **114**, 4385-95.
Toralova, T., Susor, A., Nemcova, L., Kepkova, K. and Kanka, J. (2009). Silencing CENPF in bovine preimplantation embryo induces arrest at 8-cell stage. *Reproduction*.
Ueda, S., Kondoh, N., Tsuda, H., Yamamoto, S., Asakawa, H., Fukatsu, K., Kobayashi, T., Yamamoto, J., Tamura, K., Ishida, J. et al. (2008). Expression of centromere protein F (CENP-F) associated with higher FDG uptake on PET/CT, detected by cDNA microarray, predicts high-risk patients with primary breast cancer. *BMC Cancer* **8**, 384.
Urbani, L. and Stearns, T. (1999). The centrosome. *Curr Biol* **9**, R315-7.
Varis, A., Salmela, A.-L. and Kallio, M. J. (2006). Cenp-F (mitosin) is more than a mitotic marker. *Chromosoma* **115**, 288-95.
Vergnolle, M. A. and Taylor, S. S. (2007). Cenp-F links kinetochores to Ndel1/Nde1/Lis1/dynein microtubule motor complexes. *Curr Biol* **17**, 1173-9.
Walenta, J. H., Didier, A. J., Liu, X. and Krämer, H. (2001). The Golgi-associated hook3 protein is a member of a novel family of microtubule-binding proteins. *The Journal of Cell Biology* **152**, 923-34.
Wang, H., Hu, X., Ding, X., Dou, Z., Yang, Z., Shaw, A. W., Teng, M., Cleveland, D. W., Goldberg, M. L., Niu, L. et al. (2004). Human Zwint-1 specifies localization of Zeste White 10 to kinetochores and is essential for mitotic checkpoint signaling. *J Biol Chem* **279**, 54590-8.
Wei, Y., Bader, D. and Litvin, J. (1996). Identification of a novel cardiac-specific transcript critical for cardiac myocyte differentiation. *Development* **122**, 2779-89.
Yang, Z., Guo, J., Chen, Q., Ding, C., Du, J. and Zhu, X. (2005). Silencing mitosin induces misaligned chromosomes, premature chromosome decondensation before anaphase onset, and mitotic cell death. *Mol Cell Biol* **25**, 4062-74.
Yang, Z. Y., Guo, J., Li, N., Qian, M., Wang, S. N. and Zhu, X. L. (2003). Mitosin/CENP-F is a conserved kinetochore protein subjected to cytoplasmic dynein-mediated poleward transport. *Cell Res* **13**, 275-83.
Yutzey, K., Gannon, M. and Bader, D. (1995). Diversification of cardiomyogenic cell lineages in vitro. *Developmental Biology* **170**, 531-41.
Yutzey, K. E., Rhee, J. T. and Bader, D. (1994). Expression of the atrial-specific myosin heavy chain AMHC1 and the establishment of anteroposterior polarity in the developing chicken heart. *Development* **120**, 871-83.
Zhou, X., Wang, R., Fan, L., Li, Y., Ma, L., Yang, Z., Yu, W., Jing, N. and Zhu, X. (2005). Mitosin/CENP-F as a negative regulator of activating transcription factor-4. *Journal of Biological Chemistry* **280**, 13973-13977.
Zhu, X., Chang, K. H., He, D., Mancini, M. A., Brinkley, W. R. and Lee, W. H. (1995a). The C terminus of mitosin is essential for its nuclear localization, centromere/kinetochore targeting, and dimerization. *J Biol Chem* **270**, 19545-50.
Zhu, X., Mancini, M. A., Chang, K. H., Liu, C. Y., Chen, C. F., Shan, B., Jones, D., Yang-Feng, T. L. and Lee, W. H. (1995b). Characterization of a novel 350-

kilodalton nuclear phosphoprotein that is specifically involved in mitotic-phase progression. *Mol Cell Biol* **15**, 5017-29.